ADDIS ABABA UNIVERSITY

ADDIS ABABA INSTITUTE OF TECHNOLOGY

SCHOOL OF GRADUATE STUDIES

Design and Simulation of the Distributer and nozzle of a Micro hydro pelton turbine.

A Thesis Submitted to the Graduate School of Addis Ababa University in Partial Fulfillment of the Requirements for the Degree of Masters of Science

In

Mechanical Engineering (Thermal Engineering)

By: - Sase Negash

Advisor: - Dr.Ing Edessa Dribssa

Co-Advisor:- Tilahun Nigussie

MARCH, 2018

Addis Ababa University

Addis Ababa Institute of Technology

School of Mechanical and Industrial Engineering

Design and Simulation of the Distributer and nozzle of a Micro hydro pelton turbine

By

Sase Negash

Submitted in partial fulfillment of the requirements for the degree of Master of Science **(M.Sc.)**

Approved By Board of Directors

Edessa Dribssa (Dr.Ing)	______________________	_________________
Advisor	Signature	Date
Tilahun Nigussie	______________________	_________________
Co – Advisor	Signature	Date
_________________	______________________	_________________
Internal Examiner	Signature	Date
________________	______________________	_________________
External Examiner	Signature	Date
_________________	_____________________	____________________
Chairman, Department Of Graduate Committee	Signature	Date

DECLARATION

Addis Ababa University School of Graduates

This is to certify that the thesis prepared by Sase **Negash**, entitled: "***Design and Simulation of the Distributer and Nozzle of a Micro Hydro Pelton Turbine***", do here by declare this thesis is my original work and that it has not been submitted partially, or in full for a degree in any university/institution, which compiles with the regulations of the university and meets the accepted standards with respect to originality and quality.

Signature: ________________________

*Date:*____________________________

Advisor: Edessa Dribssa (Dr.Ing) Signature:_____________Date:____________

Co Advisor: Tilahun Nigussie Signature: ___________ Date: ___________

Head of School:_______________ Signature: ______________ Date:___________

ABSTRACT

Pelton turbine is a type of hydraulic turbine in which energy carried by water is converted into kinetic energy by providing nozzle at the end of the penstock. The performance of this turbine depends on the nozzle shape and the distributer. In this paper attempts were made to study the effect of different nozzle shapes, nozzle angle, distributer bend, split angle, spear shape and spear angle.

CATIA V5 and Ansys Fluent software were used to design and analysis of the numerical simulation for all the models developed. For the design and simulation of nozzle and distributer, a jet diameter of 54.4mm, flow rate of $0.14m^3/s$ and the total head of 50m were taken. And also the nozzle angle of (30-45) in degree and the spear angle of (20-25) in degrees were fed to Ansys and then it generates 82 samples. So, the effect of each angle in the range was analyzed. The value obtained from Ansys parameter correlation depicts that nozzle angle of 30 degree and spear angle of 20 degree gives maximum efficiency. And finally the variation of blocking distance on efficiency and performance of the intended result was critical, sample values in mm from (0-93) was evaluated and best performance was found at blocking distance of 80mm. And more over, as the flow rate varies seasonally or due to flow rate regulation, ranges of flow rate in m^3/s from 0.1 up to 0.009 per single nozzle was considered for the baseline and optimal design.

Results obtained from numerical simulation on contours of static pressure, contours of velocity magnitude, and velocity vectors were colored inside the fluid interior for all models. So the comparison and analysis made on the model is based on the color magnitude on the legend bar of velocity and pressure. The result showed that, increasing the pipe diameter of distributer results in the reduction of head loss. However, since the optimal diameter is 142 mm, further increment in pipe diameter increases the cost of pipe. The other critical and notable factor to mention from the study was the nozzle angle and nozzle efficiency. i.e. As the nozzle angle increases the nozzle efficiency decreases due to back flow at the exit of the nozzle. In the end, increasing pipe diameter of distributer decreases the hydraulic energy inside the nozzle.

The performance of the nozzle at different flow rate and different closing distance were analyzed and efficiency of 96.8 % was achieved. Finally after the nozzle and distributer optimized separately, then by integrating both components i.e. distributer and nozzle and their simulation were analyzed and 96.5% efficiency was obtained.

Keywords: micro-hydro Pelton turbine, distributer, nozzle, spear, CFD and optimization.

ACKNOWLEDGEMENT

First and foremost, I would like to thank God Almighty for giving me the strength, knowledge, ability and opportunity to undertake this research study and complete it satisfactorily. I would like to express my deepest gratitude to my advisor Dr. Ing. Edessa Dribssa for his support, guidance, inspiration and suggestions during my research and next I would like to express my filling to my Co-advisor Mr**.** Tilahun Nigussie for His support, encouragement and credible ideas have been great contributors in the completion of the thesis and also for giving me valuable input datas for my research.

Finally, I would like to thanks and give my appreciation to all of my family members and my friends Especially Mr. Tesfaye Asefa and Mr.Habtamu Dagne those who were supporting and motivating me for the achievement of this study.

TABLE OF CONTENTS

LIST OF FIGURES

LIST OF TABLE

NOMANCLATURE

Z = the elevation head

H = the potential head of the site.

V_A = velocity at the surface of river bed

P_A = the atmospheric pressure,

P_B = the static pressure is atmospheric at the exit of the nozzle

H_L = head loss encountered from the point of inlet of the penstock to exit of the nozzle

$(\mathbf{C_v})$ = Coefficient of Velocity

$(\mathbf{C_c})$ = Coefficient of Contraction

$(\mathbf{C_D})$ = Coefficient of Discharge

$\mathbf{C_p}$ =Coefficient of pressure accounts for pressure drop in the nozzle

V_o= the actual velocity of nozzle at the exit

V = the velocity at the point of interest(nozzle inlet)

H_n = net head for the nozzle

H_l = head loss for the nozzle

$\mathbf{C_l}$ = head loss coefficient

H_j = head available at the jet

D_H = hydrualic diametre

A = Wetted crossectional area of the fluid ,

D_0 = outer diameter of the wetted area

D_i = inner diameter of the wetted area

P_{hs} = hydro static pressure

P_{hd} = hydrodynamic pressure

H_d = head loss in the distributer

V_{exit}=the velocity exit from the distributer which is found from CFD

$N =$ Number of nozzle,

$Q_o =$ Total flow rate

$H_g =$ Gross head,

$LP =$ Penstock length

$D_P =$ optimum diameter or economic diameter

$Cec =$ Coefficient of energy cost

$Cmp =$ coefficient for the pipe materials

$H_p =$ head loss in penstock

$\nabla p_{cr} =$ critical pressure at minimum thickness of penstock material

$E_W =$ Bulk water modulus

$E =$ Modulus of penstock material

$Ap =$ cross − sectional area of the penstock

$Dpt =$ diametre of penstock

Hs =Surge pressure head

$t =$ effective thickness of penstock

$hf =$ frictional head loss

$hm =$ minor head loss

$v =$ kinematic viscosity

$d_j =$ diameter of jet

$C =$ closing(blocking) distance or nozzle oppening

$d_{exit} =$ nozzle exit diametre

$Lb =$ spear tip length,

$da =$ bulb radius of curvature(spear height),

$do =$ spear shaft diameter,

$\beta =$ conical nozzle angle, $\alpha =$ conical spear angle,

$Rn =$ Nozzle radius of curvature ,

Rs = spear fillet radius,

dn = nozzle diameter

D1 = diameter of shaft diameter

R = Curve of nozzle exit radiu

dn = Nozzle internal diameter

X_{nb} = The distance between nozzle and bucket

F_a = The maximum force applied to the

k = radius of gyration,

L_r = length of rod

Q_n = flow rate for each nozzle

R_d =the total arm length of the deflactor

F_d =hydrodynamic force on the deflactor.

T_d = The bending moment acting on the deflector arm

F_C = friction factor acted upon by bearings

F_{dr} = The required force in each deflector

n = Number of bolts,

d_c = core diameter of the bolts.

t_f = Thickness of flange,

D_o = Outside diameter of flange

D_P = Pitch circle diameter of boltsThe:

P_c = circumferential pitch of the bolt

CHAPTER ONE

INTRODUCTION

This chapter explains the introductory part of the thesis and tells the over view of the work, which has been done during the whole research period. The chapter highlights about background, significance of the study followed by objectives of the research and organization of the thesis provided here after.

1.1 BACKGROUND OF THE STUDY

Human beings have been used the power of flowing water for thousands of years. The ancient Greece used this hydropower to grind corn and wheat to flour. The word *Hydro* comes from the Greek word for water. *Hydropower* traditionally represents the energy generated by damming a river and using turbine systems to generate electrical power. Water wheels were used extensively in the ancient times, but it was only at the beginning of the 19th Century that the invention of the hydro turbines got popularized.

It was a French engineer, Benoit Fourneyron, who developed the first commercially successful hydraulic turbine (circa 1830). Later Fourneyron built turbines for industrial purposes that achieved a speed of 2300 rev/min, developing about 50kW at an efficiency of over 80 percent and The first radial inflow hydraulic turbine was introduce with an excellent efficiency by American engineer James B. Francis for a head of 10 to 100m [43].

1.2 DEFINITION AND MAJOR CLASSIFICATION OF HYDRAULIC TURBINES

Hydraulic turbine can be defined as a rotary machine and, water is used as the source of energy. Water or hydraulic turbines convert kinetic and potential energies of the water into useful mechanical power and if needed to electrical energy. According to the way of energy transfer, there are two types of hydraulic turbines namely.

1. Impulse turbines and

2. Reaction turbines

1. In impulse turbines water coming out of the nozzle at the end of the penstock is made to strike a series of buckets fitted on the periphery of the runner. The runner revolves freely in air and the casing is not important in impulse turbine. The runner of the Pelton turbine consists of double hemispherical cups fitted on its periphery. The predominant type of impulse machine is the *Pelton turbine*, which is suitable for a range of heads of about 50–2000 m.

2. In a reaction turbine, water enters all around the periphery of runner and the runner remains full of water every time. The water leaves from the runner is discharged into the tailrace with a different pressures. Therefor casing is necessary for reaction turbines. The reaction turbine is further subdivided into the *Francis type*, which is characterized by a radial flow impeller, and the *Kaplan or propeller type*, which is an axial-flow machine, which uses the potential and kinetic energy of water and converts it into useful mechanical energy.

Based on flow direction, they are further classified as:

- Tangential Flow
- Radial Flow
- Axial Flow
- Mixed Flow

The efficiencies of the three principal types of hydraulic turbine just mentioned are shown in Figure 1.1 as functions of the power specific speed.

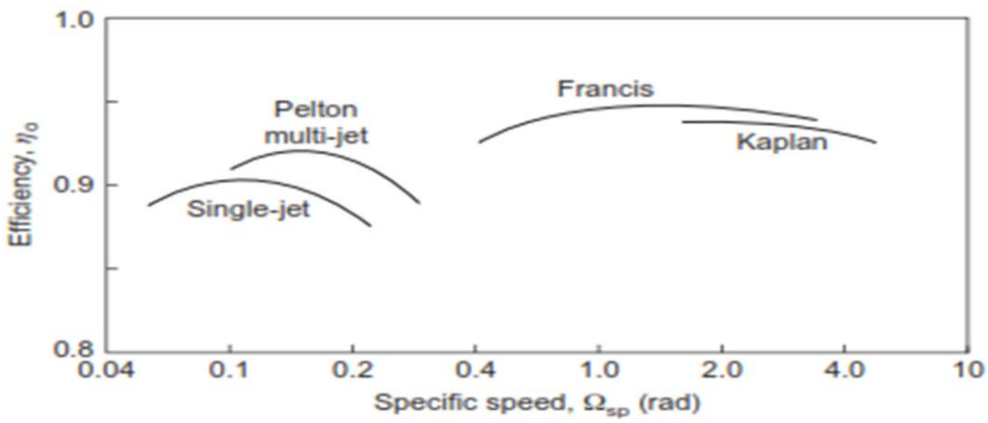

Figure 1.1 Typical design point efficiencies of Pelton, Francis, and Kaplan turbines [43].

1.2.1 SMALL-SCALE HYDROPOWER

Small-scale hydropower was the most common way of electricity generating in the early 20th century. The first commercial use of hydroelectric power to produce electricity was a waterwheel on the Fox River in Wisconsin in 1882 that supplied power for lighting to two paper mills and a house [22]. Depending on individual circumstances, many people find that they need to develop their own source of electrical power. Other renewable energy sources, such as solar and wind, can be used to produce electrical power. The choice of energy source depends on several factors, including availability, economics and energy and power requirements. Micro-hydropower systems offer a stable, inflation-proof, economical and renewable source of electricity that uses proven and available technologies. These technologies can produce as little as 100W of electricity at low cost, at very competitive rates, appropriately designed and implemented systems can provide inexpensive energy for many years.

There can be several reasons for wanting to build a micro-hydropower system. It can be used to generate electricity to fulfill basic needs for lighting, electronic devices, computers, small appliances, tools, washing machines, dryers, refrigerators, freezers, hot water, space heating or cooking. Other reasons is helping to protect the environment by avoiding the use of fossil fuels or to be independent of the power grid. Who are considering off-grid power generation? Applying micro-hydropower technology in remote locations where electricity is provided by diesel generators offers an opportunity to replace a conventional fuel with a renewable energy source. It has been demonstrated that water power can produce many times more power and energy than several other sources for the same capital investment.

A micro-hydropower system is a non-depleting and non-polluting energy source that has provided reliable power in the past and is one of the most promising renewable energy sources for the future [11].

So micro hydro pelton turbine has a long history and installed in in many African countries including Ethiopia even though Ethiopia installed only one percent from her 15000MW.Global installed capacity of Small hydro is around 50GW against the estimated potential of 180 GW Due to its short gestation period, small hydro is attracting worldwide attention. Several solutions have been proposed and successfully implemented for micro-hydro schemes [13].

1.2.2 **PELTON TURBINE COMPONENTS**

Pelton turbines are impulse turbines used for high head and low flow hydro applications. Performance and reliability related components of a Pelton turbine consist of a distributor/manifold, housing, needle valve, nozzle, impulse runner and discharge chamber [8]

Housing:-Housing is a rigid unit which consists of needle servomotor piping, feedback mechanisms, and the deflector shafts. The shape of the wetted side of the housing is important for directing the exit water effectively away from the runner.

Runner: -The runner consists of a set of specially shaped buckets mounted on the periphery of a circular disc and which generates mechanical energy from the flowing hydraulic energy which in the converted in then electrical energy.

Discharge Chamber: - The function of the discharge chamber is to enable water exiting the runner to fall freely toward the drainage. It also functions as a shield for the concrete work and prevents concrete deterioration due to the action of the water jets. Correct water level regulation (surge chambers) inside this chamber is critical for maximum efficiency.

Nozzle: - A nozzle is often a pipe or tube of varying cross sectional area, and it can be used to direct or modify the flow of a fluid (liquid or gas). Nozzles are frequently used to control the rate of flow, speed, direction, mass, shape, and/or the pressure of the stream that emerges from them.

Distributor/Manifold:-The function of the distributor (or manifold) is to provoke an acceleration of the water flow toward each of the main injectors. The advantage of this design is to keep a uniform velocity profile of the flow. Depending on the age of the turbine unit and original hydraulic design, the distributor size may contribute to losses and turbulence.

Non-performance but reliability related components of a Pelton turbine include the deflector, turbine shaft, and guide bearing.

Turbine Shaft: - The turbine shaft is a transmitter of energy between the turbine and the generator. When the flowing liquid hits the turbine blade then it produce mechanical energy. This mechanical energy in turn converted into electrical energy. The shaft typically has a bearing journal for oil lubricated hydrodynamic guide bearings on the turbine runner end.

Guide Bearing: - The function of the turbine guide bearing is to resist the mechanical imbalance and hydraulic side loads from the turbine runner, thereby maintaining the turbine runner in its centered position in the runner seals. It is typically mounted as close as practical to the turbine runner and supported by the head cover. Turbine guide bearings are usually oil lubricated hydrodynamic bearings.

Deflectors: - The deflectors serve to bend the jet away from the runner at load rejections to avoid a high speed increase. It also protects the jet against exit water spray from the runner. The deflector arc is bolted to the deflector support structure frame with the control valve of the needle servomotors. A seal ring around the deflector shaft bearing housing prevents water and moisture from penetrating into the bearing.

By the outline of a nozzle and a spear head, the surface are shaped so as to reduce the annular area steadily toward the exit, where they are usually conical.

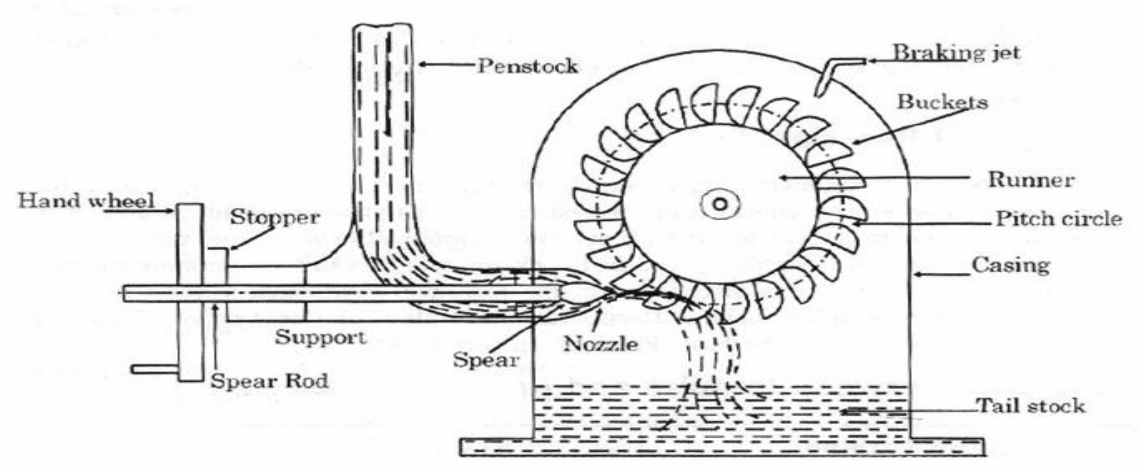

Fig 1.2 Components of Pelton turbine[5].

The typical application of Pelton turbines is in low specific speed conditions, .so among the different types of hydraulic machinery, the Pelton turbine shows an impressive part load performance.

1.3 SIGNIFICANCE OF THE STUDY

Hydropower resource is basic to generate power and Ethiopia is one of the richest in micro hydropower sites. The country needs micro hydro turbine technologies which convert the hydro power into electricity. Ethiopia has the greatest hydro power potential in the east Africa with a capacity of 15 000 MW, but its installed capacity not more than two percent [13].

The rural community is in need of electricity. Non-commercial sources like firewood, dung and agricultural waste are major sources of energy in rural Ethiopia. The household sector takes up over 80 percent of the energy supplies. Almost all the energy used by these households is biomass based. As a result, deforestation and land degradation have gone beyond control leading to extreme loss of soil fertility. The result that hydro power has significant contribution by providing multiple benefits particularly in rural households. The country needs micro hydro technologies which convert the hydro power into electricity. There is an ongoing PhD research in the Addis Ababa institute of Technology which aims at building the capacity of harnessing a micro hydro resource to generate off grid electricity. Design of runner for a Pelton turbine completed: the distributer and nozzle not yet. So this research proposed to participate in the design and optimization of a distributer and nozzle of this turbine.

This thesis gives the inspiration in micro hydro-power benefit with the objectives of Design and simulate nozzle and distributer of Pelton turbine to increasing and improve the net efficiency of the Pelton turbine and clean energy use in rural area without huge construction dams and reducing the cost of electricity production without facing problems to environment (atmosphere) from carbon emission.

The optimization of distributer, nozzle and spear have been analyzed using computational fluid dynamics (CFD). Computational fluid dynamics (CFD) performs numerical analysis of a fluid flow field once a finite volume grid has been created. One of the biggest challenges in the engineering industry is being able to come up with efficient and optimal designs for complex fluid flow. One of the strongest tools offered now a day is Fluent. Fluent is a very useful program recently acquired by Ansys. So this thesis inputs significant benefit in generation of small scale hydro power by design and optimize pelton turbine components such as nozzle, spear and distributer for its highest performance value. It would be easy to manufacture and install small hydro power in off grid area after all components of the pelton turbine designed and simulated well.

Finally the thesis has a significant role in producing the components of the micro hydro pelton turbine in an optimized capacity to support off grid rural electrification.

1.4 OBJECTIVE

1.4.1 GENERAL OBJECTIVE

The general objective of this thesis is to design and simulate the distributer and nozzle of Pelton turbine using commercial software in different shape and get best performance optimization.

1.4.2 SPECIFIC OBJECTIVE

- Collect geometric data of the runner of the micro hydro Pelton turbine designed by a PhD candidate.
- Design and simulation of the distributer
- Design the spear and nozzle of a micro hydro pelton turbine
- Optimize the design of the distributer and nozzle using a commercial CFD softwares.
- Make structural analysis of the distributer and nozzle and select appropriate material.
- Design manually operated deflector and structural Analysis
- Prepare work shop and assembly drawing of the components.

1.5 RESEARCH METHODOLOGY

Method of analysis shows the overall steps of the thesis activity. Methodologies employed in this thesis to achieve the objective of the study includes the following steps.

1.5.1 An intensive survey of literature about micro hydro pelton turbine distributer and nozzle.

This step involves collecting data from different relevant literatures, books, research and experimental result which is used as an input data for this paper.

1.5.2 Geometry and design of distributer, nozzle, spear and deflector to be decided analytically.

From the collected data overall design of distributer, nozzle, spear and deflector was done.

1.5.3 Model and Simulation

For modeling and simulation purposes, distributer and nozzle with its spear alignment is drawn on catia V5 and then exported to Ansys work bench 14. To perform the simulation, modeling, boundary condition setup, meshing, and solving were critical.

The simulation is run and has characterized the following:

Head loss in the distributer has been investigated for:

- Different diameters.
- Different splitting angles.
- Different bending radius.

Nozzle-spear assembly, pressure drop and actual outlet velocity from the analysis of CFD at

- Different nozzle openings or blocking distance from 0 to 93 mm.
- Different nozzle angles ranging 30-45 in degree.
- Different spear angles ranging 20-25 in degree.
- Velocity and Pressure distribution in the surface of the nozzle using CFD are analyzed

1.6 ORGANIZATION OF THE THESIS

This thesis work consists of six chapters.

The first chapter discuss the general overview of the thesis which is introduction part. The selected sites for this thesis, the power of water and the way of utilizing it, statement of the problem, the objective of the study and methodology are also presented in this chapter.

Chapter two is a literature review part. In this chapter different literatures related to micro hydro pelton turbine distributer and nozzle issues both in developing and developed countries, the energy potential as a whole in Ethiopia especially the hydropower resources and more about

MHP are briefly discussed. Moreover, the Methods used in the determination of head and flow rate of flowing rivers are covered in this chapter.

Chapter three mainly focuses on the derivation of equations and basic concepts of MHPT. Different theorems are also discussed which feeds for chapter four.

Chapter four. This chapter contains the main work of the thesis which is analytical and numerical solution will be performed here .i.e. the penstock, distributer, nozzle, spear and deflector will be optimized here using empirical formula as well CFD.

Chapter five is all about the results & discussion which obtained at chapter 4 and then selection of the optimized design will be done here.

Chapter six Conclusions, recommendations and suggestions for future work are presented.

CHAPTER TWO

LITRATURE RIVIEW OF PREVIOUS WORKS

This chapter contains different literatures on micro hydro pelton turbine distributer and nozzle. Varieties of international research papers have been discussed here by comparing the method and the outcome of their researches. And then from the perspectives of these previously done researches, this thesis has undergone further study for its intended objectives.

2.1 LITRATURE REVIEW

Many researchers around the world have introduced that Pelton turbine is used for high head for converting hydraulic energy into mechanical energy. In this turbine, the discharge required is comparatively low. Penstock conveys water from head race to distributor fitted with nozzle. The nozzle converts all the available energy of water into kinetic energy of jet. Number of nozzles depends on specific speed of turbine. As number of nozzle increases, diameter of runner decreases. The force of water jet on buckets is tangential and it produces torque on shaft due to which runner rotates. The performance analysis of turbine is an important aspect to analyze its suitability under different operating conditions. Also computational fluid dynamic (CFD) modeling is used to characterize different basic parameters of the turbine. Some of the researches undergone and found at hand are described below.

Mesa associates, Oak ridge national laboratory for the U.S. department of energy on their research paper "**Hydro Power Advancement Project**" state that, Pelton turbines are impulse turbines used for high head (usually 100 to 1000 m or above) and low flow hydro applications. The Pelton runner normally operates in air or near atmospheric pressure with one to six jets of water impinging tangentially on the runner. The Pelton turbine unit comes in two shaft axis arrangements: horizontal and vertical. This is dictated by the overall hydro plant design. The horizontal shaft turbine (maximum of 4 jets) is more conducive for maintenance activities but requires a larger powerhouse. Alternatively, the vertical shaft turbine (maximum of 6 jets) is more difficult to perform maintenance. The purpose of the needle and nozzle is to concentrate the jet in a cylindrical and uniform shape in order to maximize the energy transformation in the runner. Wear on the needle and nozzle causes a jet deformation which results in decay of efficiency and an appearance of cavitation [8].

This paper is very useful for this research in developing the concept and design even though it lacks simulation of the nozzle and the distributer

Micro-hydro-electric power is both an efficient and reliable form of clean source of renewable energy. It can be an excellent method of harnessing renewable energy from small rivers and streams. The micro-hydro project designed to be a run -of-river type, because it only requires very little or no reservoir in order to power the turbine. The water will run straight through the turbine and back into the river or stream to use it for the other purposes. This has a minimal environmental impact on the local ecosystem [11].

It is useful for the current research because basic and general concepts about head are discussed and represented graphically.so the overall layout of hydraulic turbine is clearly put in the research are used for this research.

Dimitrios Michailidis and his advisor Prof. Dr. Gerard J.W. van Busselon on the thesis of **Conceptual Design of a DOT Farm Station**. Nozzles and spear valves are devices, used in impulse turbines only, to control the direction or the characteristics of water flow. The main deference between them is that the cross sectional area of a nozzle stays constant, whereas it can vary in the case of a spear valve by moving it forwards or backwards. Depending on the kind of nozzle that is used, the jet converges by a divergent portion of the nozzle diameter. What is more, there is a change in the velocity of water as it flows through the nozzle as a consequence of its design. Both of these phenomena are described by the contraction, Cc, and the velocity coefficient, Cv, of a nozzle, respectively. These two parameters characterize the performance of a nozzle and if multiplied together result in the discharge coefficient, CD [46].

This paper is critical for my research because all of the necessary coefficients and parameters are analyzed for the nozzle even if the structural and design analysis of the nozzle are not clearly explained and also no distributer analysis.

Bilal Abdullah Nasir international journal of (ijeet) on his research **Design of High Efficiency Pelton Turbine for Micro Hydro Power Plant**. One or more water jets (nozzles) can be provided with the Pelton turbine depending on the water flow rate and the nozzle capacity The Pelton turbines have been given increasing interest by the research community within multiple fields. This is due to the increasing demand for energy on a global basis in addition to the growing focus on meeting the increasing demand by utilizing renewable energy resources. An increase in efficiency (installing micro hydraulic turbine) in the order 0.1 % would lead to large increase in electrical power production which shows demand increment of micro hydro power plant for rural society [2].

This paper is best international journal which clearly shows the design of each components of micro hydro pelton turbine especially for my case it shows the design of nozzle, deflector and the penstock with their parameters. But no enough simulation of these components.

Mario Peron, Etienne Parkinson, Lothar Geppert and Thomas Staubli on their research paper "**Importance of Jet Quality on Pelton Efficiency and Cavitation**" states that the jet of a Pelton turbine is more and more seen as a major influence parameter for the performance of a Pelton turbine. A water jet in a Pelton turbine shows large variations of length and time scale. Within very few centimeters between the internal region of the nozzle and the first jet diameter downstream of detachment [7].Since jet quality is one of the critical things in optimization of nozzle efficiency this research clearly shows the simulation only on jet quality. The design and other procedure of the nozzle simulation are not put.

Aung Kyaw Minn, Htay Win and Nyein Aye San on their international journal of scientific research
Design of 225kW Pelton Turbine have done" **Performance Testing Of Model 12 Pelton Turbine"** Model 12 Pelton turbine is tested in a Laboratory which is suited in Mandalay technological University. The resource of required water is carried from the ground tank. The water from the ground tank is pumped to the artificial water way by using the pump. The required jet opening is set by turning the hand wheel in anti-clockwise direction. The speed of the turbine is measured by using a tachometer. In this test, nozzle position of Pelton turbine is placed five positions. There are 1/5, 2/5, 3/5, 4/5 and fully open position. The pitch circle diameter of model 12 Pelton turbine is 96 mm and jet diameter is 10 mm. At 1/5 opening position the turbine maximum efficiency is below 90% at opening 2/5 position the maximum efficiency is 80% [1].which is very low efficiency. Even if the efficiency of the nozzle is very low and talking about testing it is very useful reference in deciding the detail internal flow of the nozzle analytically and numerically.

Vishal Gupta, Dr. Vishnu Prasad and Dr. Ruchi Khare on their research" **Effect Of Jet Shape On Flow and Torque Characteristics Of Pelton Turbine Runner**" describe the quality of jet has a great efficiency. In Pelton turbine, the energy carried by water is converted into kinetic energy by providing nozzle at the end of penstock. The shape of jet affects the force and torque on the bucket and runner of turbine. The nozzle of circular cross section is commonly used. Water, at high head, flows through the penstock and at the end of penstock, one or more nozzles are fitted to convert all the available energy of water into kinetic energy. The water comes out of the nozzle as jet and impinges on the buckets, causing it to revolve. The impact of water jet produces force on bucket causing wheel to rotate. The jet of water splits equally by splitter. Model testing is the most common but this is time consuming, costly and does not provide detailed flow information.CFD is used to improve optimization. Many authors have worked for finding out most efficient shape of nozzle. Still performance prediction of Pelton turbine for different shapes of jets is a thrust area for research because of multiphase and transient flow [6].

According to their research , efficiency of jet is shown in the following table which is less than 90% but my research aims that the efficiency is above 95%.The square shape is easier for manufacturing because of regular shape in machining but less efficient than circular one.

Table 2.1 Efficiency of different jet shapes [6].

Jet shape	*Circular*	*Triangular*	*Square*	*Elliptic*
Numerical efficiency	*88.03*	*77.8*	*84.72*	*76.56*

Abhishek Sharma, Vishnu Prashad and Anil Kumar on their research about "**Numerical Simulation of Pelton Turbine Nozzle for Different Shapes of Spear"** they have done simulation for design of spear for nozzle by applying computational fluid dynamics analysis and using ANSYS software. Detail flow analysis of the desired model has been done for design optimization. Their design altered till the best performance or desired output is obtained. CFD can provide the solution for different operating condition and geometry configuration in less time and cost and found very useful for design and development. In their works, three shapes of spear at different mass flow rates have been analyzed using ANSYS-CFX 10 software, the pressure and velocity distribution are obtained and compared. Using the analysis result, the loss variations with the nozzles for different spear shapes are computed [3]. Their results are presented in the following table.

Table 2.2 The velocity, pressure and discharge coefficients [3]

B.condition	Pressure(pa	V(m/s)	Area(m^2)	Head (m	H_L(m)	Loss coefficient	C_V	C_P	C_d
Inlet	291700	5.74	0.4215	31.41	0.48	0.01528	0.8910	0.952	0.773
outlet	58836.5	22.12	0.1975	30.936	0.48				
Inlet	451528	7.175	0.4215	48.65	0.32	0.0065	0.8998	0.942	0.789
outlet	87639.5	27.8	0.1975	48.32	0.32				
Inlet	661768	8.611	0.4215	71.23	0.382	0.0053	0.8931	0.940	0.769
outlet	137604	33.389	0.1975	70.89	0.82				

As can be seen from the table the velocity coefficient (C_v) is very low if we calculate the hydraulic efficiency of nozzle $={C_v}^2$. $The\ maximum\ \ C_v\ value\ is\ \ 0.899816\ \ and\ square$

$this\ \ value\ gives\ \ around$ 80.8% , Which is very low. But the paper is directly useful for this research in determining and comparing the CFD results.

Aldo Cateni, Livio Magri and Gianalberto Grego on their research **“Economics Of Efficiency Testing** And Monitoring 7th International Conference On Hydraulic Efficiency Measurements, Optimization Of Hydro Power Plants Performance Importance Of Rehabilitation And Maintenance**”.** In particular for the runner profiles studied the purpose of needle and nozzle is to concentrate the jet in a cylindrical and uniform shape in order to maximize the energy transformation in the runner. Wear on needle and nozzle causes a jet deformation which results in a decay of efficiency and possibly an appearance of cavitation. A test nozzle was connected to the manifold of the HPP Handeck in order to measure the jet deformations from different upstream bends, nozzle geometries and obstacles. In worn nozzles, the boundary layer is thickened and disturbed, due to an increased waviness of the walls in the nozzle pipe and nozzle mouth [41].At their research the maximum optimization achieves below 93% efficient pelton turbine. And the research explained how the shape of the nozzle affect the efficiency of the nozzle which is very essential for this research even though there is no analytical design procedure for the nozzle.

Takashi Kubota and hitomi kawekami on their research**” Observation of Jet Interference in 6 Nozzle Pelton Turbine**” stated about the head of micro hydro pelton turbine. A pelton turbine has been applied to higher heads.in recent years it applies to medium and low heads less than 100m.This trend is due to the re-evaluation of the flowing advantage of pelton turbine. And about efficiency of the nozzle they states that through the regulation of the number of nozzles, a multi-nozzle pelton turbine can be operated under the wide range of output power maintaining high efficiency without vibration increase compared to Francis turbine. Since deflector is used in each nozzle can deflect a jet in a moment from the runner through its rapid closer [16]. Which includes my head ranges (50m) because range of pelton turbine most of the table shows above 100m and efficiency can be increased by increasing number of jets.

J. Veselý and M. Varner Stated in their **research Upgrading Of 62.5MW Pelton Turbine Paper Undergoing Research Strait Nozzle** .The commercial CFD software Fluent was used for the flow simulations through straight flow nozzle of rehabilitated turbine. CFD flow simulation through straight flow nozzle was realized as a two phase’s turbulent axisymmetric flow Efficiency of the nozzle depends on the nozzle and needle shapes and the needle opening. Numerical flow simulation (CFD) was applied for the straight flow nozzle hydraulic efficiency evaluation [12] .This paper are very useful for the current thesis in showing the clear procedure of the CFD even if no information of how the distributer is analyzed.

Deepak Bisen1, Prof. Sunil Shukla and Dr. P.K.Sharma on their research paper: "**Optimization and Simulation of Hydro-Turbine Nozzle in Based on Ansys Analysis**". They present Optimization and Simulation of hydro-turbine nozzle in based on Ansys analysis. Based on three-dimensional numerical flow analysis, the flow characteristics through the water turbine with nozzle are predicted. The Pressure and Velocity distribution of hydro-turbine nozzle at different points were calculated and analyzed for a Structural analysis and CFD analysis. The simulation results show that using nozzle can increase the pressure drop across the turbine and extract more power from available water energy. These results provide a fundamental understanding of the composite water turbine [10] .Even though the flow is in three dimension the basic principle of the pressure and velocity distribution are the same.

Reiner Mack, Bartlomiej Gola, Martin Smertnig, Bernhard Wittwer and Peter Meusburger on their research paper "**Modernization Of Vertical Pelton Turbines With The Help Of CFD And Model"** testing Fifteen years ago the hydraulic design of Pelton turbines was based on model tests only. The first step into the computer supported hydraulic design of Pelton runners was done by Kubota. The first application of CFD for Pelton turbines in an industrial environment was presented by Mack et al. and they mainly doing their research based on CFD to optimize pelton turbine components.one of their research area is distributer.Both distributor lines in the prototype are casted components as they were common during the time of their installation. Their hydraulic shape made use of acceleration bends without edges as they are typical for to days Tri-Cone welded solution. Since no modification was for seen for the hydraulic shape in the distributors and a reliable prediction with numerical methods was available, a standard distributor design was used for the model test and the influence of the individual designs was predicted with computational fluid dynamics [21]. From this paper the distributer needs high technology to manufacture and also there is high loss.

Muh. Anis Mustaghfirin, Akio Miyara, Azridjal Aziz and Fumiaki Sugino on their research paper about **Distributer Design , Geometry Analysis and Simulation** ; Uniformity of Two-phase Flow Distribution in Curved Round Distributor:- Distributor plays a major role on uniformly of the fluid flow distribution through multiple channels, particularly in two phase flow. Uniformity and low pressure drop are the major issue which shall be solved

Velocity contour of their research work is as follows.

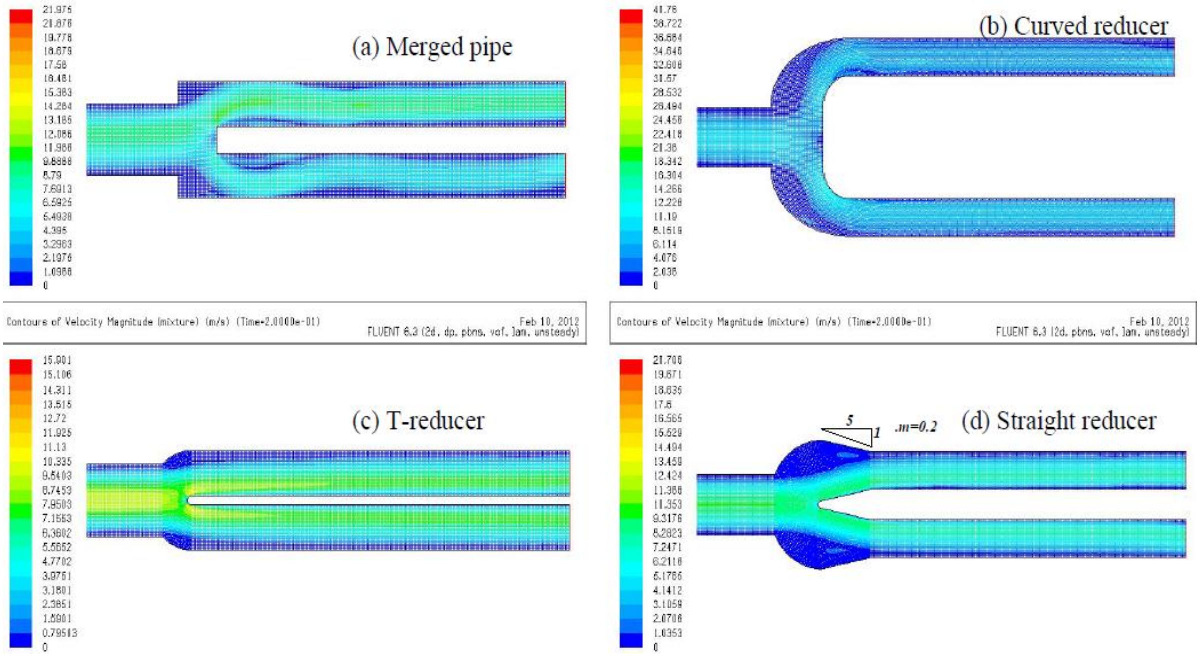

Fig 2.1 Velocity contour of distributer [25].

Even if these type of distributer uses for other purpose the bending of the bifurcation is not good in fluid flow mechanics. As can be seen from the figure the bending of the bifurcation is at 90 degree which creates much back flow and collision of fluid with the bending surface. And the velocity distribution also the same throughout the flow which is minimum velocity feeding for nozzles and as consequence less jet power will resulted [25].

Phoevos-Charalampos K. Koukouvinis on **Development of a Meshfree Particle Method for the Simulation of Steady and Unsteady Free Surface Flows**: application and validation of the method on impulse hydraulic turbines**.** In fluid mechanics, the numerical simulation is performed using as governing equations, relations which are established from conservation laws; such laws state that certain quantities, such as mass, momentum and energy must be conserved during the evolution of the described system. These governing equations are expressed as a system of non-linear, partial differential equations, which, through a number of numerical methods, are eventually transformed into a system of simple algebraic equations. The system of algebraic equations is then possible to be solved, in order to obtain a solution. The subject of Computational Fluid Dynamics (CFD) is the development of numerical methods which enable the solution of the mathematical model representing fluid flows. Through Numerical operations involving: Governing equations, Boundary and initial conditions, Domain discretization, Numerical discretization and Resulting algebraic equations. As computer computational power increases, more and more refined and advanced methods and computational models are developed in order to describe and solve complicated flow fields and flow patterns. Today CFD has become an integral part in the design process of products, devices, machines or vehicles where fluid flow phenomena play an important factor on the performance. Optimization studies are commonplace in industries, where thousands of virtual designs are evaluated using CFD in order to improve desired characteristics [24].

The main components which the review focused is on nozzle and distributer.Most of the research which is done on nozzle and spear indicate that their efficiency is below 90%. As most of the researches indicates the efficiency of the nozzle and distributer did not exceed 90% this research is aimed at optimizing the performance and efficiency of the nozzle and distributer above 90 %.

In the review some of the researches reviewed were used as best reference for the current research while the other is less useful.

CHAPTER THREE

DESIGN OF NOZZLE AND DISTRIBUTER

This chapter contains basic equation, mathematical formulation and contains the main work of the analytical design of the thesis which involves the design and analysis of nozzle and distributer. The detail design starts from design of penstock, distributor, nozzle, and spear explicitly. The design of the nozzle and distributer basically depends on the derived equations.

The equations includes head loss in penstock, nozzle and distributer and the basic equation such as velocity, flow rate ,efficiency and the dynamic and static pressure will be clearly equated here. The coefficients like velocity, discharge and contraction coffient will be derived. To summarize, this section discusses basic turbine theory, nozzle and distributer design, including defining a series of concepts, terms and variables that are used in turbine components such as penstock, distributer, and nozzle evaluation and design.

3.1 THE CONCEPT OF HEAD AND FLOW RATE

Head and flow rate are the two most important things in hydraulic turbine. Head is a water pressure which is created by the difference in elevation between the water intake and the turbine

Flow is a water quantity and is expressed as a volume per second or minute .Both head and flow rate must be present to produce power

In a potential Micro hydropower site, head is the vertical distance of waterfall. When evaluating a potential site, head is usually measured in feet, meters, or units of pressure. Head also is a function of the characteristics of the channel or pipe through which it flows; you can use your site's head calculation along with its flow calculation to determine the site's potential power output. When determining head, you need to consider both gross head and net head. Gross head is the vertical distance between the top of the penstock that conveys the water under pressure to the point where the water discharges from the turbine.

3.2. HEAD LOSS IN PIPES

Hydro power is obtained from the potential and kinetic energy of water flowing from a height. The energy contained in the water is converted into electricity by using a turbine coupled to a generator.

Net head is the gross head minus the head losses that occur when water flows from the intake to the turbines through canals and penstock. Water loses energy (head loss) as it flows through a pipe, fundamentally due to the friction against the pipe wall depends on the wall material roughness and the velocity head. The friction in the pipe walls can be reduced by increasing the pipe diameter. However, increasing the diameter increases the cost, so a compromise should be reached between the cost and diameter.

Water flowing through a pipe system with bends, sudden contractions and enlargement of pipes, racks, valves and other accessories experiences losses in addition to the friction loss, a loss due to inner viscosity. This loss depends on the velocity. The loss of head produced by water flowing through an open valve depends on the type of the valve.

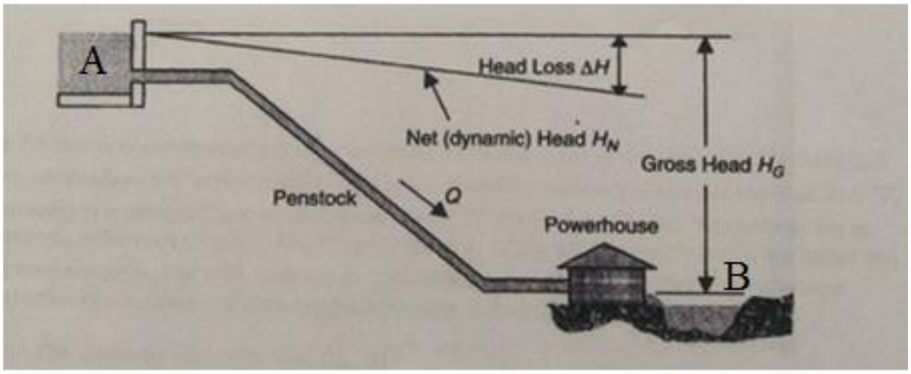

Fig.3.1. Components of impuls turbine [20].

Note: H the potential head can be obtained using Bernoulli's equation to analyze the fluid flow from point A to point B as in fig.3.1. Using the Euler's equation to obtain Bernoulli's equation by integrating along a streamline for steady, incompressible, frictionless flow which gives to Eq.3.1

$$H = \frac{P}{g\rho} + \frac{v^2}{2} + Z \qquad 3.1$$

Where; $\frac{P}{g\rho}$ = the head due to local static pressure,

$\frac{v^2}{2}$ = the head due to local dynamic pressure,

Z = the elevation head,

H = the potential head of the site.

From eqn. 3.1

$$H = \frac{P_A}{g\rho} + \frac{{v_A}^2}{2} + Z_A = \frac{P_B}{g\rho} + \frac{{v_B}^2}{2} + Z_B \qquad 3.2$$

At the surface of the river bed, the fluid moves very slowly compared to the flow along the pipe. We say that $V_A = 0$, also the pressure is atmospheric pressure, $P_A = 0$.

At the exit of the nozzle the static pressure is atmospheric. i.e. $P_B = 0$

Substation of the values in equation 3.2 and taking in to account the total head loss in between A to B gives the following equation

$$Z_A - Z_B - H_L = \frac{{v_j}^2}{2} \quad 3.3$$

Where

$H_L = head\ loss\ encountered\ fron\ point\ of\ inlet\ of\ penstock\ to\ the\ exit\ of\ nozzle.$

$Z_A - Z_B$ Is the elevation of the river bed and the turbine?

3.3 NOZZLE PARAMETRES DERIVTION

It is assumed that the Head H_n is the net head behind the nozzle, and that all pipeline and valve losses have been accounted for elsewhere. There are, of course, losses in the nozzle itself, and the actual velocity of discharge will be less than the theoretical value. This is catered for by the use of Coefficient of Velocity(C_v), Coefficient of Contraction(C_c), and Coefficient of Discharge(C_D).The purpose of these coefficients are as follows [32].

$C_{V:}$:- is a parameter which tell us how the actual velocity of the flow deviate from the theoretical velocity.

$C_{D:}$ - is a nozzle design parameter which determines the effective area of the fluid region for fluid flow along the longitudinal axis of the flow.

C_C :-s a parameter which tell us how the jet diameter is deviated from the nozzle exit diameter

Coefficients are Coefficient of velocity is defined by the equation:

$$C_V = \frac{actual\ velocity}{theoretical\ velocity} \quad 3.4$$

Actually the coefficient of discharge is a nozzle design parameter which determines the effective area of the fluid region for fluid flow along the longitudinal axis of the flow.

$$C_D = \frac{\text{actual flow rate}}{\text{theoretical flow rate}} = \frac{Q}{A_o\sqrt{2gH_n}} \quad 3.5$$

$Where\ A_o - area\ of\ flow$

As it can be seen from fig 3.2 the triangular shape of the spear tip which is drawn in bold line is to determine area of flow and the closing distance which is illustrated as follows.

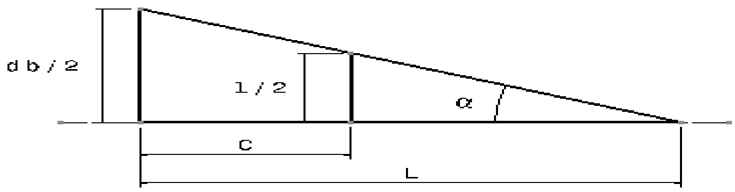

Fig 3.2 Half cross section of spear to determine closing distance.

$A_o = \frac{\pi}{4}({d_b}^2 - l^2), using\ simple\ mathematical\ model\ where$

$$l^2 = \left(\left[(2\tan\alpha)\left(\frac{0.068}{2\tan\alpha} - C\right)\right]^2\right) \quad 3.6$$

Closing distance is the longitudinal space available between the nozzle exit and the spear where a flow is allowed to let out the system. As the closing distance decreases area of flow reduces, and closing distance increases area of flow increases.so the area of flow depends on the closing distance as it can be seen in the following figure

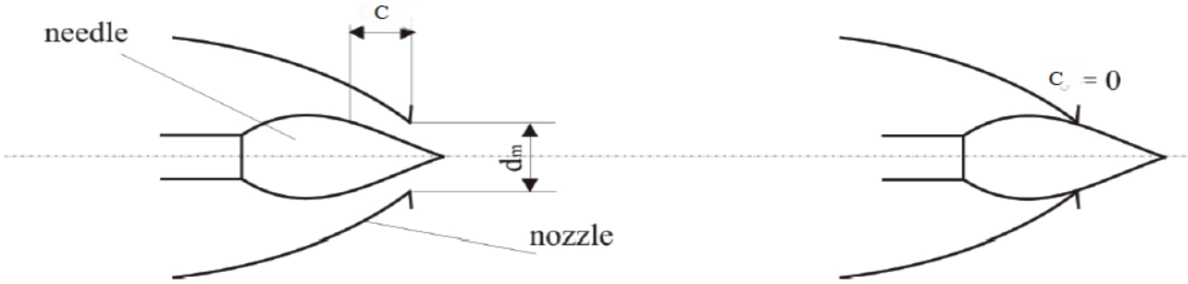

Fig 3.3 Closing distance variation[14]

$Where\ d_b - the\ diameter\ of\ the\ nozzle\ exit$

$\mathrm{l} -$ the diameter of the spear tip at closing distance of C

$$C_C = \frac{actual\ cross - sectional\ area}{geometrical\ cross - sectional\ arae} = \frac{(d_j)^2}{{d_b}^2} \quad 3.7$$

Where $\mathrm{d_b}$ – the diameter of the nozzle exit

$d_j - diameter\ of\ jet$

C_C can be calculated by equation 3.8 if the discharge and velocity coefficients are known

$$C_C = \frac{C_D}{C_v} \qquad 3.8$$

Jet diameter is therefore determined by:

$$d_{jet} = C_c \times d_{exit} \qquad 3.9$$

The coefficient of pressure accounts for pressure drop in the nozzle which is calculated from this equation:

$$C_p = \frac{(P - P_o)}{\frac{1}{2}\rho {V_o}^2} \qquad 3.10$$

Where P-static pressure at the point of interest, P_o-free stream static pressure

V_o-free-stream velocity (nozzle exit)y, ρ-free stream density

For incompressible flow along the axial direction of the nozzle axis, the Bernoulli equation is:

$$P + \frac{1}{2}\rho V^2 = P_o + \frac{1}{2}\rho {V_o}^2 \qquad 3.11$$

This equation is general (energy equation at exit and inlet of nozzle) because it is true for ideal case but V_O at the nozzle exit is vary in actual case when it simulated at different nozzle spear arrangement.

Where V − the velocity at the point of interest(nozzle inlet).

Rearranging the terms for $P-P_o$ interms of the rest terms gives

$$\mathrm{P} - \mathrm{P_o} = \frac{1}{2}\rho_o(\mathrm{V}^2 - {\mathrm{V_0}}^2) \qquad 3.12$$

Substitution into the coefficient of pressure formula gives:

$$C_p = 1 - \left(\frac{V}{V_o}\right)^2 \qquad 3.13$$

The velocity V at the inlet of the nozzle is calculated from the velocity head which is theoretical value or without loss and V_O is determine from actual analysis due to friction and other losses under CFD simulation.

3.3.1 HEAD LOSS IN THE NOZZLE

Nozzle is a device which converts the total head available at the nozzle inlet into velocity head. This conversion incorporates velocity coefficient for head loss [32]. The square of the velocity coefficient is determined by:

$$C_V{}^2 = \frac{velocity\ head\ after\ the\ nozzle}{total\ available\ head\ behind\ nozzle} = \frac{\left(\frac{V_{actual}{}^2}{2g}\right)}{H_n} \qquad 3.14$$

Head behind the Nozzle = Head after the nozzle + Head loss in Nozzle. Therefore the head loss is calculated by:

$$H_l = \left(H_n - \frac{V_{actual}{}^2}{2g}\right) \qquad 3.15$$

Rearranging the terms for H_l and substitution of equation gives:

$$H_l = H_n(1 - C_V{}^2) \qquad 3.16$$

Where C_V=the Coefficient of velocity of the flow jet, determined by actual velocity which

decided from the CFD result .

Head loss coefficient is a factor which accounts for a head loss out of the total head which is determined by this formula:

$$C_l = \frac{H_l}{H_n} = \frac{H_n(1 - C_v{}^2)}{H_n} = (1 - C_v{}^2) \qquad 3.17$$

3.3.2 EFFICIENCY AND NET POWER OUTPUT OF THE NOZZLE

Hydraulic efficiency of nozzle is a measure of how much hydraulic energy is converted to kinetic energy [29].

$$\eta_{nozzle} = \frac{\frac{1}{2g}V_{actual}{}^2}{head\ beahind\ nozzle} = \frac{1}{2gH_n}V_{actual}{}^2 = \frac{(C_V\sqrt{2gH_n})^2}{2gH_n} = C_V{}^2 \qquad 3.18$$

The theoretical velocity (neglecting losses in the nozzle) at the nozzle exit is calculated by:

$$V_{theo} = \sqrt{2gH_n} \qquad 3.19$$

The power of the jet is dependent upon the flow rate of the water and the specific energy (K.E) in the jet .Thus the power of the jet per a single nozzle is determined by

$$P = \rho Q g h = \rho Q \frac{V_{actual}^2}{2} \qquad 3.20$$

Where $H_j - head\ available\ at\ the\ jet(Actual = \frac{V^2}{2g})$

3.4 HYDRAULIC DIAMETER

The hydraulic diameter is the wetted diameter of the flow cross-section.

The hydraulic diameter for fluid flowing through any cross-sectional area is calculated by the formula:

$$D_H = \frac{4XA}{P} \qquad 3.21$$

$Where\ A = Wetted\ crossectional\ area\ of\ the\ fluid\ ,\ P = wetted\ perimeter$

$$D_H = \frac{4XA}{P} = 4 \times \frac{\frac{\pi}{4}\left({D_o}^2 - {D_i}^2\right)}{\pi(D_0 + D_i)} = D_0 - D_i \qquad 3.22$$

$Where\ D_0 - outer\ diameter\ of\ the\ wetted\ area\ of\ the\ nozzle$

$D_i - inner\ diameter\ of\ the\ wetted\ area$ Of the spear

3.5 HYDROSTATIC, HYDRODYNAMIC AND TOTAL PRESSURE

Let us consider a fluid flowing through a pipe of varying cross sectional area. Considering two points A and B as shown in Figure, such that A and B are at a height Z_A and Z_B respectively from the datum.

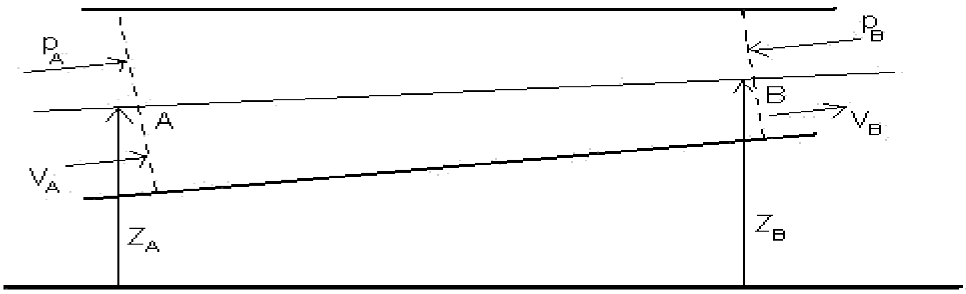

Fig 3.4 Datum lines for hydro-static and hydro-dynamic pressure[internet]

If we consider the fluid to be stationary, then,$(\partial P/\partial z)_{hs} = -\rho g$ where the subscript 'h_s' represents the hydrostatic case. So

$$P_{A,hs} + Z_A \rho g = \rho g(Z_B) + P_{B,hs}, \qquad 3.23$$

$$P_{A,hs} - P_{B,hs} = \rho g(Z_B - Z_A) \qquad 3.24$$

Where $p_{A,hs}$ is the hydrostatic pressure at A and $p_{B,hs}$ is the hydrostatic pressure at B.Ths., from above we can conclude that the Hydrostatic pressure at a point in a fluid is the pressure acting at the point when the fluid is at rest or pressure at the point due to weight of the fluid above it.

Now if we consider the fluid to be moving, the pressure at a point can be written as a sum of two components, Hydrodynamic and Hydrostatic.

$$P_A = P_{A,hs} + P_{A,hd} \qquad 3.25$$

Using the above equation in Bernoulli's equation between points A and B.

$$P_{A,hd} - P_{B,hd} = \frac{V_B{}^2 - V_A{}^2}{2g} \qquad 3.26$$

The above equations convey the following. The pressure at a location has both hydrostatic and hydrodynamic components. The difference in kinetic energy arises due to hydrodynamic components only. In a frictionless flow, the sum of flow work due to hydrodynamic pressure and the kinetic energy is conserved. Such conservation shall apply to the entire flow field if the flow is irrotational. The hydrostatic component is often called static pressure and the velocity term, dynamic pressure. The sum of two, P_0 is known as total pressure. This is conserved in isentropic, irrotational flow.

3.6 HEAD LOSS IN DISTRIBUTER

The key question in analyzing different type of manifolds/ distributer is the uniformity of the flow distribution and the pressure drop. The uniformity of the flow is disturbed due to the split angle of the bifurcation and the bendings. It can be possible to reduce the disturbance due to bending by increasing the radius. And also as the split angle gets low the non-uniformity of the flow decreases. Incorporating head losses in the distributer and neglecting the elevation difference, the Bernoulli equation will be:

$$\frac{P_{in}}{\rho g} + \frac{1}{2g} V_{in}{}^2 = \frac{P_{exit}}{\rho g} + \frac{1}{2g} V_{exit}{}^2 + H_d \qquad 3.27$$

$Rearranging\ for\ H_d$ gives:

$$H_d = \frac{(P_{in} - P_{exit})}{\rho g} + \frac{1}{2g}\left(V_{in}{}^2 - V_{exit}{}^2\right) \qquad 3.28$$

Where $H_d - head\ loss\ in\ the\ distributer$

3.7 GIVEN DATA:

The following data was taken from the PHD Candidate microhydro pelton turbine reaserch at Addis Abeba institute of thechnology by Tilahun Nigussie.

- Total flow rate $(Q_o) = 0.14\frac{m^3}{s}$
- Gross head, $H_g = 50\text{m}$
- Jet diameter $(d_j) = 54.4\text{mm}$ which is basic for the nozzle design
- $\text{LP(Penstock length)} = 60\text{m}$
- Number of jets (N_j) =2

3.8 PENSTOCK DESIGN.

The penstock is the piping that brings the water from the river or stream to the point where it begins to be directed to the turbine. Penstocks (pipes) are used to conveying water from the intake to the power house. They can be installed over or under the ground, depending on factors such as the nature of the ground itself, the penstock materials, the ambient temperature and the environmental requirements [18]. The internal penstock diameter (Dp) can be estimated from the flow rate, pipe length and gross head.

3.8.1 SELECTION OF MATERIAL FOR PENSTOCK.

The factors to be considered while deciding upon the material to be used for a particular penstock are Availability, Surface roughness, Design life and maintenance, Method of jointing and Relative cost [28].

3.8.2 COMPARISON OF DIFFERENT MATERIALS

i) Steel and cast iron pipe are widely used in hydropower design and is preferable for very high head plants that allow a long service life. Expansion joints should be provided at certain intervals, depending on local climatic conditions;

ii) Pre stressed concrete pipe presents a reduce cost but greater difficulty in installation;

iii) Plastic and glass fiber-reinforced plastic pipe induces small friction loss, but must be buried or wrapped to protect it from sunlight effect;

iv) Reinforced concrete pipe, should sewage pipe producers exist and it has a long service life, little maintenance, low cost, but high difficulty in installation and resistance problems. Mild steel, uPVC and HDPE are the most common used materials. Steel material is chosen for its availability, strength and durability characteristics.See penstock material on appendix on table 3.1.

3.8.2 CONCEPTS ON PENSTOCK DESIGN

Penstock is a significant component of the MHPT scheme and needs to be designed and selected carefully as it represents a major expense in the total budget.

Here the main aspects to consider are head loss and capital cost. Head loss due to friction in the pipe decreases dramatically with increasing pipe diameter. Conversely, pipe costs increase steeply with diameter. Therefore a compromise between cost and performance is considered for design and selection of pipe diameter and material. While designing penstocks, the first principle is to identify available pipe options and then to decided upon acceptable head loss (5% of the gross head is generally considered) [18, 36].

As the PHD candidate recommended it has been selected steel material due to its durability, with stand water hammer effect,low periodic maintainance and it does not require additional masonry work.

3.8.2 ECONOMIC DIAMETER

In penstock design one of major factor is determining the diamter pipe line because of its cost and loss.The economic diameter is obtained considering the incremental energy benefits from a lower energy loss associated to a larger diameter, as well as stability of operational conditions(i.e. water hammer and wear) with the total investment cost increase.Nevertheless, emperical formulations are recommended to economic diameter estimation for small hydropower plants by several authors, on the basis of data from existing penstocks[36].

$$D_P = Cec \times Cmp \times {Q_0}^{0.43} Ho^{-0.24} \qquad 3.29$$

$Where\ D_P =\ optimum\ diameter\ or\ economic\ diameter\ (m)$

$Cec = Coefficient\ of\ energy\ cost\ (zones\ where\ the\ energy\ cost\ is\ low\ =\ 1.2,$

$medium\ = 1.3\ and\ high\ or\ no\ alternative\ source\ = 1.4;$

$Cmp =\ coefficient\ for\ the\ pipe\ materials\ (for\ steel\ = 1;\ or\ plastic\ = 0.9);$

$Ho = net\ head\ at\ the\ exit\ of\ penstock(m);$

$Q_0 = design\ discharge\ (m\hat{}3/s)$

$For\ steel\ penstock\ material:$

$Cec = 1.4, Cmp = 1,$

The net head available in the penstock is calculated by:

$$H_o = H_g - H_p \tag{3.30}$$

$Where\ H_g = gross\ head\ and\ H_p = head\ loss\ in\ penstock$

$To\ determine\ the\ penstock\ diameter\ first\ assume\ \ 5\%\ of\ \ the\ pipe\ loss\ of\ the\ gross\ head$

$which\ is\ the\ reference\ to\ determine\ minor\ and\ frictional\ loss\ in\ the\ pipe\ separately.$

$$H_o = H_g - H_p = 50 - 50 \times 0.05 = 47.5m$$

$$D_P = Cec \times Cmp \times {Q_0}^{0.43} Ho^{-0.24} = 1.4 \times 1 \times (0.14)^{0.43} (47.5)^{-0.24} = 238mm$$

3.8.3 MINIMUM THICKNESS OF STEEL PIPE

The pipe minimum thickness corresponds the pipe failure due to atmospheric pressure by the occurance of vacuum.

For this situation, when a long pipe is forced by an external pressure p_2 greater than internal pressure p_1, creates a differential critical pressure Δp_{cr} that can be obtained by the following equation [36].

$$\nabla p_{cr} = (p_2 - p_1)cr = \frac{2E}{1 - V^2} (t|D)^3 \tag{3.32}$$

The steel elasticity modulus (E = 2.06x10^{11} N/m2), ν the steel Poisson coefficient (ν= 0.3), t the pipe thickness and D_P the pipe diameter. By substitution of the former values on equation 3.32, yields the following result

$$\nabla p_{cr} = 4.55X10^{11} (t|D)^3 \tag{3.33}$$

According to European Convention for ConstructionalSteelwork (ECCS) in order to take into account eventual geometric imperfections, it is proposed the following relation

$$p_{atm} = \frac{7.35}{F} \nabla p_{cr} \tag{3.34}$$

where P_{atm} is the atmospheric (p_{atm}= 1.013x10^{5}N/m^2) and F a safety factor (e.g. F =2.5).

Based on the above equation subtituting ∇p_{cr} and p_{atm} gives that the minimum steel thickness

$$\frac{t}{D} \geq 4.23X10^{-3} \tag{3.35}$$

Substituting for $D = 237mm$ gives the value of thickness $t \geq 1.031mm$.For this design standard pipe with nominal diameter of 10 inch (250mm), outside diameter 10.75 inch or

(273mm), 266mm internal diameter and 3.40mm thickness and having specific weight of 22.61Kg/m is selected as per ASTM metric standard as shown in appendix C

3.8.4 DESIGNING THE PENSTOCK FOR WATER HAMMER EFFECT

Sudden changes in the velocity of water in a pipeline results in pressure transients that develop along the length of the pipeline, a phenomenon known as water hammer [14, 36].

In hydro power systems, water hammer is usually caused by sudden opening or closure of valves at the bottom of the pipeline, by changes in turbine operation and by pipe bursting.

Several measures exist that can be incorporated to reduce the risk of water hammer in a Pipeline. These include: Increasing the diameter of the pipeline, Ensuring longer opening and closing time of valves at the bottom of the pipeline and Installation of a bypass line around the turbine.

$$Hs = Vw * {}^{\Delta V}/_{g} \ (m) \qquad 3.36$$

$$Vw = \sqrt{\frac{1}{\rho * \left(\frac{1}{E_W} + \frac{Dp}{E * t}\right)}} \ (m.s^{-1}) \qquad 3.37$$

$$\Delta V = \frac{Q}{N_j \times Ap} (m.s^{-1}) \qquad 3.38$$

$$Where\ E_W = Bulk\ water\ modulus = 2.1 \times 10^9 \frac{N}{m^2} \quad and$$

$$E = Modulus\ of\ penstock\ material\ (for\ steel = 206 \times 10^9 \frac{N}{m^2})$$

$$N_j = number\ of\ jet = 2$$

$$Ap = \ area\ of\ the\ penstock = \frac{\pi Dp \times t^2}{4} = \frac{\pi(266)^2}{4} = 55.6 \times 10^{-3} m^2$$

$$Water\ density, \rho = 998.2 Kg/m^3$$

$$Substituting\ each\ values:$$

$$Vw = \sqrt{\frac{1}{\rho \times \left(\frac{1}{Kwm} + \frac{Dpt}{Mp * tp}\right)}} = \sqrt{\frac{10^9}{998.2 \times \left(\frac{1}{2.1} + \frac{266}{206 * 3.4}\right)}} = 925.2 m/s$$

$$\Delta V = \frac{Q}{nj \times Ap} = \frac{0.14}{2 * 55.6 * 10^{-3}} = 1.26\frac{m}{s}$$

$$Hs = Vw * {}^{\Delta V}/_{g} = 925.2 * {}^{1.26}/_{9.81} = 118.8m$$

$The\ safety\ factor\ against\ surge\ pressure\ will\ be$:

$$S.F = \frac{t \times S_{sp}}{5 \times 10^3 \times Dp \times H_t}(> 2.5)$$

$Where\ t = effective\ thickness\ of\ penstock(m)$

$S_{sp} = tensile\ strength\ of\ penstock\ material\ (\ 400MPa)$

The total head including the surge is calculated by:

$$H_t = H_g + H_s = 50 + 118.8 = 168.8m$$

Checking safe condition for water hammer effect plus the gross head:

$$S.F = \frac{t \times S_{sp}}{5 \times 10^3 \times Dpt \times H_t} = \frac{3.4mm \times 400 \times 10^6}{5 \times 1000 \times 266mm \times 168.8m} = 6(> 2.5)$$

Therefore the penstock is safe if water hammer effects is there.

3.8.5 HEAD LOSS IN PENSTOCK

The head losses in the pipeline are expressed as

$$Ht(total\ head) = Ho(net\ head) + hf + hm \qquad 3.39$$

Where hf is the frictional losses caused by wall shear that is distributed along the length of the pipeline and hm is the minor losses induced by a change in magnitude and/or direction of the velocity of the water in the pipeline [35]. These losses that are caused by valves, elbows and other fittings are commonly referred to as minor losses. Several methods do exist to determine the frictional losses that are induced by wall shear in the pipeline.

3.8.6 DETERMINATION OF FRICTION FACTOR IN PENSTOCK

Friction factor can be found in three ways:

- Graphical solution: Moody Diagram
- Implicit equations: Colebrook-white Equation

- Explicit equations: Swamee-Jain Equation

Method 1: Moody Diagram

In this paper the Moody diagram was used to estimate the frictional losses in the penstock.

It is clear that in order to use the Moody diagram we must be able to obtain values of surface roughness. These have been measured and tabulated (and sometimes Plotted) for an extensive range of materials used in piping systems [35]. Apendix D provides some representative values.

For commericial steel $\epsilon = 0.045\text{mm}$

Relative roughness, ϵ/D, becomes: $0.045/266 = 0.000169$

The Reynolds number is calculted with this formula:

$$\text{R}_\text{e} = \frac{\text{V} \times \text{D}_P}{\text{v}} \qquad 3.40$$

Where V is the velocity of the fluid, D_P is the cross − sectional diameter of the pipe,

$$\text{v} = \text{ kinematic viscosity} \left(= \frac{\mu}{\rho}\right) = 1.005\text{e} - 6\frac{\text{m}^2}{\text{s}}$$

$$\text{V} = \frac{\text{Q}}{\text{A}} = \frac{4\text{Q}_o}{\pi(\text{D}_P)^2} = \frac{4 * 0.14}{\pi(0.266)^2} = 2.52\frac{\text{m}}{\text{s}}$$

$$\text{R}_\text{e} = \frac{\text{V} * \text{D}_P}{\text{v}} = \frac{2.52\frac{\text{m}}{\text{s}} * 0.266\text{m}}{1.005\text{e} - 6\frac{\text{m}^2}{\text{s}}} = 7\text{e}5$$

Appendex E shows the flow conditions flow regime Vs Reynolds nomber. So for reynolds number 7e5 is that,the flow regime is turbulant.

$Reading\ the\ Moody\ chart\ for\ friction\ factor(f)\ at\ relative\ rougness\ 0.000169\ and$

$Re = 7e5\ would\ be\ 0.014$

Now we can calculate the frictional head loss:

$$h_f = f\frac{L * V^2}{D * 2g} \qquad 3.41$$

Where f-friction factor, L-the length of penstock, V-the velocity of the water, D-internal diameter of penstock.

$$h_f = f\frac{L * V^2}{D * 2g} = 0.014 * \frac{60 * (2.52)^2}{0.266 * 2 * 9.81} = 1.022m$$

The minor losses in the pipeline are calculated once the number of the different fittings that will be incorporated into the pipeline is known, since the loss coefficients that represent these components need to be known. The minor losses are calculated from:

$$Hm = \frac{8\sum K}{g}\left(\frac{Q}{\pi {D_{pt}}^2}\right)^2 \qquad 3.42$$

where K is the loss coefficient of each component in the pipeline. The loss coefficients of fittings are reffered to the following tables. K values .

Table 3.5 Different loss coefficient for penstock design [35].

		Main Pipeline	
Fitting	K-Value	Quantity	Total
Entrance	0.8	1	0.8
90^0 bend	0.19	3	0.57
45^0 bend	0.09	5	0.45
Sum of K-Values			1.82

$\sum K$ Value would be 1.82.

$$Hm = \frac{8\sum K}{g}\left(\frac{Q}{\pi {D_{pt}}^2}\right)^2 = \frac{8 * 1.82}{9.81}\left(\frac{0.14}{\pi(0.266)^2}\right)^2 = 0.6m$$

The total head loss in the penstock would be,$H_m + H_f = 0.6 + 1.022 = 1.62m$

Interms of percentage: $\frac{1.62}{50} X\ 100 = 3.24\%$

Total head loss in the penstock in percent is 3.24% which is an exllent design and acceptable

3.9 DISTRIBUTER DESIGN

Bifurcations and other complex pipe junctions frequently form an integral part of a hydro scheme. Distributers are pipes which parts the flow in to the nozzles.

The following table shows the tabulation of the five types of bifurcation

Table 3.6 Clarification of each distributer.

Bifurcation option	Parts of bifurcation Under option	Split angle (degree)	Bending radius(mm)	Length(m)
1	Inlet	Reference Frame		
	Outlet lower	0	300	3.3
	Outlet upper	30	300	3.3
2	Inlet	Reference Frame		
	Outlet lower	20	300	1.3
	Outlet upper	30	300	1.5
3	Inlet	Reference Frame		
	Outlet lower	30	200	0.9
	Outlet upper	40	200	1.0
4	Inlet	Reference Frame		
	Outlet lower	30	300	1.0
	Outlet upper	40	300	1.2
5	Inlet	Reference Frame		
	Outlet lower	30	300	2.0
	Outlet upper	40	300	1.7

Hydro-Works uses the modern method of internal reinforcing where it is appropriate, and computational fluid dynamic (CFD) analysis is used to ensure weather the flow is stable flow and low head losses[25,29]. So the design and analysis of the distributer is carried out by globally accepted software called Ansys .Basically the design of distributers depends on the manufacturing technology available to produce it. There are many types of consideration due to splitting angle, bending radius, distributer diameter in designing of distributer bifurcation but for the current design five types of consideration is used to simulate the distributer interms of manufacturing and jointing capabilities as shown in above table 3.6.

3.9.1 DESIGN THE GEOMETRY OF DISTRIBUTER USING CATIA V5.

The following figure is a simple layout which shows how the splitting angle and other consideration of the distributer parameter with its nozzle set are aligned with 400mm pitch diameter of runner . The distributer is drawn by catia V5 and tabulated in the above table 3.6 interms of split angle, bending radius, and length. The geometry analysis are calculated depending on the runner pitch diameter. The following figure shows the geometrical constraints at split angle of 70^0(the sum of the lower and upper splitting angle).

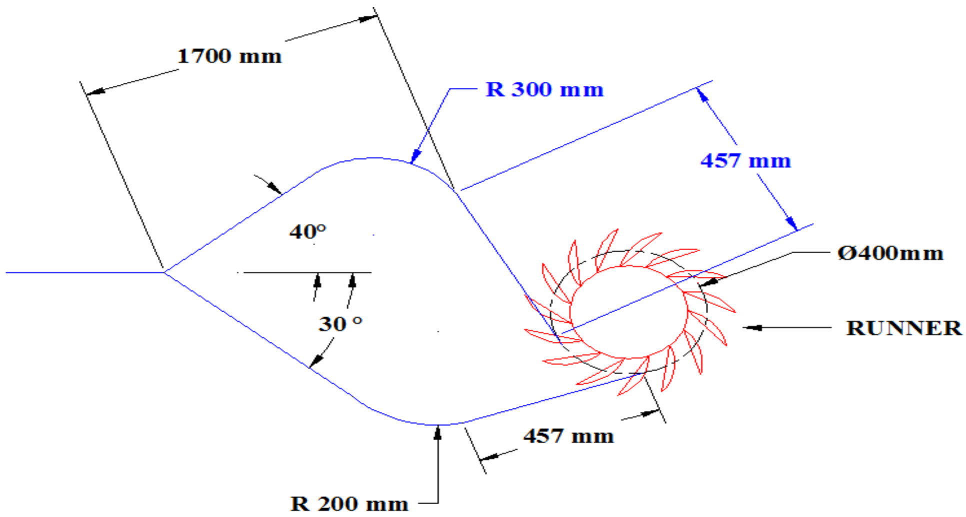

Fig 3.5 Distributer geometry with the runner diameter.

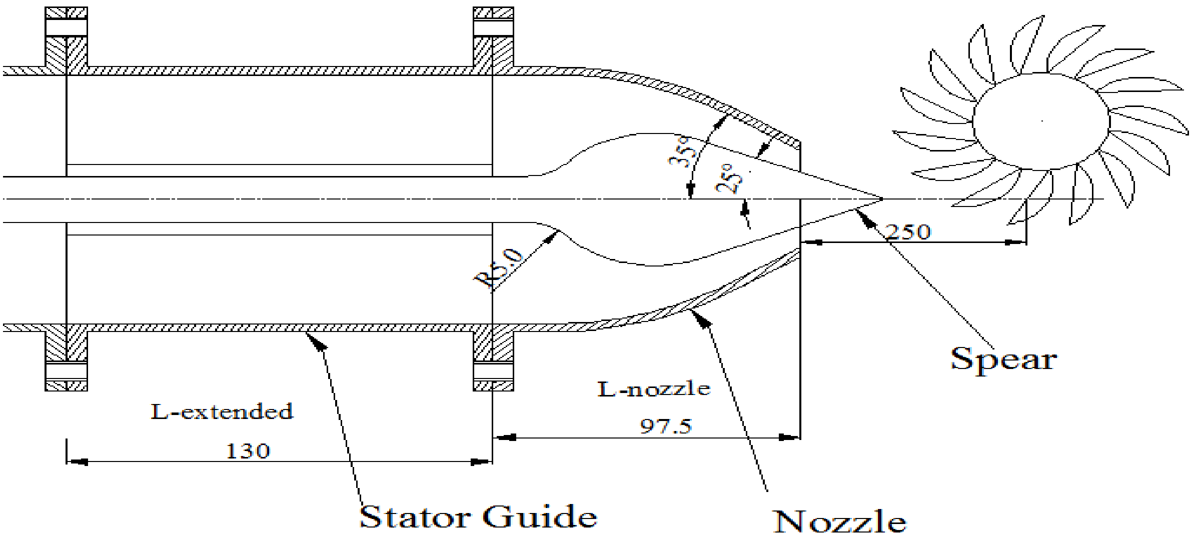

Fig 3.6 The nozzle length and its clearance between the runner and nozzle exit.

From figure 3.5 and 3.6 the exteded length(stator guide),the nozzle length and the clearance between nozzle exits and The distance between nozzle and bucket taking into account the minimum clearance between the nozzle and buckets was given as 250mm are taken from nozzle design which gives 457mm.

3.10 NOZZLE DESIGN

A nozzle is a gradually converging short tube which is fitted at the outlet of the distributor for the purpose of converting the total energy of the flowing water into kinetic energy. Nozzles are used where high velocities of flow are required to be developed [1, 2, and 10].

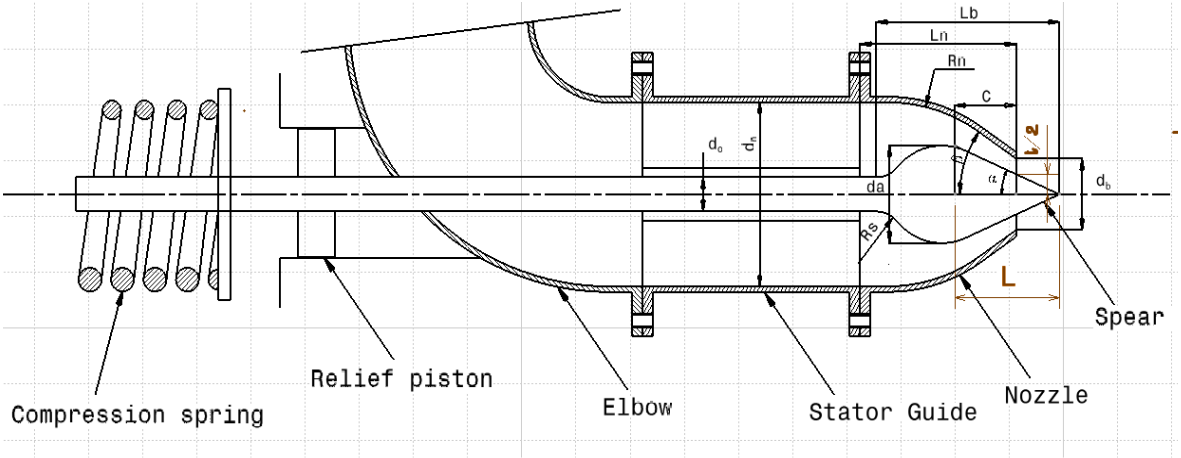

Fig 3.7 Nozzle –Spear alignment with the stator guide and distributer

In impulse turbines, it is required to convert whole of hydraulic energy into kinetic energy.

The flow regulating device are frequently used to control the mass flow rate, direction, and shape of the stream that emerges from them.

Velocity increases rapidly in the passage through the nozzle, and surface are exposed to the risk of wear. They can be severely eroded by abrasive matter in the water, resulting in a disturbed jet, loss of efficiency, and wear on the bucket.

Discharge is regulated by the spear moving axially. When the penstock and the nozzle are filled with water, forces act upon the nozzle with the tendency to move it out of position. Load changes can have the same effect. While the turbine is in operation vibrations occur, with an effect of moving the turbine from its position. These are reasons why the nozzles and the turbine must be fixed together and why the turbine must be rigidly fastened on its place [2, 3].

3.10.1 MATERIAL SELECTION FOR NOZZLE

Selection of material of nozzle is also the main property function in the efficiency of the nozzle design. The best material suited to work in corrosive environment is stainless steel, so we shall have discuss different types and properties of stainless steel. We mean steels alloyed with at least 12% chromium [7, 46].

Martensitic steels:-Martensitic steels have the highest strength but also the lowest corrosion resistance of the stainless steels.

Martensitic steels with high carbon contents may be regarded as tool steels. Owing to their high strength in combination with some corrosion resistance, martensitic steels are suitable for applications which subject the material to both corrosion and wear. An example is in *hydro-*

electric turbines. A martensitic-austenitic structure is obtained by increasing the nickel content slightly compared with the martensitic steels. These steels also often have a slightly lower carbon content. The range of applications is largely the same as for martensitic steels

Due to corrosion and wear resistance I have selected Martensitic steel (13Cr 4Ni stainless steel) for my MHPT design scheme.as shown in the following table.

Table 3.7 For Properties of 13Cr 4Ni stainless steel [7].

13Cr-4Ni Chemical composition(mass fraction) wt.%		
Chemical	Min.(%)	Max.(%)
C		0.05
Si	0.30	0.60
Mn	0.50	1.00
Cr	12.0	14.0
Ni	3.50	4.50
Mo	0.40	0.70
P		0.030
S		0.030

Table 3.8 Mechanical properties of 13Cr 4Ni stainless steel [7].

13Cr-4Ni Mechanical Properties		
Tensile strength	231-231	σb/MPa
Yield Strength	154	σ 0.2 ≥/MPa

3.10.2 GEOMETRY OF NOZZLE AND SPEAR.

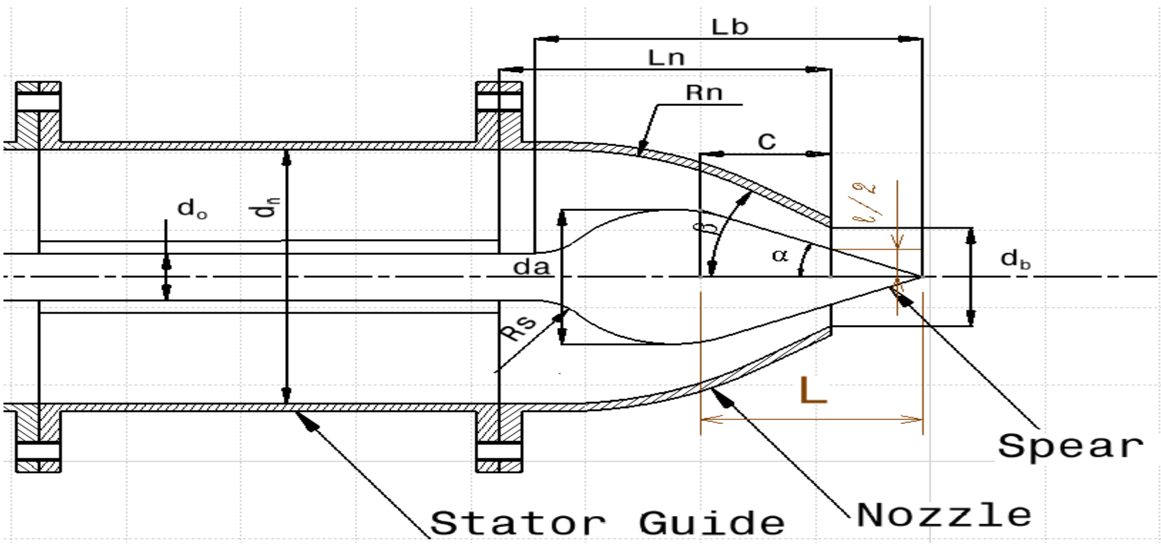

Fig 3.8 Nomenclature of spear and nozzle dimension.

$Where \quad Lb = spear\ tip\ length, \qquad da = bulb\ radius\ of\ curvature(spear\ height),$

$do = spear\ shaft\ diameter,$

$\beta = conical\ nozzle\ angle, \alpha = conical\ spear\ angle,$

$c = closing\ space(blocking\ distance\ )$

$db = orifice\ diameter(nozzle\ outlet\ diameter),$

$d = jet\ diameter, Rn = Nozzle\ radius\ of\ curvature\ , Rs = spear\ fillet\ radius,$

$dn = nozzle\ diameter$

When calculating the diameter of the nozzle it must be considered that the cross-sectional area of the jet will be smaller than the area of the nozzle exit opening by a contraction factor (coefficient of contraction).The jet contraction factor is in the range of 1.6 for holes with sharp edges, to 1.05 for nicely rounded edges [40].

If exit is sharp edge there is high contraction of jet which exit from the nozzle which need high manufacturing capability and if rounded edge the contraction factor is somehow less.

1. Nozzle exit diameter is calculated under consideration of contraction factor
Taking the contraction factor 1.25, the orifice diameter will be, $db = 1.25d = 1.25 \times 54.4mm = 68mm$

2. The bulb size is larger than the nozzle exit diameter by 20% to 30%. Take 25%, the bulb radius of curvature will be , $\mathrm{da} = 1.25 \times \mathrm{db} = 1.25 * 68\mathrm{mm} = 85\mathrm{mm}$[40]

3. The spear angle is in the range of 20° to 25°, so take α=25° [10].

4. The nozzle angle is in the range of 30° to 45°, so take β=35° [10].

5. To determine the blocking space (closing distance), C, we shall have to see the triangle needle tip. Where L is length of needle tip excluding the bulb part see fig 3.2

$$For\ l: \quad l = \frac{db}{2} = \frac{68}{2} = 34mm$$

Using mathematical modelling

The needle tip length will be, $L = l/\tan\alpha \ = 34/\tan(25°) = 72.9mm$

By similarity of triangles theorem, we have

$L/(L-c) = (db/2)/(l/2)\ rearranging\ the\ eqation\ interms\ of\ C\ it\ will\ be$

$$C = L\left(1 - \frac{l}{db}\right) = 72.9\left(1 - \frac{34}{68}\right) = 36.45mm$$

To be more safe take the value of blocking distance**(c)**$38mm$

6. Diameter of spear shaft, $d1 = 0.58\ times\ jet\ diameter, d1 = 0.58 \times 54.4 \cong 32mm.$

The spear shaft is around an half less than the jet diameter this is because of the spear fillet radius and spear bulb radius. The following parameters also determine in reference to the jet diameter [1, 2, and 40].

7. Length of needle tip, $\mathrm{Lb} = 3.17$ times jet diameter $\mathrm{Lb} = 3.17 \times 54.4 \cong 173\mathrm{mm}$

8. Curve of nozzle exit radius, $\mathrm{R} = 2.2$ times jet diameter, $\mathrm{R}_n = 2.2 \times 54.4 \cong 120\mathrm{mm}$

9. Nozzle internal diameter, $\mathrm{dn} = 3.125 \times$ jet diameter $= 3.125 \times 54.4 = 170\mathrm{mm}$

10. Spear fillet radius, $\mathrm{Rs} = 0.408 \times \mathrm{djet} = 0.408 * 54.4 = 22.5\mathrm{mm}$

11. The nozzle must be designed in such a way that the pressure loss is as small as possible and that thus the nozzle coefficient is increased. An increased velocity of the water means higher losses in pressure. That is why the part of the nozzle, in which the water has a high speed, has to be as short as possible. So Nozzle length can be calculated in terms of penstock diameter and jet diameter $\mathrm{Ln} = \frac{\mathrm{dp-d}}{\tan\beta}$

Where $\mathrm{dp} =$ penstock diameter and $\mathrm{d} =$ jet diameter

$\mathrm{Ln} = (266 - 54.4)/\tan 35 \cong 302\mathrm{mm}$

12. The nozzle exits have to be located as close to the Pelton runner as possible to prevent the jet from diverging the designed diameter. The distance between nozzle and bucket taking into account the minimum clearance between the nozzle and buckets was given as:

$\mathrm{X_{nb}} = 0.625 \times \mathrm{D_r} = 0.625 \times 400 = 250\mathrm{mm}$

The nozzle exits have to be located as close to the Pelton runner as possible to prevent the jet from diverging the designed diameter. The required distance was bigger than the calculated above, due to inconsistencies in the manufacture of buckets and the need to have a minimum distance of safety between the nozzle and Pelton runner [2]

CHAPTER FOUR

MODELING AND SIMMULATION OF NOZZLE AND DISTRIBUTER

This chapter contains the main work of the thesis which involves the modeling and simulation of nozzle and distributer. The modeling of the nozzle and distributer basically depends on the geometric values which is decided in chapter three using empirical and analytical formulas.

4.1 COMPUTATIONAL FLUID DYNAMICS (CFD) AND THE PROCEDURE USED TO ACCOMPLISH THE SIMULATION

Pelton turbines in the past have been leading to an achievement of the hydraulic efficiency of over 90 %. Further optimization and enhancement of turbine efficiencies through model tests, however, seem to be difficult to achieve, because the potential for further improvement cannot be accurately revealed, identified, and quantified, neither by flow visualization nor by measurements of the system efficiency. Because of the related high costs in the model tests and mainly because of the advanced achievements in both the analytical calculations and the numerical simulations based on computational fluid dynamics (CFD) [24].

The necessity of validation of CFD simulations has its background in the fact that the CFD simulations are based on the use of particular and different turbulence models in solving the Naiver-Stokes equations. So the computational results might first have to be validated.

Ansys fluent software is an engineering program which estimates the flow parameters based on Principles of fluid flow numerically.

- Principle of conservation of mass: it states that “Mass can neither be created nor destroyed”. Continuity equation has been derived on this principle.
- Principle of conservation of energy: it states that “Energy can neither be created nor destroyed”. On the basis of this Principles the energy equation is derived.
- Principle of conservation of momentum: it states that “the impulse of the resultant force, or the product of the force and time increment during which it acts is equal to change in momentum of the body. Momentum equation is derived in this basis.

Continuity equation:- The rate of increase of the fluid mass contained within the region must be equal to the difference between the rate at which the fluid mass enters the region and the rate at which the fluid mass leaves the region.

However, if the flow is steady, the rate of increase of fluid mass within the region is equal to zero, then the rate at which the fluid mass enters the region is equal to the rate at which the fluid mass leaves the region.

$$\frac{\partial \rho}{\partial t}+\frac{\partial(\rho V_X)}{\partial X}+\frac{\partial(\rho V_Y)}{\partial Y}+\frac{\partial(\rho V_Z)}{\partial Z}=0$$

Momentum equation:-According to Newton’s Second Law of motion, inertia force acting on a body in any direction is equal to resultants of all body and surface forces in that direction.

$$\frac{\partial V_X}{\partial t}+V_X\frac{\partial V_X}{\partial X}+V_Y\frac{\partial V_X}{\partial Y}+V_Z\frac{\partial V_X}{\partial Z}=F_X-\frac{1}{\rho}\frac{\partial P}{\partial X}+\frac{\mu}{\rho}\left(\frac{\partial^2 V_X}{\partial X^2}+\frac{\partial^2 V_X}{\partial Y^2}+\frac{\partial^2 V_X}{\partial Z^2}\right)$$

$$\frac{\partial V_Y}{\partial t}+V_X\frac{\partial V_Y}{\partial X}+V_Y\frac{\partial V_Y}{\partial Y}+V_Z\frac{\partial V_Y}{\partial Z}=F_Y-\frac{1}{\rho}\frac{\partial P}{\partial X}+\frac{\mu}{\rho}\left(\frac{\partial^2 V_Y}{\partial X^2}+\frac{\partial^2 V_Y}{\partial Y^2}+\frac{\partial^2 V_Y}{\partial Z^2}\right)$$

$$\frac{\partial V_Z}{\partial t}+V_X\frac{\partial V_Z}{\partial X}+V_Y\frac{\partial V_Z}{\partial Y}+V_Z\frac{\partial V_Z}{\partial Z}=F_Y-\frac{1}{\rho}\frac{\partial P}{\partial X}+\frac{\mu}{\rho}\left(\frac{\partial^2 V_Z}{\partial X^2}+\frac{\partial^2 V_Z}{\partial Y^2}+\frac{\partial^2 V_Z}{\partial Z^2}\right)$$

since these equation are difficult to solve analyticaly we must use numerical method of solving the problem using ansys software (fluent)

4.2 MODELLING OF THE DISTRIBUTER

The five types of distributer consideration are drawn by catia V5 and inserted to ANSYS 14, by using different design parameters’ like split angle, bending radius, and length the simulation will be done. The following model shows the geometrical constraints at split angle of 70^0.

The following procedure were used in the simulation of distributor

3D Modeling of the distributer:-The 3D model is prepared from the assembly of nozzle, spear, distributer and three junction elbow as one body using CATIA V5 and imported in to Ansys workbench design modeler software. It has been cleaned up split edges and faces for further use in meshing up to the software permits. The fluid body is symmetrical in the upper and lower bifurcation, here the geometry is split into two bodies which symmetry to each other. One symmetrical body is used and the other suppressed to save the time and computer RAM needed to run the mesh and solution.

The following figure shows tasks made in Ansys design modeler (DM)

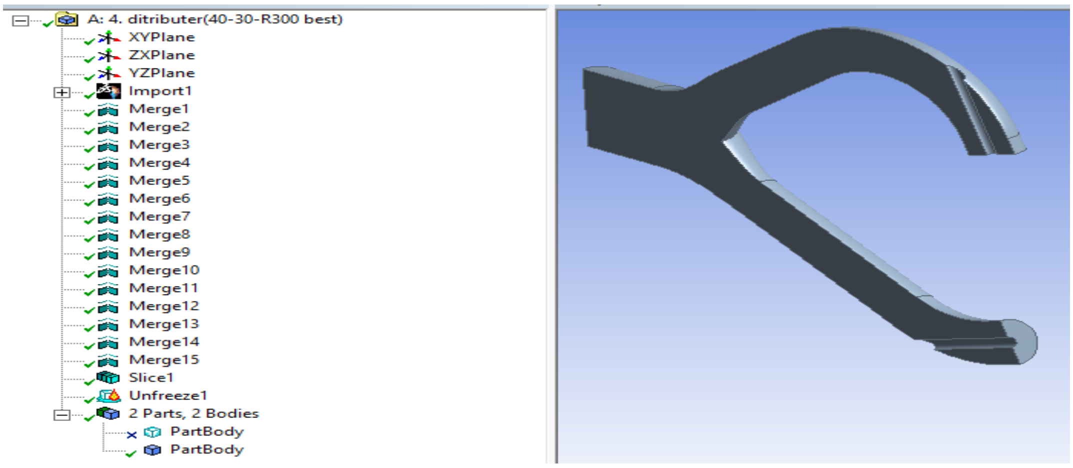

Fig 4.1 Geometry clean up and symmetry body operated in Ansys

Discretization (Meshing) of the fluid region:-Figure 4.1 shows the general setting used to discretize the fluid model for the analysis purpose. The method used here to discretize the fluid body is automatic. In Ansys language automatic means the combination of tetrahedral and sweep method. It finds sweep able body automatically discretizes and the rest becomes tetrahedral. In my case all meshes are tetrahedral and no sweep able body found in the fluid region since the fluid region is a single body.

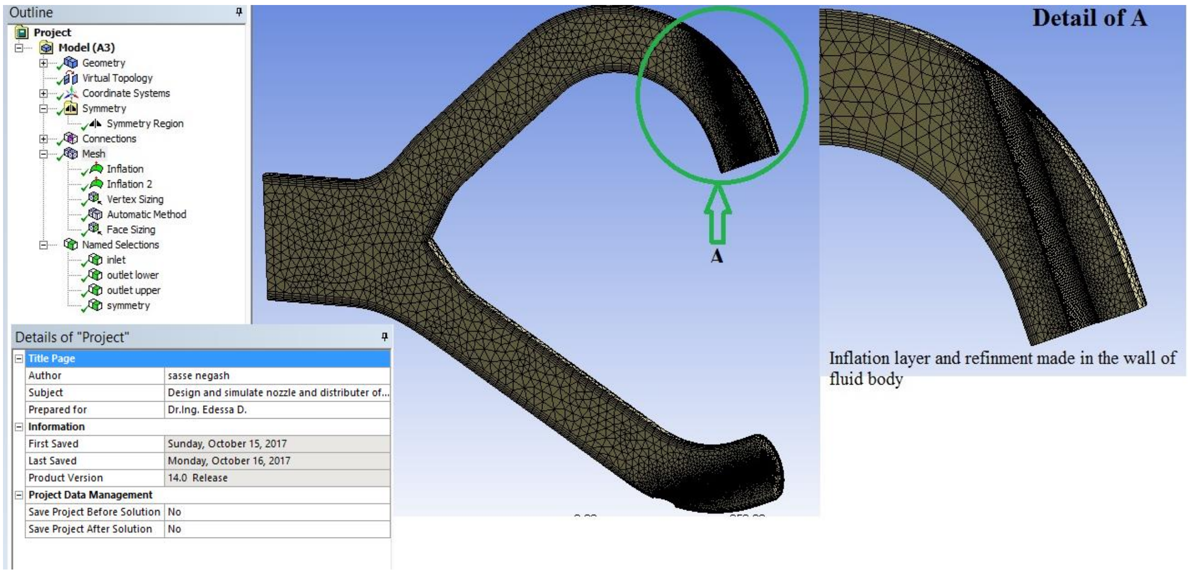

Fig4.2 3D Mesh model

Named selections are used here for easy selection in fluent solver pages for boundary values insertion. Patch conforming tetrahedral method uses edges and faces the first step to start meshing method and at last the volume.

In sizing control on curvature is used in advanced size function to refine only at curvature and bending zones to capture more cells for fluent solver since there are losses at that area more than the straight one. The mesh method is set to patch conforming to control and refine regions where small hole and pocket regions are available. As it can be seen from above figure spear wall fluid region is well captured by the method.

Grid Dependent Test for Distributer:-The quality of the mesh plays a significant role in the accuracy and stability of the numerical computation. The attributes associated with mesh quality are node point distribution, smoothness, and skewness. Regardless of the type of mesh used in a domain, checking the quality of the grid is essential. A good technique of limiting the mesh quality for a specific application like CFD is to see the result deviation as the mesh gets fine and good.

The following table shows the mesh quality improvement related to the results

Table 4.1 Grid dependent test table for the distributer

P197 - Mesh Max Face Size	P196 - Mesh Min Size	P198 - Mesh Max Size	P125 - V_in	P126 - V_lower	P127 - V_upper	P128 - static pressure in	P129 - static pressure lower	P130 - static pressure upper	P191 - Mesh Elements	P192 - Mesh Nodes	P194 - Mesh Max	P195 - Mesh Average
mm	mm	mm	m s^-1	m s^-1	m s^-1	Pa	Pa	Pa				
40	15	45	2.5548	4.5177	4.5948	4.7366E+05	4.6324E+05	4.6235E+05	24529	10131	0.99847	0.87667
30	5	35	2.536	4.6758	4.6796	4.7371E+05	4.6367E+05	4.6269E+05	1.2999E+05	37508	0.99944	0.87965
20	3	25	2.5244	4.6605	4.6635	4.7373E+05	4.6383E+05	4.6306E+05	2.3685E+05	68773	0.99965	0.88657
10	3	15	2.5193	4.6254	4.6423	4.7375E+05	4.6399E+05	4.6332E+05	3.8203E+05	1.1225E+05	0.99978	0.88887

Looking the velocity results interms of the mesh refinement it becomes insignificant as mesh size gets small. Here refining the mesh anymore is not important since the result is no more improving for this CFD application. Therefore, the mesh is verified! Low Orthogonal Quality or high skewness values are not recommended

4.2.1 FLUENT PROBLEM SETUP PAGES

General problem setup page:- Pressure based, absolute velocity formulation, and steady flow is set in general page.

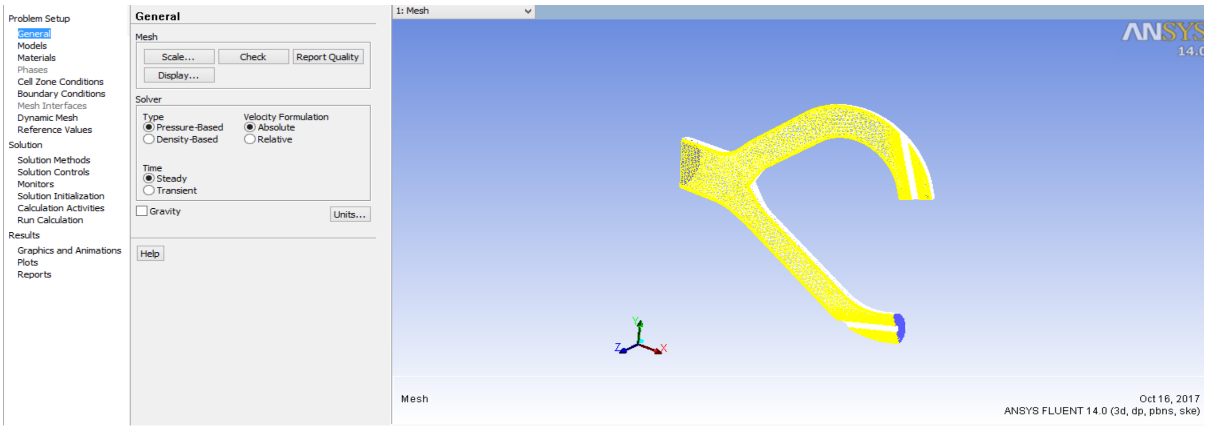

Fig 4.3 General problem set up page page

Model: standard K-e, standard wall function is used to model the turbulent fluid scheme.

Problem set up model:-Multiphase is off because only single phase is used i.e. water in liquid state. The energy also off since there is no heat transfer (heat exchange) or there is no matter considering temperature and Standard k epsilon wall function is used to model turbulent flow since the flow is under the viscous tab in the following set up figure.

In flow modeling page: only turbulent modeling is applicable for this flow equation. The Viscous tab lists different types of viscous modeling.

Reynolds no estimates the flow pattern whether the flow is turbulent or laminar.

$$R_e(\text{at the distributer inlet}) = \frac{V * d}{v} = \frac{2.5\,\frac{m}{s} * 0.226m}{1.005e-6\,\frac{m^2}{s}} = 5.65e5$$

$R_e(\text{at the distributer exit}) = \frac{V*d}{v} = \frac{4.92\frac{m}{s}*0.11m}{1.005e-6\frac{m^2}{s}} = 1.1e6$ at the appendix C From table 3.4 the flow is turbulent at the inlet and out let of the distributer

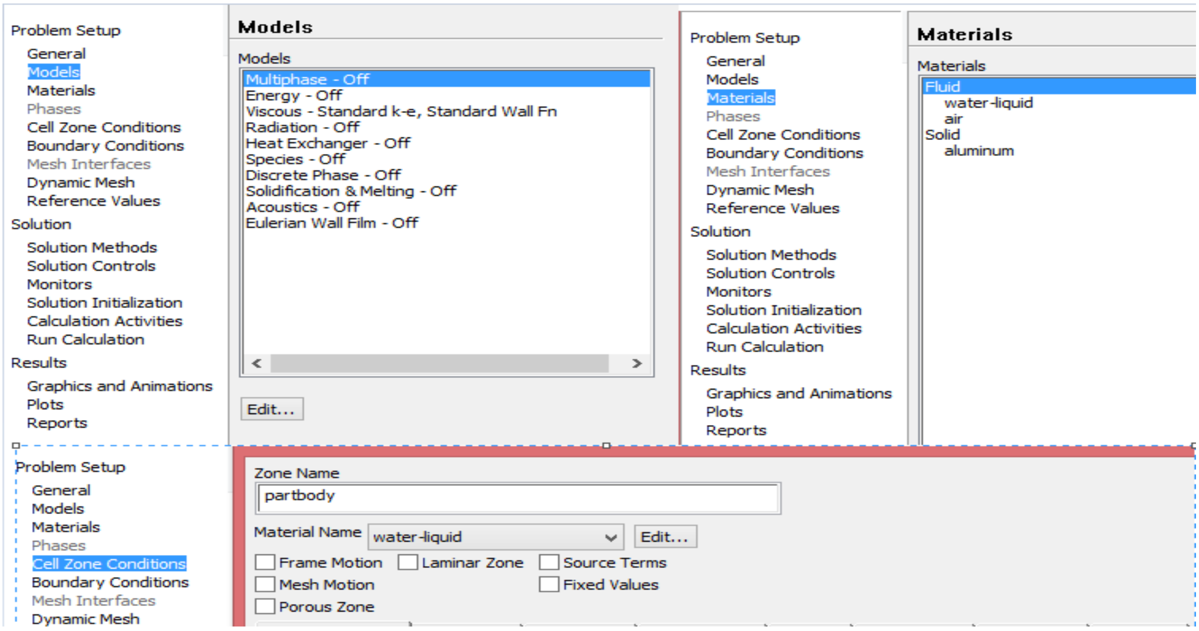

Fig 4.4 Problem set up general model and materials set up

Material:-water in liquid state is added to the list from Ansys fluent material library for later use in cell zone condition

Cell zone condition:-water is fluid for the analysis.

Boundary conditions:-there are one inlet, two outlet and symmetry boundary conditions as depicted in the following figure.

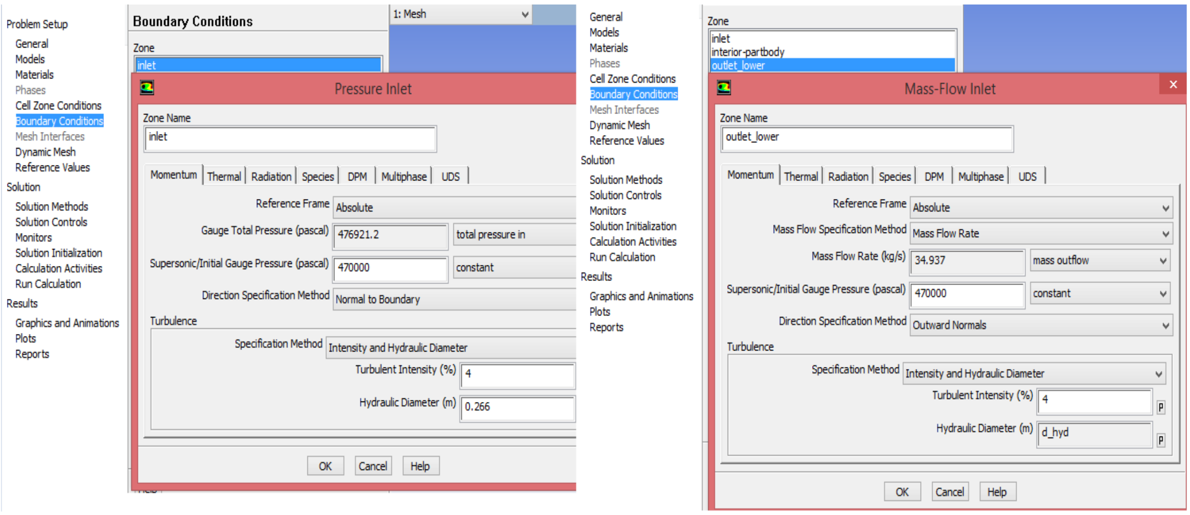

Fig 4.5 Problem set up inlet aand out let Boundary conditon

Inlet and exit of distributer: - at the inlet of the distributer the fluid has Hydraulic energy that it has obtained from the static head incorporating the loss available in the penstock.

Mass flow rate is taken at the exit of the distributer

$$Mass\ flow\ rate(exit) = \rho\frac{Q}{2} = 998.2 \times \frac{0.14}{2} = \frac{34.9\ Kg}{s}$$

And at the inlet the total gauge pressure or energy is feed to Ansys by adding the hydro dynamic and hydrostatic energy using equation 3.23

$$\mathrm{P_o} = \rho g H + \frac{1}{2}\rho\left(\frac{Q}{\mathrm{A_{pen}}}\right)^2 = 998.2 \times 9.81 \times 48.38 + \frac{1}{2} \times 998.2\left(\frac{0.07}{\pi \times \frac{0.266^2}{4}}\right)^2$$

$$= 476921.2\ \mathrm{Pa}$$

The turbulence intensity,I is defined as the ratio of the root-mean-square of the velocity fluctuations, u' to the mean flow velocity,u_{ave}.

For internal flows, the turbulence intensity at the inlets is totally dependent on the upstream history of the flow. If the flow upstream is under-developed and undisturbed, you can use a low turbulence intensity. If the flow is fully developed, the turbulence intensity may be as high as a few percent. The turbulence intensity at the core of a fully-developed duct flow can be estimated from the following formula derived from an empirical correlation for pipe flows:

$$I = \frac{u'}{u_{ave}} = 0.16(Re)^{-1/8}$$

$$I(Re = 5.65e5) = \frac{u'}{u_{ave}} = 0.16(5.56\ e5)^{-\frac{1}{8}} = 3\ \%\ (distributer\ inlet) and$$

$$I(Re = 1.1e6) = \frac{u'}{u_{ave}} = 0.16(1.1e6)^{-\frac{1}{8}} = 2.8\%(distributer\ exit)$$

Turbulence is set to intensity of 4% since there are factors like distributer bendings, elbows which increases the turbulence intensity.

Hydraulic diameter:$D_H = 266mm(distributer\ inlet)$

$D_H = 0.142 - 0.032 = 0.11m(distributer\ exit)$

Symmetry and wall:-symmetry and wall boundaries has been added to fully constrain the fluid model for the fluent solver.

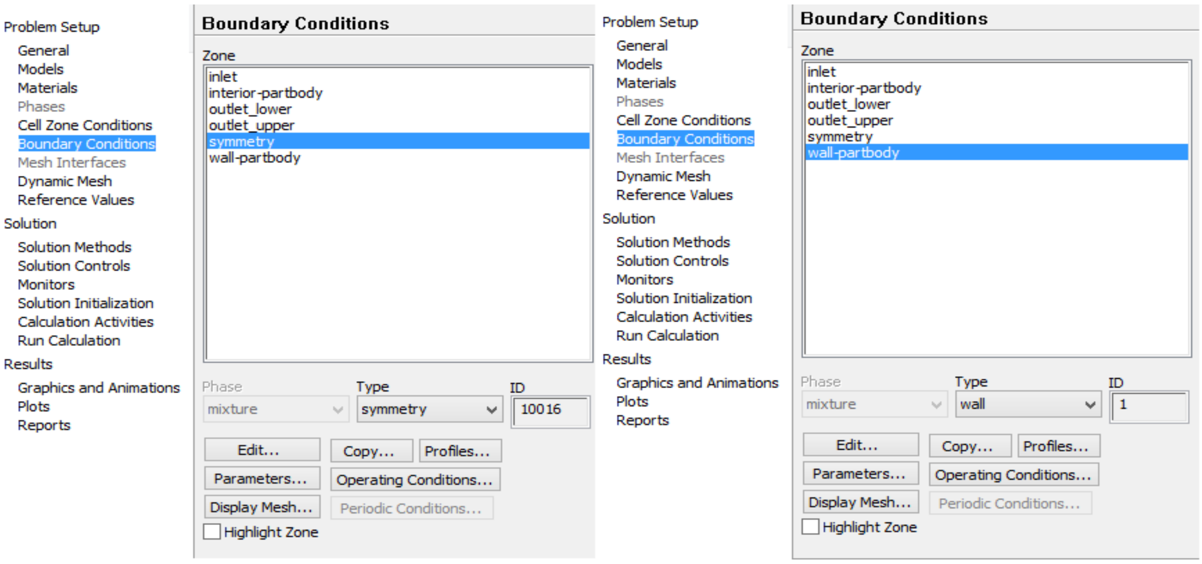

Fig 4.6 Problem set up boundary condition at different zone

Solution method:-The solution method is used to set the necessary methods. For example in the pressure-velocity couple method is used to be consider the velocity and pressure effect. In spatial discretization the pressure, the momentum, turbulent kinetic energy and turbulent dissipation rate must set to the second order equation to be solved

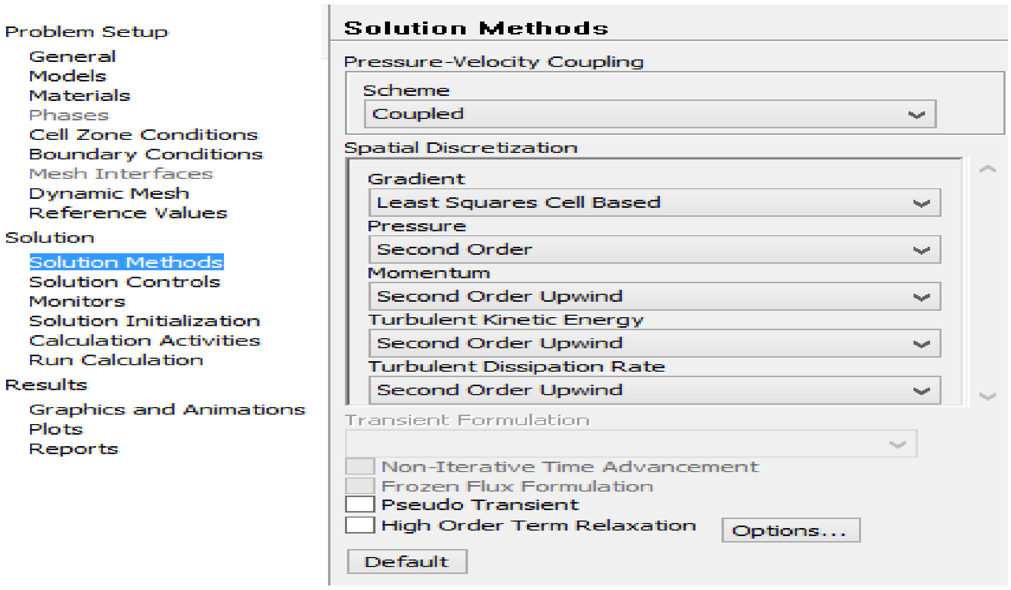

Fig 4.7 Solution method set up page

Monitor and convergence criterion:-The residuals for continuity equation, x, y, and z-velocity, k, and ε is set to 10^-6 and the convergence criterion to absolute and maximum iteration is given to be 1000 if it does not converge check again the mesh or other set up.

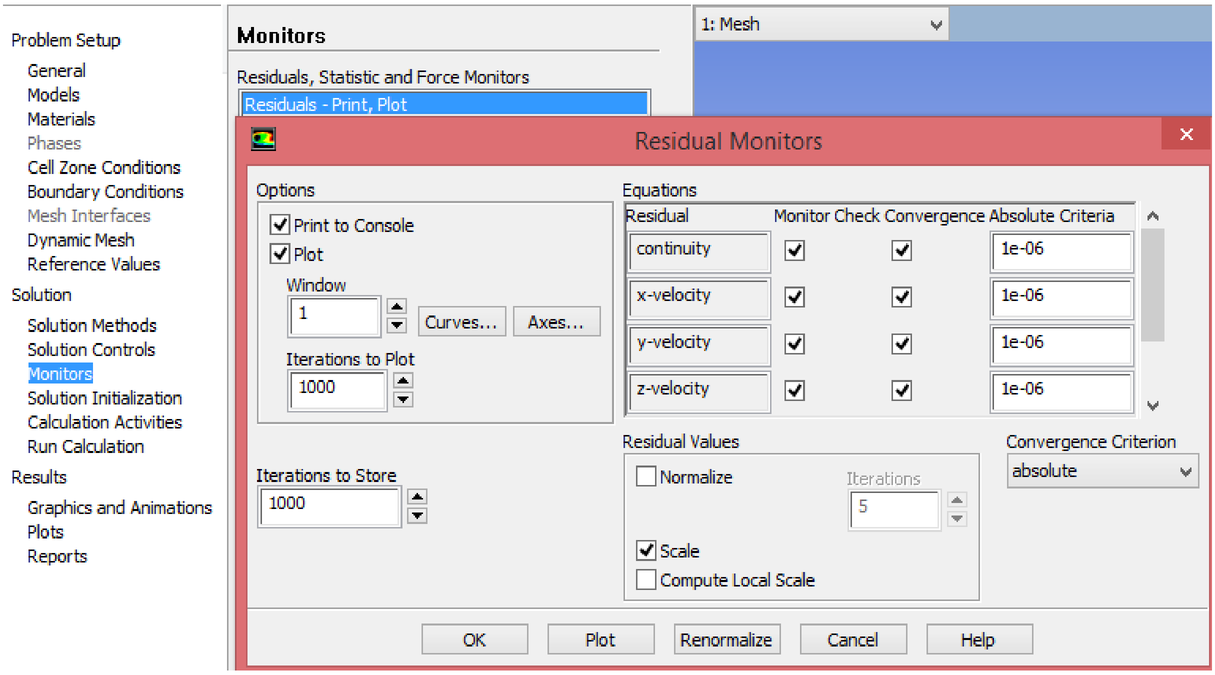

Fig 4.8 Monitoring setup

Solution initialization:-The solver is initialized by standard method computed from inlet Ansys guesses the pressure and the velocity at the inlet immediately when the total energy in the inlet is feed and solution is initialized as it displayed 470kpa and 3.72m/s in the following figure.

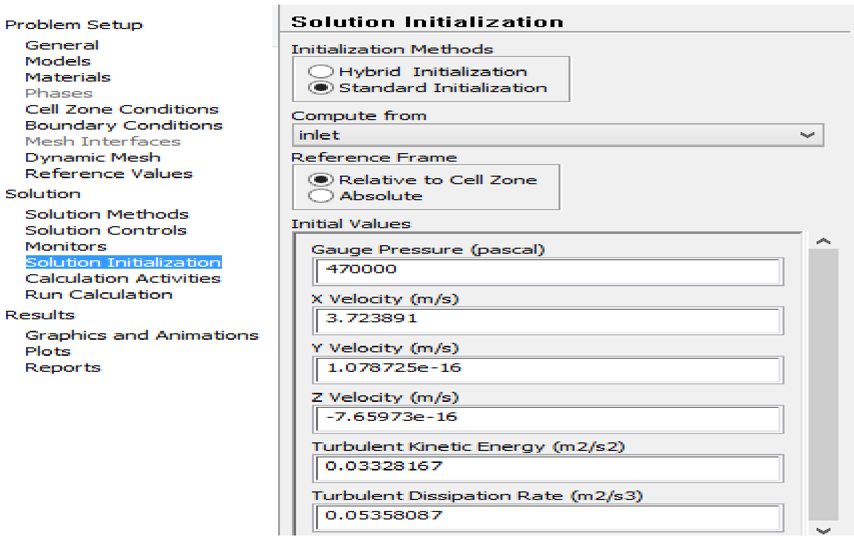

Fig 4.9 Solution initialization and initial guess

Calculation run:-the number of iteration to calculate is to 500 for first stage and if the solution not converge we continue up to 1000 and above or check the mesh again and the number of iteration interval to 1.

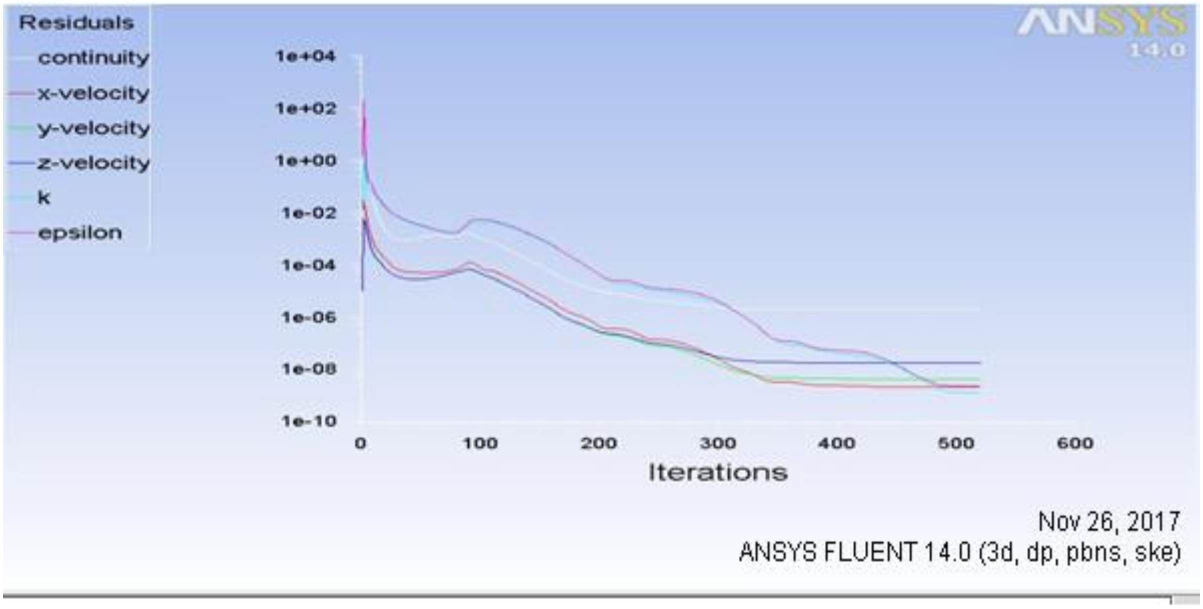

Fig 4.10 Convergence graph

The solution proceeds until either one of the convergence criteria achieved or the number of iteration reached. In this case the solution is not exactly converged at 10e-6 but nearly achieved. As the solution goes the solver in not getting lower and lower the residual curve.

Therefore it is reasonably to stop at iteration number of 500 since almost all of the equation reaches 10^{-8}.

Validation of the results:-The standard wall function k epsilon model valid if 100 < Y+ >30 so as depicted in the following graph ranges between 35 and 100 for Y^+ values.

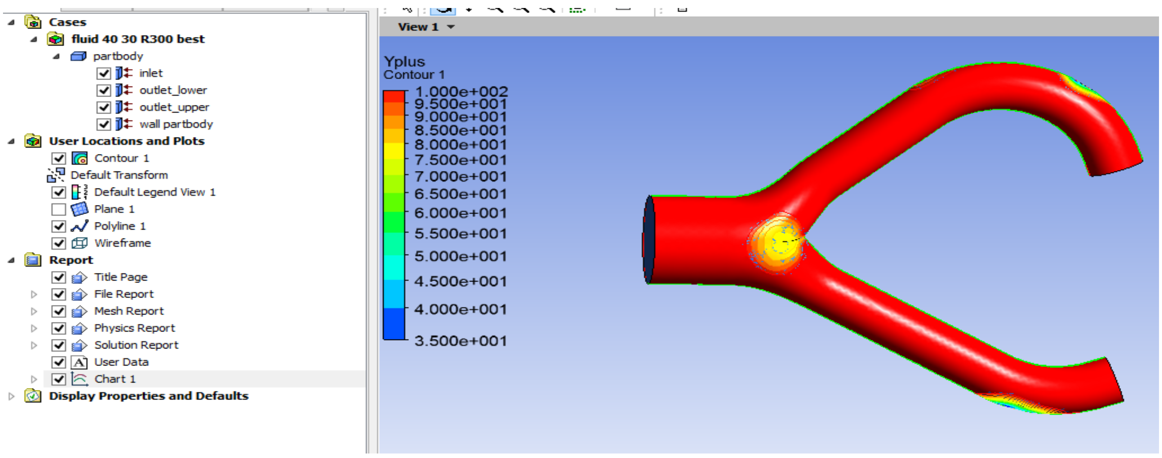

Fig 4. 11 Y+ range contour

The key question in analyzing different type of manifolds/ distributer is the uniformity of the flow distribution and pressure drop. I.e. as a whole head losses.

The total head loss in different types of bifurcation designs are simulated based on different distributer diameter , split angle, and bending radius are calculated and summarized in table in chapter five (result and discussion part) with the numerical results from Ansys fluent CFD post software.

4.3 MODELING AND FLOW SIMMULATION OF NOZZLE AND SPEAR

Geometric modeling and CFD simulation of the nozzle and spear at the whole cross section will be carried out in this step and knowing the relation of the independent and dependent variable .so in this step includes different parameters like

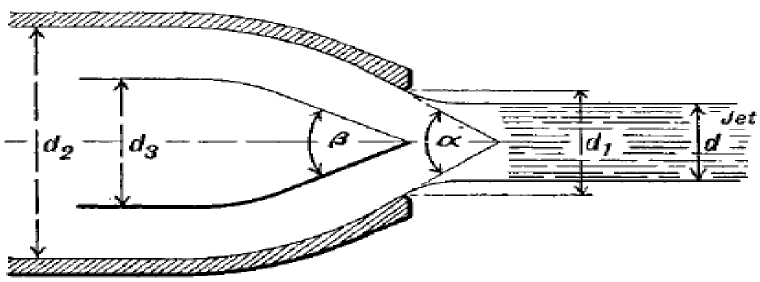

Fig 4.12 spear and nozzle angle[17]

- Velocity distribution using different nozzle angle at the whole cross section of nozzle

- Velocity distribution using different spear angle at the whole cross section of spear
- Pressure distribution inside the nozzle using different parameters like spear bulb radius, nozzle curvature, blocking distance, spear fillet radius etc.

4.3.1 ANSYS FLOW SIMULATION OF SPEAR AND NOZZLE.

Design of spear and nozzle of the Pelton turbine depends on the flow properties of the fluid. A poor design of a spear will result in a reduced flow rate, because of the backflow and voirtocity in the fluid [10]. Similarly, a poor nozzle design also reduces the conversion of hydraulic energy to kinetic energy i.e. Results low efficiency. Different design configuration were used to analyze the flow and its efficiency. The better the design the better the flow pattern and the efficiency too. A series of steps are followed to get the final Ansys report.

3D Modeling of the nozzle: -For modelling of the fluid, Ansys design modeler software is used. To start with the analysis the region of the fluid domain is taken by the free space region of the nozzle and spear. The nozzle and spear are dimensioned as already their geometry was calculated and 3D modeling of A half section of the spear and nozzle was drawn. The dimensions are parameterized for later design configuration of the analysis. A quarter (90^0) of the model is revolved to save the time needed to compute the result of the entire model by 75%.

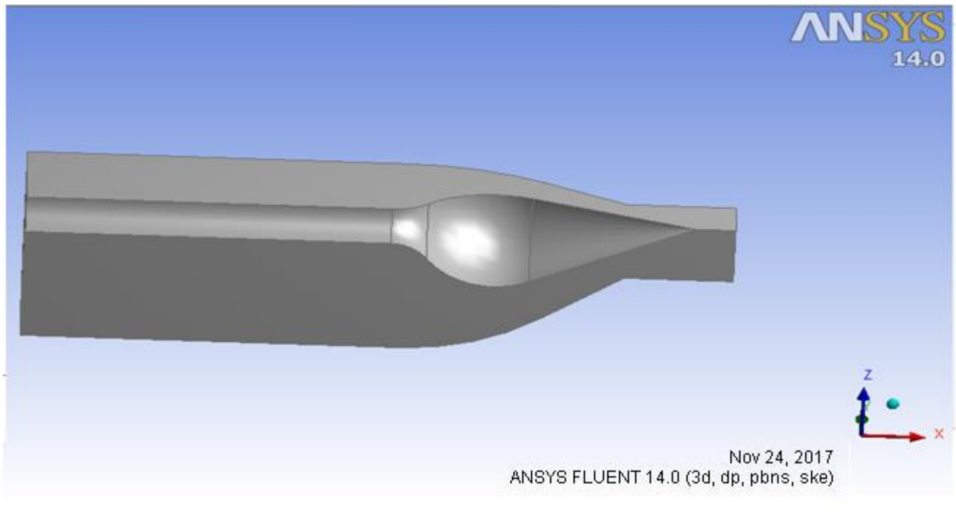

Fig 4.13 3D modeling for current design point

At the exit of the nozzle the fluid region is extended so that the boundary condition is applied at streamlined zone.

Discretization (Meshing) of the fluid region:-Ansys Fluent software is used to discretize the mesh of the fluid domain. The resolution of the mesh depends on the method used and the complexity of the fluid geometry. The refinement of the mesh is continued until its effect on result is negligible. Basically the mesh quality is determined by different parameters like aspect ratio, skewness and orthogonal quality of the mesh model. Orthogonal quality ranges from zero to one. The closer the number to 1 the better the quality. The model is inflated near the nozzle and spear wall to get fine meshes for the turbulence model to capture more gradients (slope, hill and ramps) the place which may have loss relative than other. That the result gets valid. The overall discretization procedure and method is put in the following table

Table 4.2 Mesh method description

Meshing method	Inflated surface	Sizing (sphere of influence)
Automatic	Nozzle and spear wall	At the spear tip vertex

As putted in the above table automatic mesh method is used in the discretization since there is bend , fillet and varying cross section in the flow is adjusted automatically and inflation is used at the nozzle and spear wall as well the spear tip and vertex places are used by sizing.

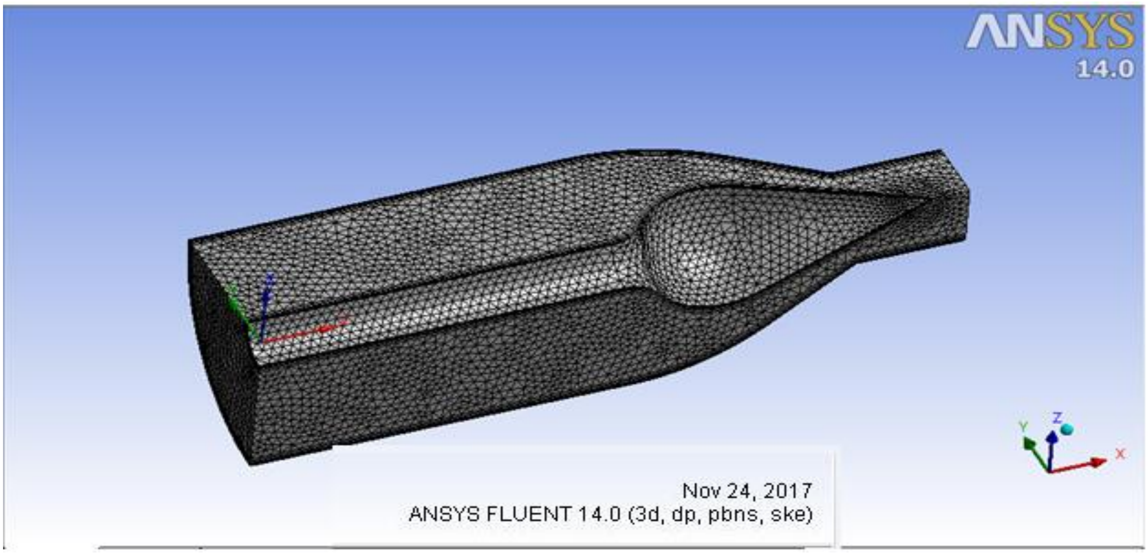

Fig 4.14 3D Model meshing

Verification of mesh quality is checked by different method. One of the decisive checking mechanism is that for different mesh size i.e. minimum, maximum and face mesh size the mesh quality is varying and stops at some point, even if there is huge difference in number of element and nodes.

Grid dependent test for the nozzle:-In order to verify the numerical accuracy of the results obtained, it is necessary to compare results on different meshes.

The following tables shows the mesh settings, results and other parameters related to the results of using the same angles and remaining different parameters unchanged ,the mesh refinement have seen in low, medium and high.

So no need to explain all the tables, the target is showing that when mesh quality, element number, element node, maximum and minimum mesh size vary the result is unchanged.

Low refinement

Table 4.3 Low *refinement* mesh quality for spear and nozzle at an angle of (25, 35*) degrees*

P120 - Mesh Max Face Size	P121 - Mesh Max Size	P122 - Vertex Sizing Sphere Radius	P123 - Vertex Sizing Element Size	P128 - Inflation Maximum Layers	P129 - Inflation Growth Rate	P118 - Mesh Min	P113 - inlet_static_pressure	P112 - V_out	P119 - Mesh Average	P138 - Mesh Nodes	P139 - Mesh Elements
mm	mm	mm	mm				Pa	m s^-1			
30	30	10	6	5	1.2	0.25688	4.6826E+05	25.255	0.88817	6116	16283

Medium refinement:

Table 4.4 Medium refinement mesh quality for spear and nozzle at an angle of (25, 35) degrees

P124 - Mesh Max Size	P125 - Mesh Max Face Size	P126 - Inflation Maximum Layers	P127 - Inflation Growth Rate	P140 - Vertex Sizing Sphere Radius	P141 - Vertex Sizing Element Size	P115 - Mesh Av...	P114 - Mesh Min	P111 - inlet_static_pressure	P110 - V_out	P136 - Mesh Nodes	P137 - Mesh Elements
mm	mm			mm	mm			Pa	m s^-1		
25	17	5	1.2	10	2.5	0.88405	0.30403	4.6909E+05	26.556	7007	19375

Final refinement:

Table 4.5 Final refinement mesh quality for spear and nozzle at an angle of (25, 35) degrees

P143 - Mesh Max Size	P144 - Mesh Max Face Size	P87 - Vertex Sizing Element Size	P88 - Inflation Maximum Layers	P142 - Inflation Growth Rate	P102 - A_in	P47 - Vout	P48 - inlet pressure	P53 - Mesh Min	P89 - Mesh Elements	P90 - Mesh Nodes	P91 - Mesh Average
mm	mm	mm				m s^-1	Pa				
20	10	2.5	5	1.2	0.021883	26.555	4.6919E+05	0.36463	24533	8812	0.89247

As it can be seen from the table the exit velocity and inlet static pressure are not getting changed or negligible as the mesh minimum quality achieves from 0.30 to 0.35. As the mesh quality varies from 03 to 0.035 the result obtained is unchanged so no need of maximizing mesh quality if no result change. Due to this we can save time so we can now conclude that the numerical solution is verified when the mesh minimum orthogonal quality reaches or nears 0.3.

For mesh method automatic meshing method is used so that fluent automatically applies the best method for CFD solver. Depending the minimum mesh quality obtained here further optimization of the rest parameters like nozzle and spear angle will be done.

The different design points will be analyzed at almost the same mesh quality (orthogonal quality, aspect ratio, skewness) and discussed later in result and discussion session. Three of the best optimized design configurations will be also analyzed and discussed in deep for refined mesh.

4.3.3 FLUENT PROBLEM SETUP PAGES

After setting up mesh parameters the next step will be setting up different fluent pages.

In general page the quality of the mesh interms of aspect ratio (inflation) and orthogonal quality is enquired and tabulated in the above table. Pressure based, and steady flow solver setting is setted. Gravity remain unchecked. The solver set up is the same us of distributer the model, the material and the cell zone condition are the same except the boundary condition value the method also the same in analysis so no need of repetition. The flow is 3D model and symmetry.

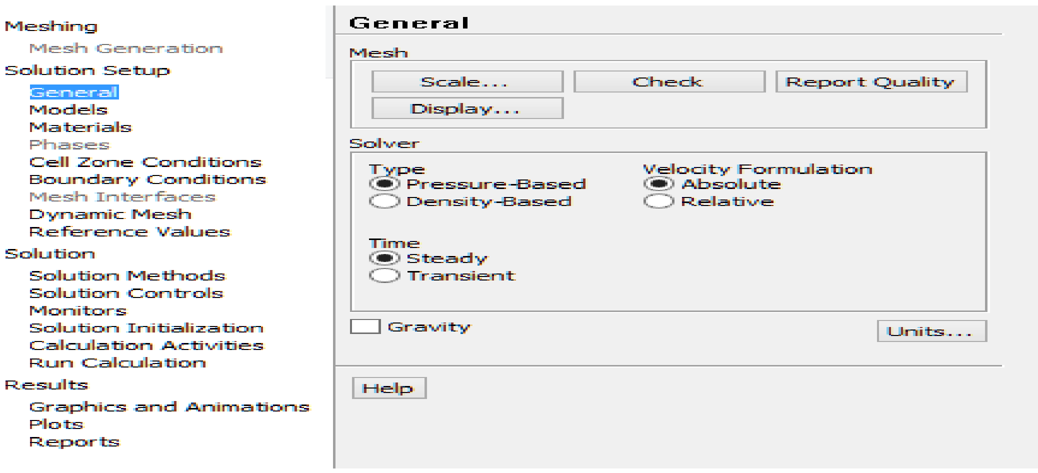

Fig 4.15 Ansys problem setup page

Reynolds no estimates the flow pattern whether the flow is turbulent or laminar.

$$R_e(\text{at the nozzle inlet}) = \frac{V * d}{v} = \frac{4.92\frac{m}{s} * 0.140m}{1.005\frac{m^2}{s}} * 10e6 = 8e5$$

$$R_e(\text{at the nozzle exit}) = \frac{V * d}{v} = \frac{30.8\frac{m}{s} * 0.068m}{1.005\frac{m^2}{s}} * 10e6 = 2.1e6$$

This shows that the flow is turbulant with standard wall function as guided by the following table. Appendix E shows , wall treatment conditions and non-dimentional first cell distance for different reynolds number.

Model:-Standard K-epsilon, standard wall function model is used to characterize turbulent flow regime through the nozzle since it is accurate for higher Reynolds number flow. *The value listed in the table i.e. 0.09, 1.44 and 1 is Ansys default value.*

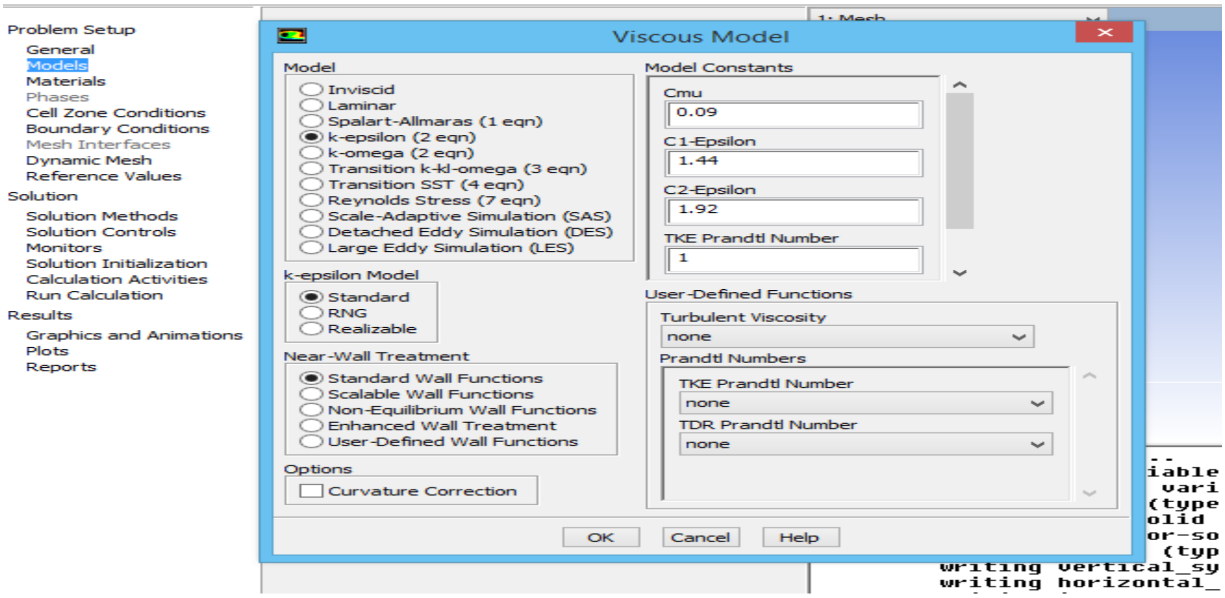

Fig 4.16 Fluent problem setup modeling

From fluent material data base water is copied to the list in drop down menu to select it as fluid cell zone later.

Boundary Condition page:- The boundary conditions are applied at the inlet and outlet surfaces of the domain.

Inlet Boundary Condition:-Total gage pressure is set at inlet boundary which is calculated below and its direction with normal to the inlet surface i.e., at inlet of nozzle domain is applied.

As mentioned in the distributer the same principle only the head and the A_{in} are different for the nozzle. The net head is the head behind the distributer and the inlet area for the nozzle is the distributer diameter with a diameter of 142mm.

$$Total\ gage\ pressure = hydrostatic\ pressure + hydrodynamic\ pressure$$

At the inlet of the nozzle there is a flow rate as well energy head.

$$P_o = P_{hs} + P_{hd} = \rho g H + \frac{1}{2}\rho {V_{in}}^2 = \rho g H + \frac{1}{2}\rho\left(\frac{Q}{A_{in}}\right)^2$$

Where Q is flow rate for single distributer which is $0.07m^3/s$

A_{in} inlet area of nozzle which is 142mm

H is net head available at the nozzle inlet which is found after subtraction of distributer head loss which is 47.98m

$$P_o = \rho g H + \frac{1}{2}\rho\left(\frac{Q_{nozzle}}{A_{in}}\right)^2 = 998.2 \times 9.81 \times 47.98 + \frac{1}{2} \times 998.2\left(\frac{0.07}{\pi \times \frac{0.142^2}{4}}\right)^2$$

$$= 479587.6\text{Pa}$$

Therefore the total inlet gage pressure is dependent on the inlet velocity. As though it is parameterized under Ansys fluent workbench parameter option.

The theoretical velocity (neglecting losses) at the exit of nozzle would be:

$$V_{theo} = \sqrt{2gH_n} = \sqrt{2 \times 9.8 \times 47.98} = 30.68\, m/s$$

Hydraulic diameter: $D_H = D_0 - D_i = D_0 - 32mm(parametrized\ also)$

Hydraulic diameter is the perimeter of the flow through a pipe

$D_H = 0.170 - 0.032 = 0.138m(for\ the\ current\ design\ point)$

After the simulation of the distributer the value of the diameter of the distributer is set to 142mm but the spear road diameter is unchanged so the hydraulic diameter will be the weighted flow region is diameter of nozzle minus diameter of spear.

$D_H = 0.142 - 0.032 = 0.11$

The turbulence intensity, I is defined as the ratio of the root-mean-square of the velocity fluctuations, u' to the mean flow velocity, u_{ave}.

For internal flows, the turbulence intensity at the inlets is totally dependent on the upstream history of the flow. If the flow upstream is under-developed and undisturbed, you can use a low turbulence intensity. If the flow is fully developed, the turbulence intensity may be as high as a few percent. The turbulence intensity at the core of a fully-developed duct flow can be estimated from the following formula derived from an empirical correlation for pipe flows: [32] $I = \frac{u'}{u_{ave}} = 0.16(Re)^{-1/8}$

$$I(Re = 8e5) = \frac{u'}{u_{ave}} = 0.16(800000)^{-\frac{1}{8}} = 3\%\ and$$

$$I(Re = 2.1e6) = \frac{u'}{u_{ave}} = 0.16(2.1e6)^{-\frac{1}{8}} = 2.6\%$$

Turbulence is set to intensity of 4 % since there are factors like distributer bendings, elbows which increases the turbulence intensity.

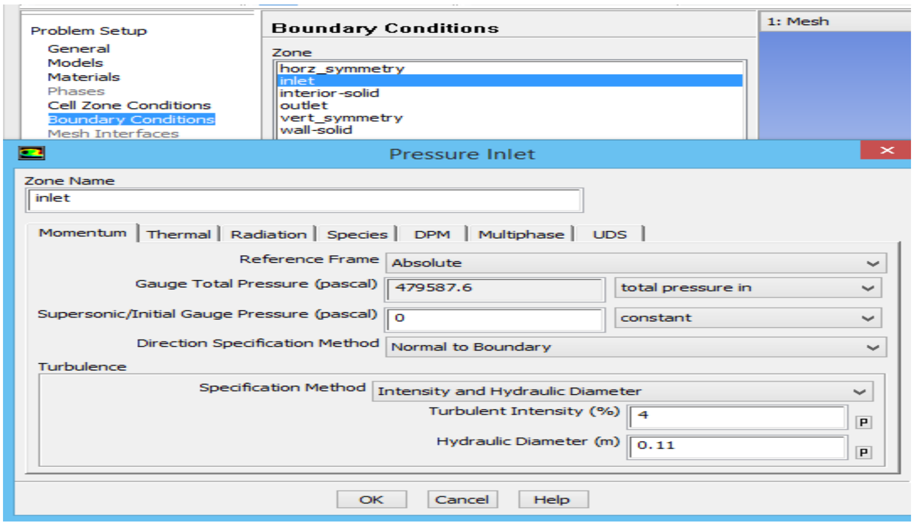

Fig 4.17 Inlet boundary condition setup for pressure

Outlet Boundary Condition:- The reference pressure at the outlet of the external domain was set equal to 1atmospheric (0 $Pa\ gage\ pressure$).

Turbulence is set to intensity of 5 %.

At the exit the diameter is 68mm and set to the out let boundary condition as 0.068m

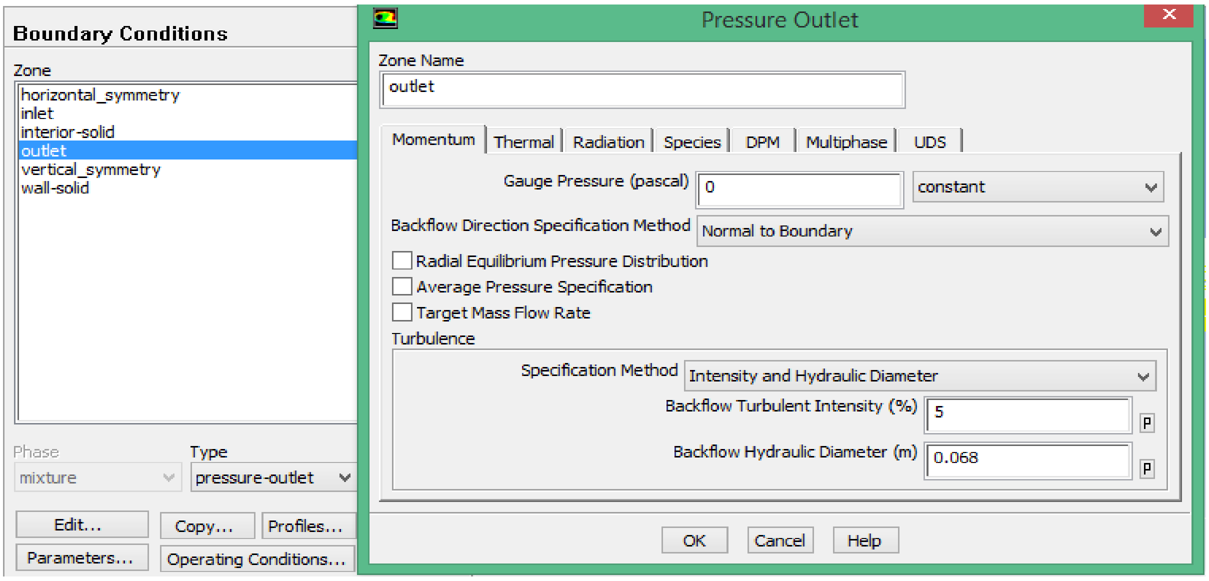

Fig 4.18 Outlet boundary c ondition setup for pressure

Wall Conditions:-The walls of all the domains are assumed to be smooth and no slip condition is assigned

Roughness height for commericial steel $\epsilon = 0.045\text{mm}$

Roughness constant, ϵ/D, becomes: $0.045/170 =$2.65e-4

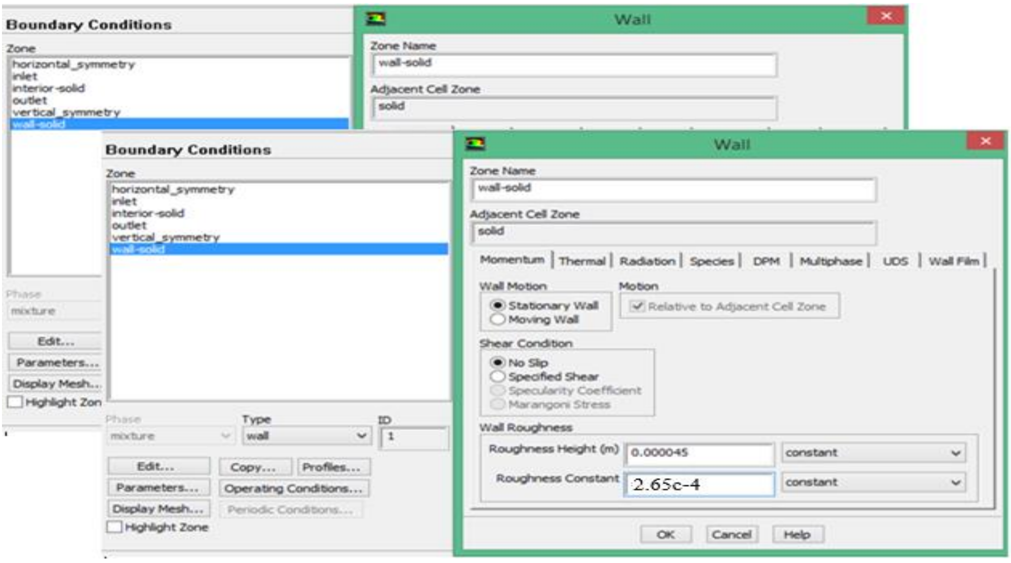

Fig 4.19 Boundary condition setup for solid wall

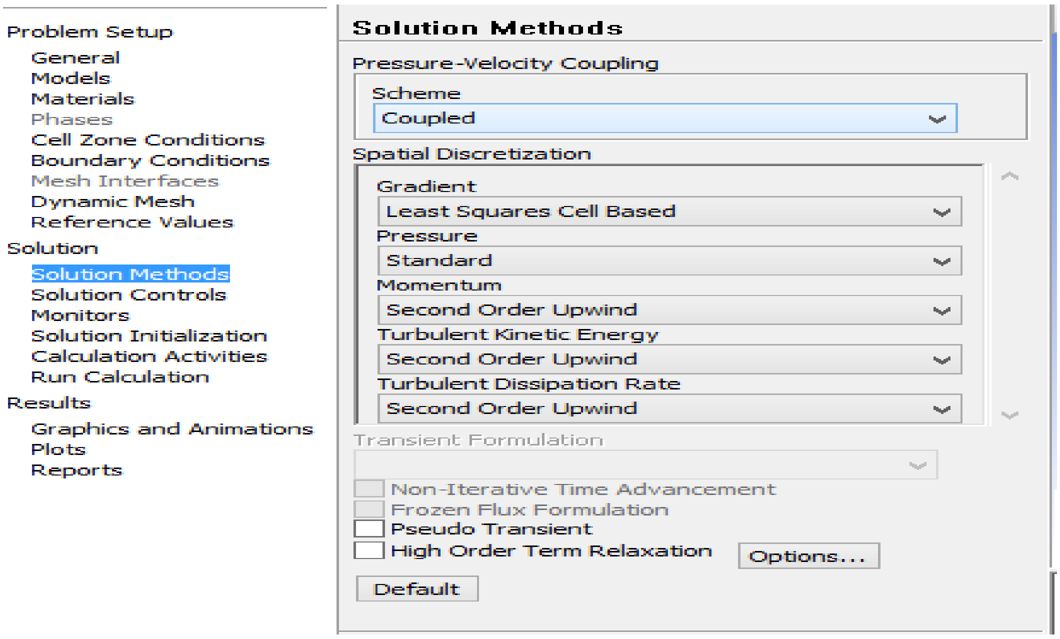

Fig 4.20 The solution method setup

The RMS residual target has been set to 1x10e-6 for termination of the continuity equation, kinetic turbulence energy (k) and turbulence dissipation (ε) calculations and 500 number of iterations for convergences.

The scaled residual curve for the current design point is as shown below

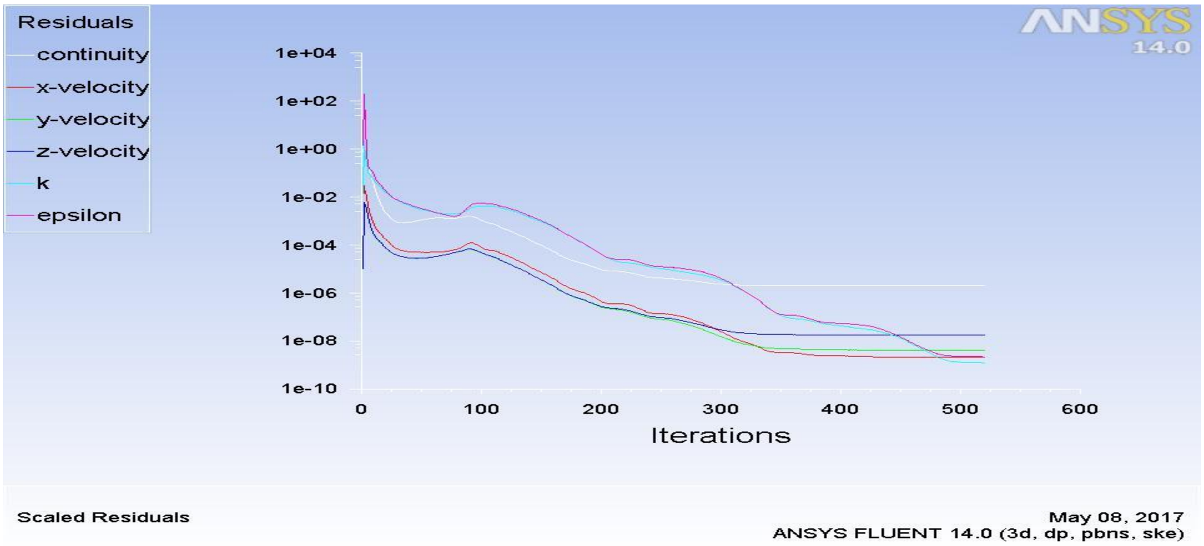

Fig 4.21 Scaled residual curve for current design point.

Validation of the simulation result:-The validation of the result using first cell distance is important specially when there is no experimental results. Therefore as you can see from the Y+ figure, the Y+ curve for refined mesh tells it is big enough to pass the range for turbulent flow regime. I.e. Y+≥ 30

The y+ values are varied for different flow condition and also it depends on the Reynold number if Y+ <5 viscous sub layers region, 5< Y+< buffer region, Y+> 30 fully turbulent region and also it varies depending on the model in this thesis standard wall function k-epsilon method is used as mention in table 4.7, the value is of the y+ region is meet and valid as shown in the following figure.

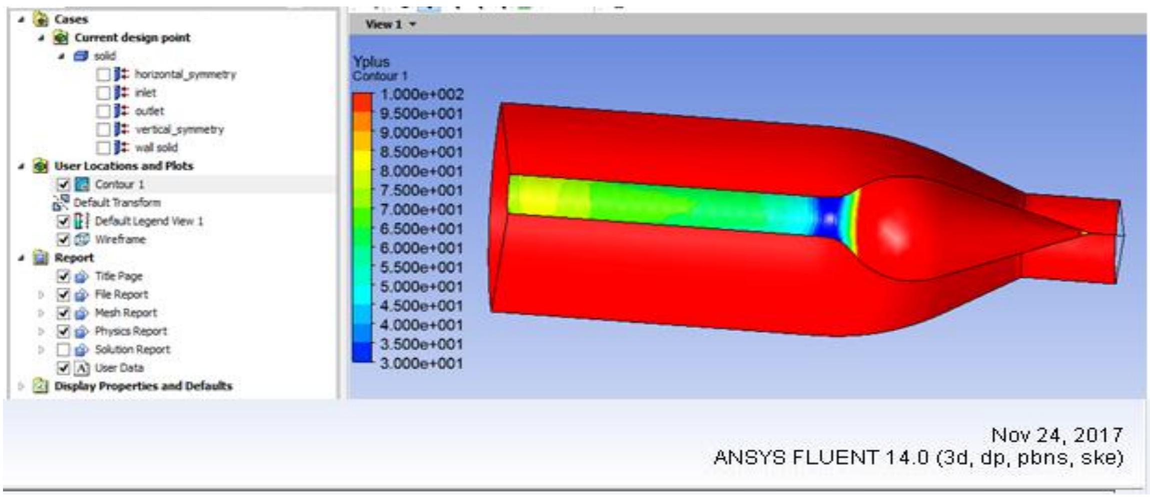

Fig 4.22 Y+ values for refined mesh

As depicted from the pressure graph mesh refinment is unnecessary changing any further since there is no change in pressure value. The result of the numerical solution is therefore *valid* at mesh quality of around 0.3.

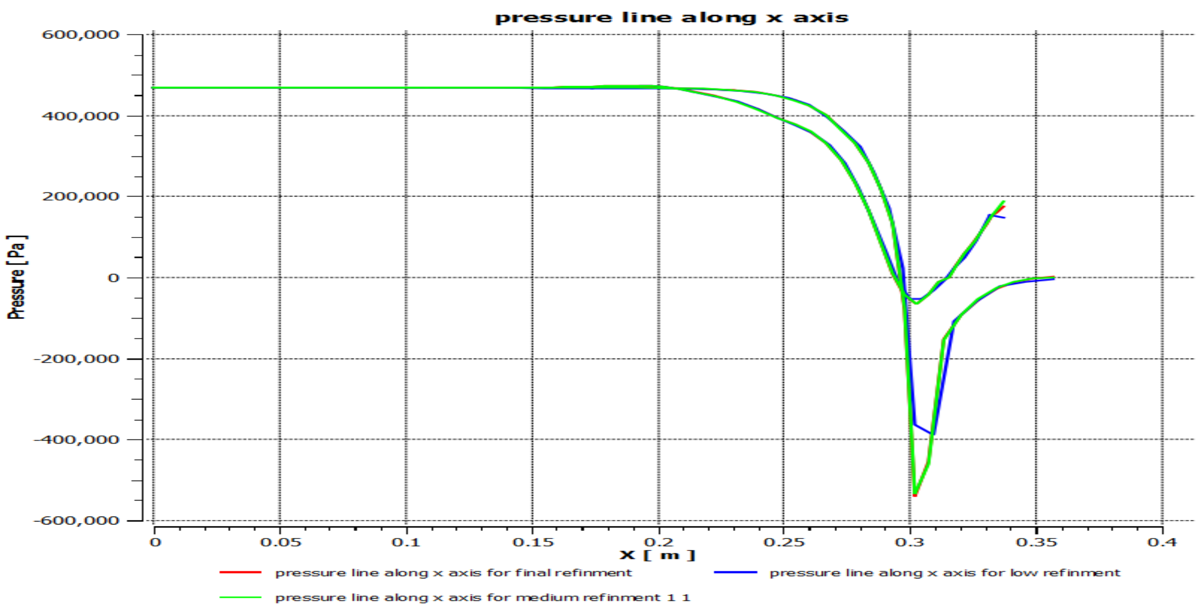

Fig 4.23 Static pressure along in the direction of flow on the curve of nozzle and spear wall.

4.4 SIMULATION OF INTEGRATED NOZZLE AND DISTRIBUTER

The simulation of the integrated distributer and nozzle is simulated using the optimal distributer and nozzle.Every and each procedure is the same as that of distributer and nozzzle simulation and here the integrated simulation head loss is equal to the head loss in the distributer plus the head loss in the nozzle.

4.4.1 GEOMETRY OF INTEGRATED NOZZLE AND DISTRIBUTER

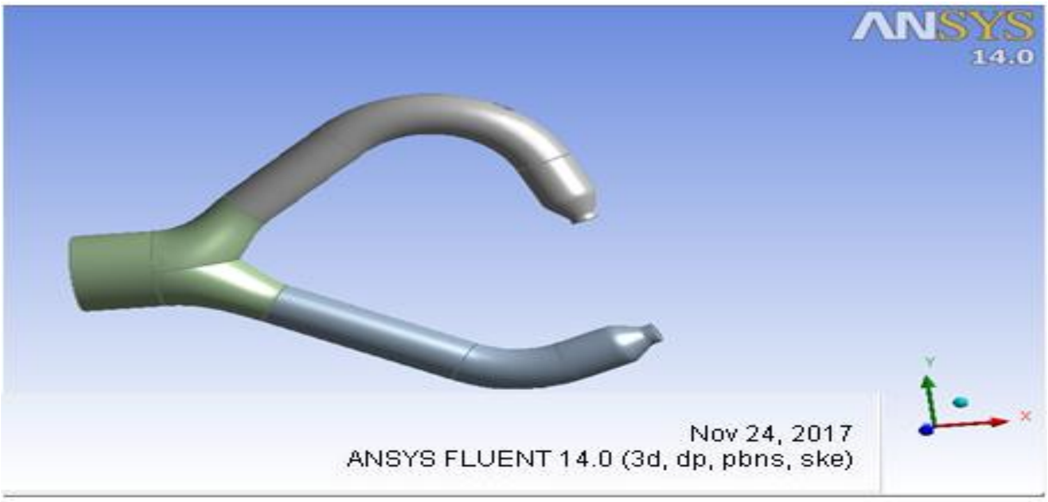

Fig4.24 the 3D model of integrated nozzle and distributer

4.4.2 THE INTEGRATED NOZZLE AND DISTRIBUTER MESH

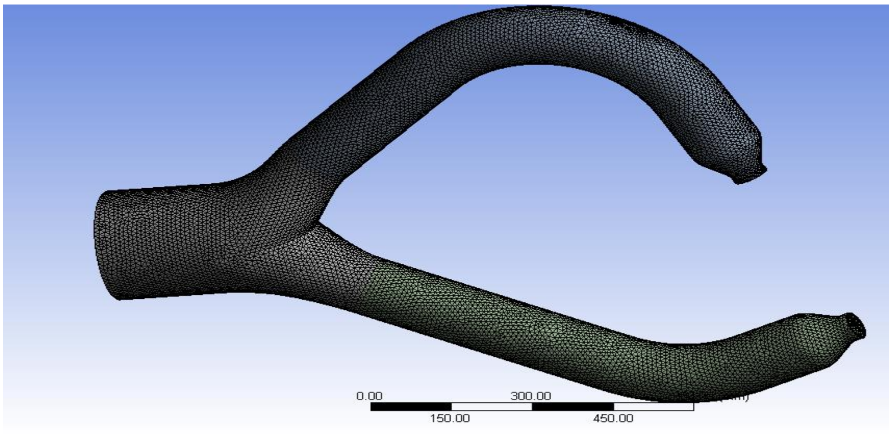

Fig4.25 mesh for the integrated nozzle and distributer

Grid dependent test for the integrated nozzle and distributer:-Looking the velocity and the total pressure results interms of the mesh refinement it becomes insignificant as minimum mesh size gets small.

Here refining the mesh anymore is not important since the result shows no more change in its value as it can be seen in able 4.6. Therefore, the mesh is verified!

Table 4.6 Mesh verification for integrated nozzle and distributer.

P18 - Mesh Min Size	P4 - Mesh Max Size	P5 - Mesh Elements	P6 - Mesh Nodes	P8 - Mesh Aver…	P10 - V_in	P11 - V_jet_lower	P12 - V_jet_upper	P14 - total pressure lower	P15 - total pressure upper
m	m				m s^-1	m s^-1	m s^-1	Pa	Pa
20	30	5.027E+05	1.5089E+05	0.89734	3.8614	29.253	29.025	4.7518E+05	4.7578E+05
10	25	5.027E+05	1.5089E+05	0.89734	3.1872	29.553	29.031	4.7616E+05	4.7579E+05
5	20	6.2256E+05	1.8584E+05	0.89588	3.1864	29.553	29.031	4.7616E+05	4.7576E+05

4.4.3 PROBLEM SETUP PAGES FOR INTEGRATED NOZZLE AND DISTRIBUTER

General problem setup page: - Pressure based, absolute velocity formulation, and steady flow is set in general page

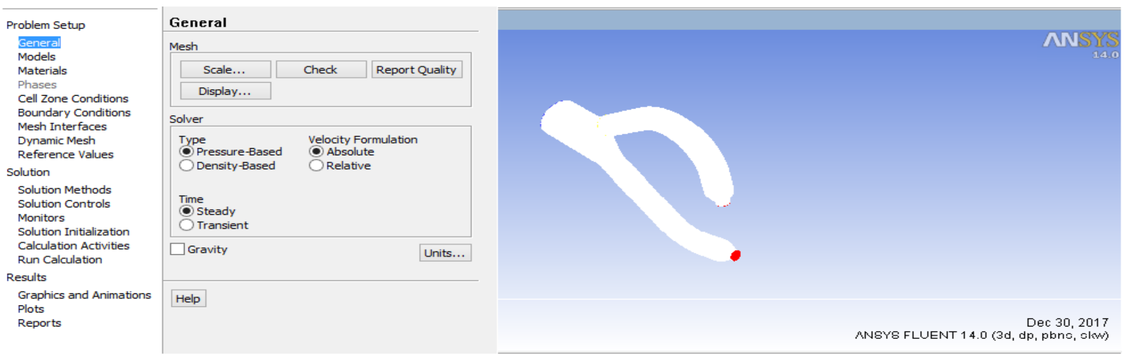

Fig 4.26 The general setup page

Reynolds no estimates the flow pattern whether the flow is turbulent or laminar.

$$R_e(\text{at the distributer inlet}) = \frac{V*d}{v} = \frac{2.5\,\frac{m}{s}*0.226m}{1.005e-6\,\frac{m^2}{s}} = 5.65e5$$

$$R_e(\text{at the nozzle exit}) = \frac{V*d}{v} = \frac{30.8\frac{m}{s}*0.068m}{1.005\frac{m^2}{s}} * 10e6 = 2.1e6$$

The Renold number shows that the flow is turbulant and *Standard K-epsilon, standard wall function* model is used to characterize turbulent flow by the following table.

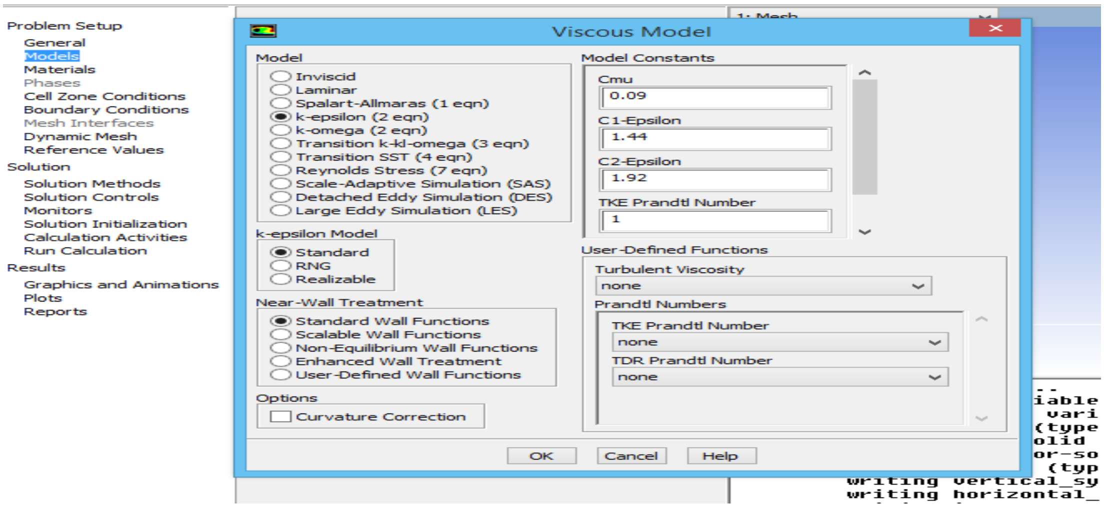

Fig 4.27 The standard k epsilon urbulan model

Material:-water in liquid state is added to the list from Ansys fluent material library for later use in cell zone condition**.**

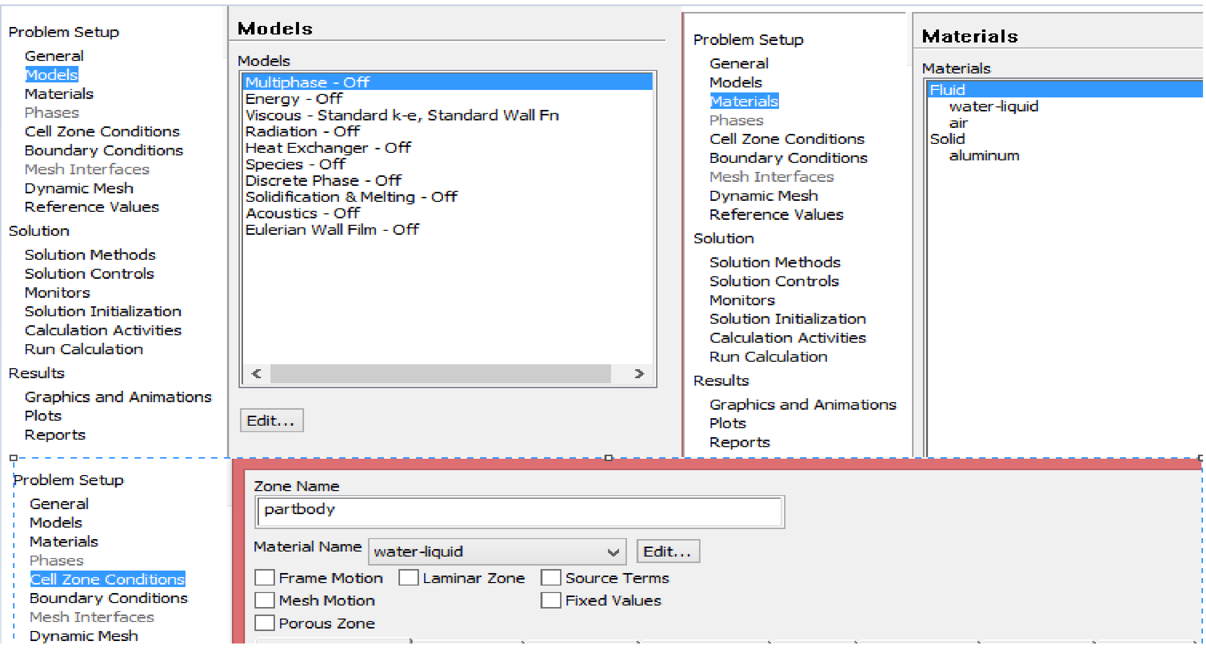

Fig 2.28 The material setup page.

Cell zone condition:-water is used for the analysis.

Boundary conditions:-there are one inlet, two outlet and symmetry boundary conditions

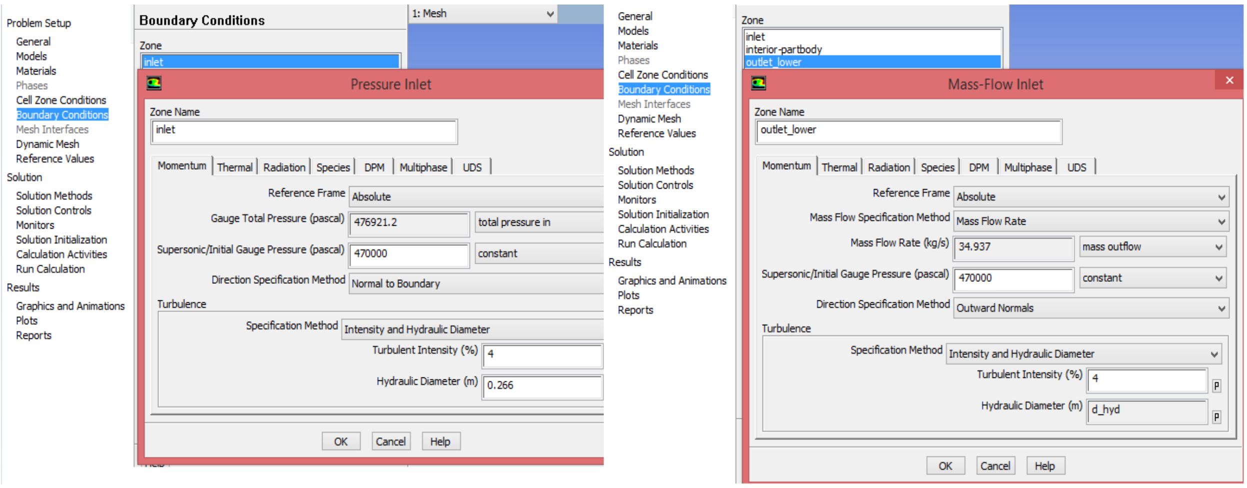

Fig 4.29 Problem set up inlet aand out let Boundary conditon.

Inlet and exit of distributer:-At the inlet of the distributer the fluid has Hydraulic energy that it has obtained from the static head incorporating the loss available in the penstock. Mass flow rate is taken at the exit of the distributer.

$$Mass\ flow\ rate(exit) = \rho\frac{Q}{2} = 998.2 \times \frac{0.14}{2} = \frac{34.9\ Kg}{s}$$

And at the inlet the total gauge pressure or energy is feed to Ansys by adding the hydro dynamic and hydrostatic energy using equation 3.23.

$$\mathrm{P_o} = \rho\mathrm{gH} + \frac{1}{2}\rho\left(\frac{Q}{\mathrm{A_{pen}}}\right)^2 = 998.2 \times 9.81 \times 48.38 + \frac{1}{2} \times 998.2\left(\frac{0.07}{\pi \times \frac{0.266^2}{4}}\right)^2 = 476921.2\ \mathrm{Pa}$$

The turbulence intensity,I is defined as the ratio of the root-mean-square of the velocity fluctuations, u' to the mean flow velocity,u_{ave}.

For internal flows, the turbulence intensity at the inlets is totally dependent on the upstream history of the flow. If the flow upstream is under-developed and undisturbed, you can use a low turbulence intensity. If the flow is fully developed, the turbulence intensity may be as high as a few percent. The turbulence intensity at the core of a fully-developed duct flow can be estimated from the following formula derived from an empirical correlation for pipe flows:

$$I = \frac{u'}{u_{ave}} = 0.16(Re)^{-1/8}$$

$$I(Re = 5.65\mathrm{e}5) = \frac{u'}{u_{ave}} = 0.16(5.56\ \mathrm{e}5)^{-\frac{1}{8}} = 3\ \%\ (distributer\ inlet) and$$

$$I(Re = 1.1e6) = \frac{u'}{u_{ave}} = 0.16(1.1e6)^{-\frac{1}{8}} = 2.8\%(distributer\ exit)$$

Turbulence is set to intensity of 4% since there are factors like distributer bendings, elbows which increases the turbulence intensity.

Hydraulic diameter:$D_H = 266mm(distributer\ inlet)\ and\ 68mm\ \ of\ nozzle\ exit$

Symmetry and wall: symmetry and wall boundaries has been added to fully constrain the fluid model for the fluent solver.

Outlet Boundary Condition: - The reference pressure at the outlet of the external domain was set equal to 1atmospheric (0 $Pa\ gage\ pressure$).Turbulence is set to intensity of 5 %.

At the exit the diameter is 68mm and set to the out let boundary condition as 0.068m

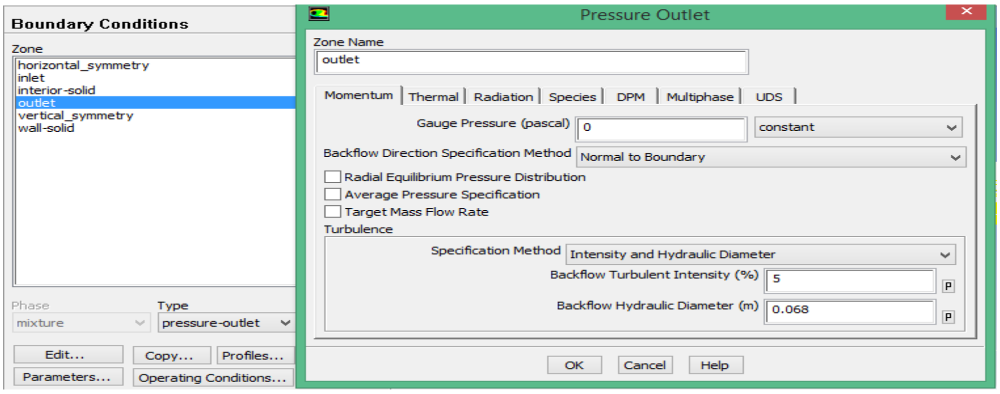

Fig 4.30 The out let boundary condition of the integrated nozzle and distributer.

The solution method is set to coupled, standard and second order upwind methods.

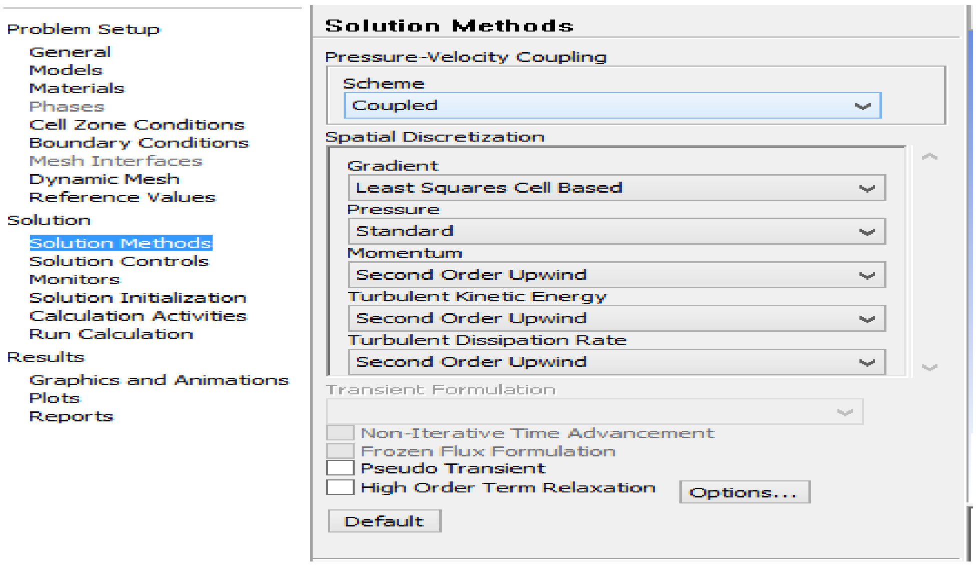

Fig 4.31 the solution method set up page

CHAPTER FIVE

RESULT AND DISCUSSION

The result and discussion of the nozzle-spear alignment, distributer and the integrated nozzle-distributer optimization is presented here using a globally accepted software, Ansys fluent. And the stress analysis, design and structural simulation of mechanical components such as nozzle, spear and deflector has been done using Ansys mechanical software on this chapter as well.

The result and discussion of distributer and nozzle with its spear alignment has been done. Depending the performance we need, the selection of our best optimized design has been taken as afinal result and conclusion will follow the result and discussion.

The result and discussion mainly focus on the decissive terms like pressure drop,out let velocity, efficiency and discharge. These terms are measured by looking the output figure of the distributer,nozzle and spear. The figures or legend bar included in the analysis were pressure contour,velocity contour,the stream line of the flow and the vorticity contour of the flow.

5.1 ANSYS FLUENT SIMULATION RESULTS OF DISTRIBUTER

Here analysis of flow simulation of distributer has been taken to under the consideration of getting minimum head loss and as well it must be manufacturable. So after the simulation has been done the decision has been made depending on the result obtained. The result is presented in the following table for each of the five bifurcation.

The following five tables shows that five bifurcation (distributer) results from Ansys simulation

Ansys simulation result for bifurcation type 1

Table 5.1 Pressure and velocity distribution for bifurcation type 1

P108 - V_lower	P143 - Q	P104 - static pressure outlet lower	P105 - static pressure outlet upper	P106 - dynamic pressure outlet upper	P107 - dynamic pressure outlet lower	P109 - V_upper	P142 - V_in	P144 - Q_lower	P145 - Q_upper	P146 - static pressure in
m s^-1	m^3 s^-1	Pa	Pa	Pa	Pa	m s^-1	m s^-1	m^3 s^-1	m^3 s^-1	Pa
4.7671	0.14	4.6121E+05	4.6109E+05	11235	11326	4.7062	2.549	-0.07	-0.07	4.7368E+05

Ansys simulation result for bifurcation type 2

Table 5.2 Pressure and velocity distribution for bifurcation type 2

P169 - dynamic pressure lower	P170 - dynamic pressure upper	P171 - dynamic pressure in	P167 - static pressure lower	P166 - static pressure in	P165 - Q	P164 - V_upper	P163 - V_lower	P162 - V_in	P168 - static pressure upper
Pa	Pa	Pa	Pa	Pa	m^3 s^-1	m s^-1	m s^-1	m s^-1	Pa
11197	11217	3186.8	4.6351E+05	4.7373E+05	0.14	4.7408	4.7238	2.5236	4.6314E+05

Ansys simulation result for bifurcation type 3

Table 5.3 Pressure and velocity distribution for bifurcation type 3

P138 - static pressure outlet	P97 - outlet dynamic pressure lower	P96 - inlet dynamic pressure	P95 - inlet total pressure	P94 - inlet static pressure	P141 - V_upper	P139 - V_in	P140 - V_lower	P98 - outlet dynamic pressure upper	P134 - Q	P135 - Q_lower	P136 - Q_upper
Pa	Pa	Pa	Pa	Pa	m s^-1	m s^-1	m s^-1	Pa	m^3 s^-1	m^3 s^-1	m^3 s^-1
4.6382E+05	11157	3187.3	4.7692E+05	4.7373E+05	4.7315	2.5248	4.715	11153	0.14	-0.07	-0.07

Ansys simulation result for bifurcation type 4

Table 5.4 Pressure and velocity distribution for bifurcation type 4

P154 - Q	P132 - dynamic pressure lower	P131 - dynamic pressure upper	P125 - V_in	P126 - V_lower	P127 - V_upper	P128 - static pressure in	P129 - static pressure lower	P130 - static pressure upper	P155 - Q_lower	P156 - Q_upper
m^3 s^-1	Pa	Pa	m s^-1	m s^-1	m s^-1	Pa	Pa	Pa	m^3 s^-1	m^3 s^-1
0.14	11128	11114	2.5241	4.706	4.7192	4.7373E+05	4.6375E+05	4.6303E+05	-0.07	-0.07

Ansys simulation result for bifurcation type 5

Table 5.5 Pressure and velocity distribution for bifurcation type 5

P147 - Q	P113 - static pressure lower	P116 - V_lower	P114 - static pressure upper	P117 - V_in	P118 - dynamic pressure lower	P115 - V_upper	P119 - dynamic pressure upper	P148 - Q_lower	P149 - Q_upper	P150 - static pressure in
m^3 s^-1	Pa	m s^-1	Pa	m s^-1	Pa	m s^-1	Pa	m^3 s^-1	m^3 s^-1	Pa
0.14	4.6193E+05	4.7028	4.624E+05	2.555	11108	4.6905	11041	-0.07	-0.07	4.7363E+05

As it can be seen in the above five tables the simulation has been done.the selection will be done based on head los and the out let velocity.The total head loss in different types of bifurcation designs is calculated and summarized as follows with the numerical results from Ansys fluent CFD post software by using equation 3.25.

The results from the upper and lower distributer are added because to know the total loss from the unit integration and select the nozzle and distributer integration with minimum loss.

Table 5.6 Head loss and pressure drop calculated values for different bifurcation

Bifurcation Consideration	Parts of bifurcation Under consideration	Split angle	Bending radius, mm	Length, m	Velocity, m/s	Head loss, m
1	Inlet	Reference Frame	-		2.55	
	Outlet lower	0	300	3.3	4.77	0.448
	Outlet upper	30	300	3.3	4.7	0.49
	Total head loss					0.94
2	Inlet	Reference Frame			2.52	
	Outlet lower	-20	300	1.3	4.72	0.23
	Outlet upper	30	300	1.5	4.74	0.30
	Total head loss					0.53
3	Inlet	Reference Frame			2.52	
	Outlet lower	-30	200	0.9	4.71	0.21
	Outlet upper	40	200	1.0	4.73	0.32
	Total head loss					0.53
4	Inlet	Reference Frame			2.52	
	Outlet lower	-30	300	1.0	4.69	0.17
	Outlet upper	40	300	1.2	4.71	0.22
	Total head loss					0.4
5	Inlet	Reference Frame			2.55	
	Outlet lower	-30	300	2.0	4.7	0.33
	Outlet upper	40	300	1.7	4.69	0.63
	Total head loss					0.96

As the length of the pipe increases the loss also increase.The simulation results prooves this reality in the above table at bifurcation considaration 1 and 5. Since the length of these distrbuter is very high there is high loss which is shown in red colour.Due to this reason reject these two types of bifurcation.When we see bifurcation type 2,3 and 4 they have almost equal hydraulic loss but different length and radius. To select the best one from these three distributer let we see the pressure contour and velocity contour.

5.1.1 PRESSURE CONTOUR FOR DISTRIBUTER

As it can be seen in the following figure 5.2 and 5.3 its pressure contour shows that low pressure at the bending radius of the distributer which is not good pressure distribution which is sudden change in pressure especially in distributer bifurcation consideration 2 and 3. In the bifurcation consideration of 1 and 5 has high loss, so bifurcation consideration 4 is smooth transition of pressure as well as less head loss was obtained due to this advantage it was selected.

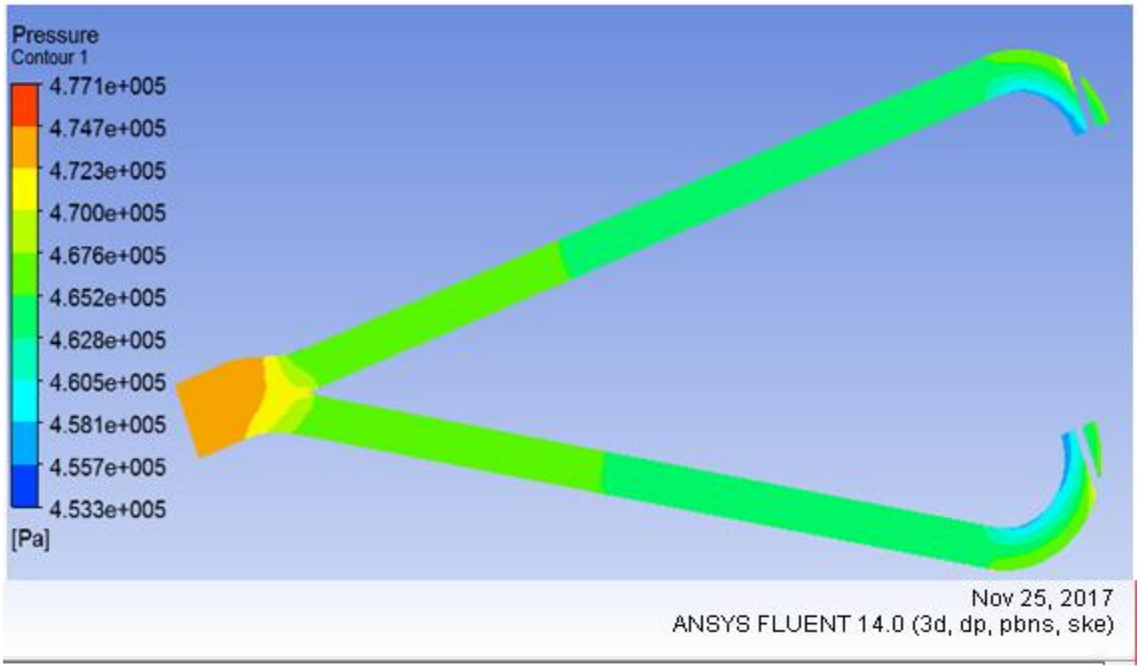

Fig 5.1 Pressure distribution for bifurcation consideration 1(Lower and upper distributer at splitting angle 20 and 30 degree respectively, bending radius 300mm, and length 3.3m)

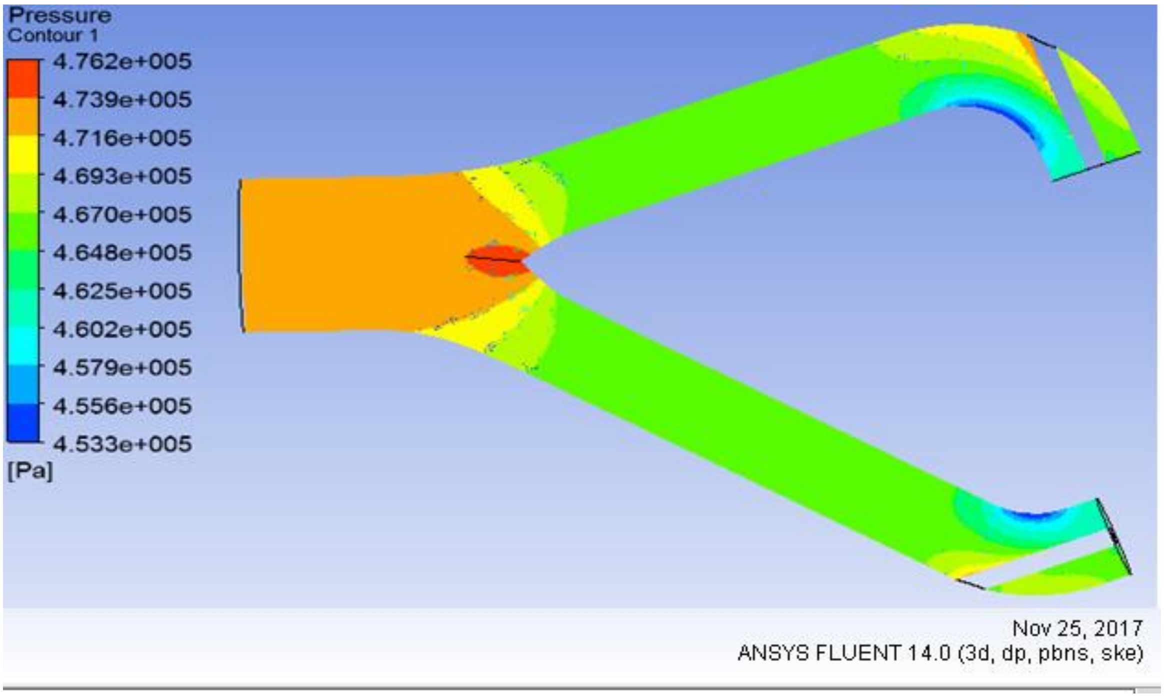

Fig 5.2 Pressure distribution for bifurcation consideration 2(Lower and upper distributer at splitting angle of 20 and 30, lower and upper distributer 1.3m and 1.5m length respectively and both 300mm bending radius)

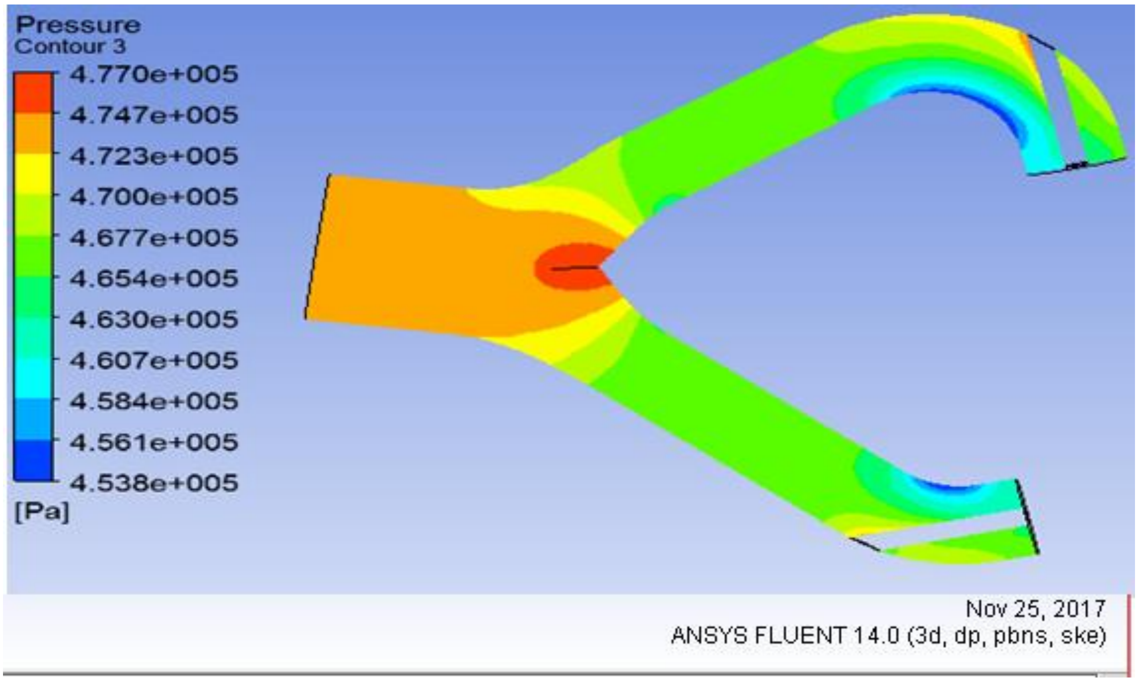

Fig 5.3 Pressure distribution for bifurcation consideration 3(Lower and upper distributer at splitting angle of 30 and 40, lower and upper distributer 0.9 m and 1m length respectively and both 200mm bending radius)

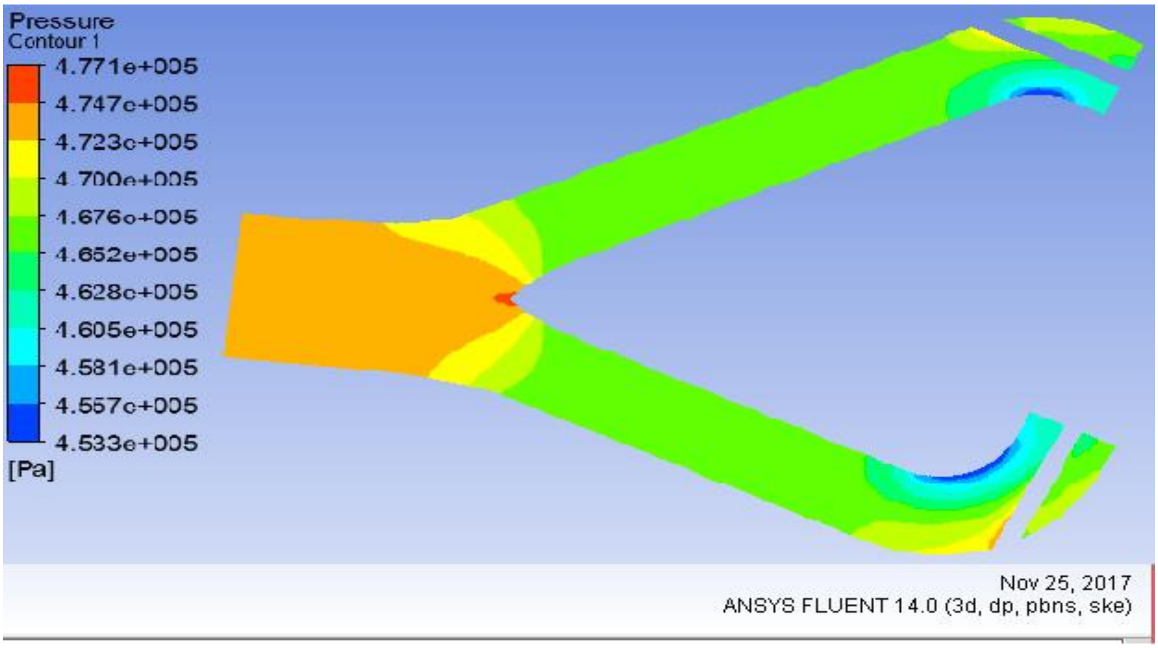

Fig 5.4 Pressure distribution for bifurcation consideration 4(Lower and upper distributer at splitting angle of 30 and 40, lower and upper distributer 1 m and 1.2m length respectively and both 300mm bending radius)

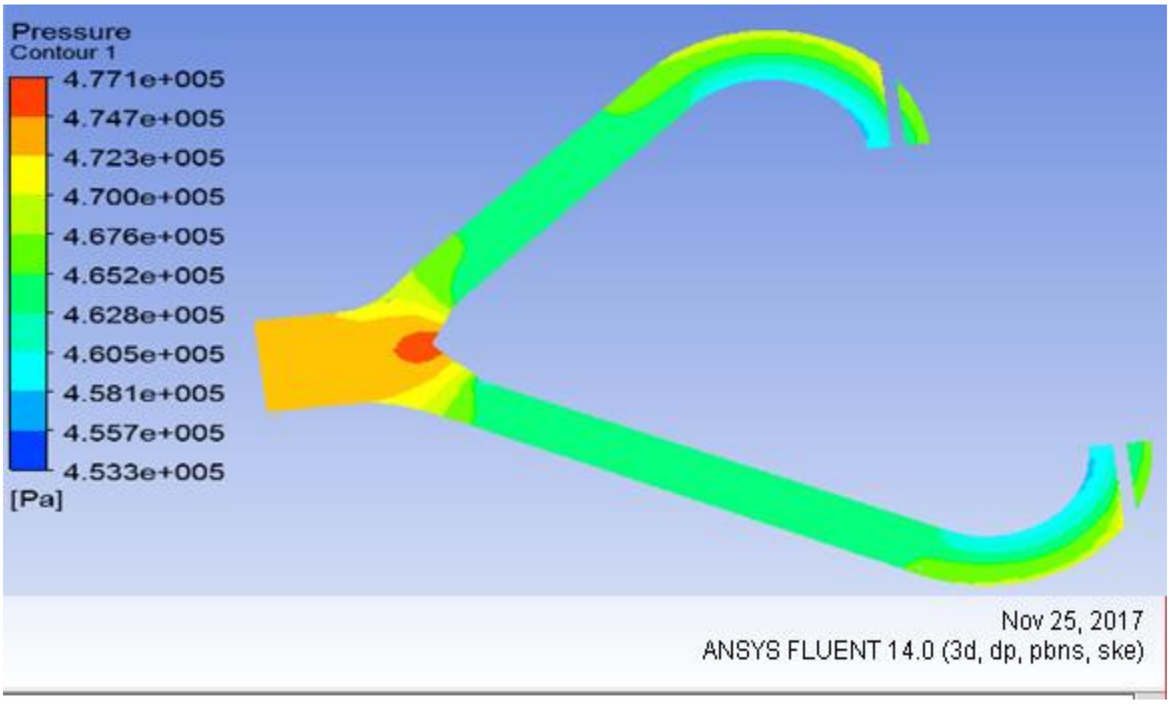

Fig 5.5 Pressure distribution for bifurcation consideration 5 (Lower and upper distributer at splitting angle of 30 and 40, lower and upper distributer 2 m and 1.7 m length respectively and both 300mm bending radius)

5.1.2 VELOCITY CONTOUR

The velocity contours shows how the velocity is distributed or the flow pattern of each bifurcation consideration. The following figure shows the distribution of the velocity with in the five types of consideration and one of them is selected.

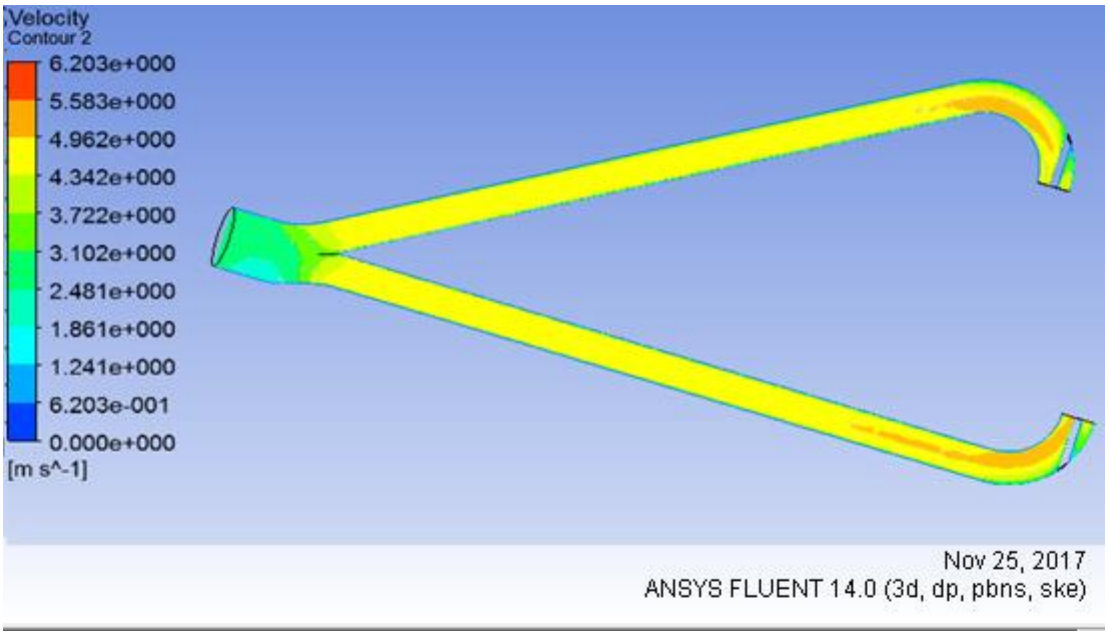

Fig 5.6 Velocity distribution for bifurcation type 1(Lower and upper distributer at splitting angle 0 and 30 degree respectively, bending radius 300mm, and length 3.3m)

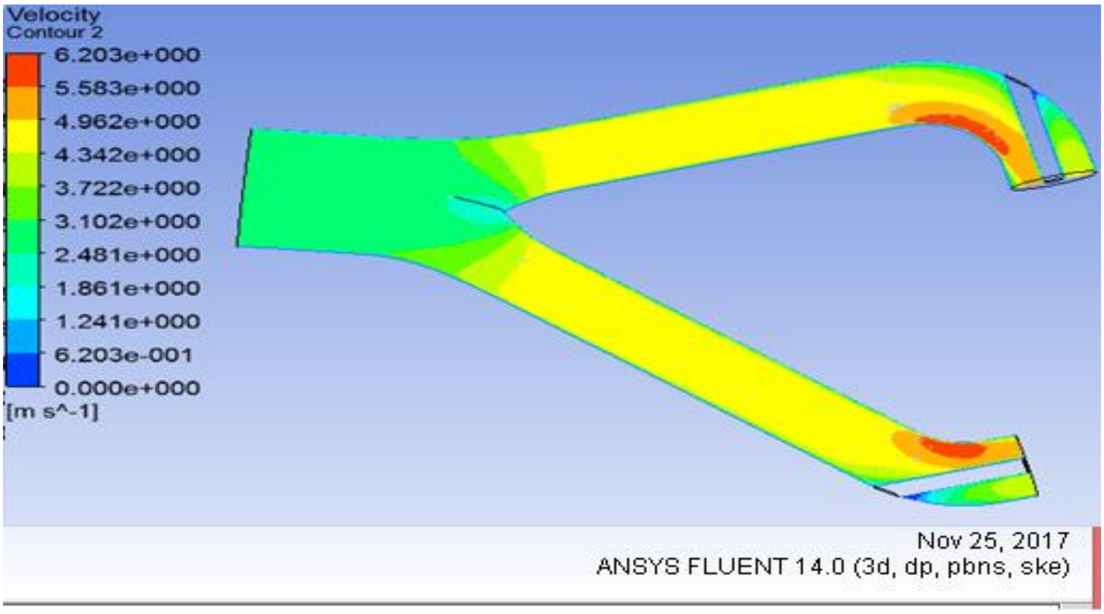

Fig 5.7 Velocity distribution of bifurcation type 2 (Lower and upper distributer at splitting angle of 20 and 30, 1.3m and 1.5m length respectively and both 300mm bending radius)

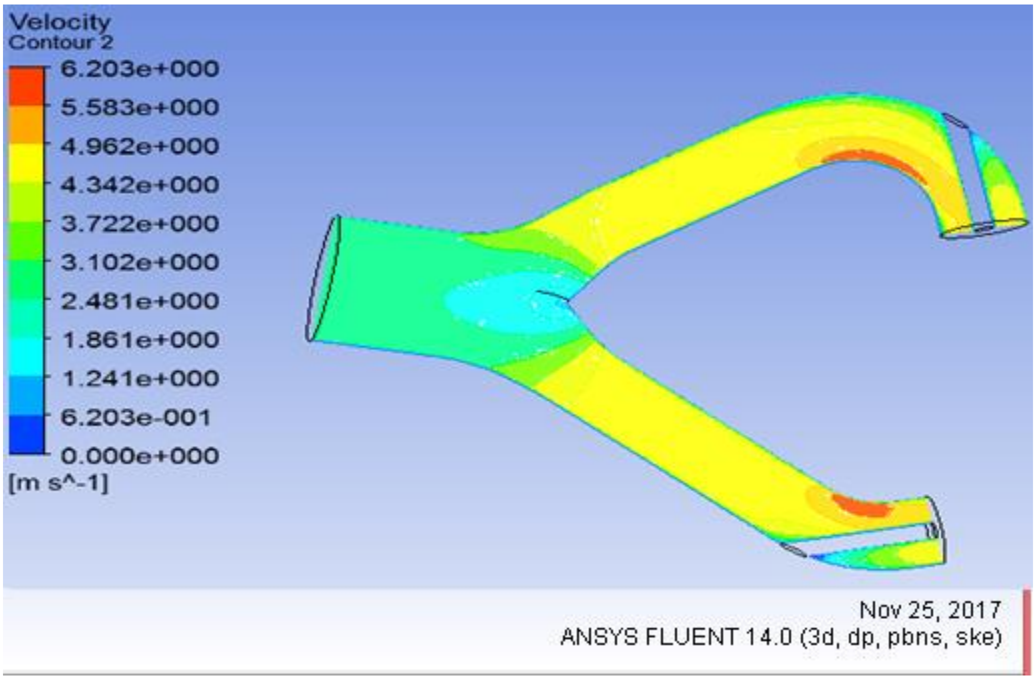

Fig 5.8 Velocity distribution of bifurcation type 3(Lower and upper distributer at splitting angle of 30 and 40, 0.9 m and 1m length respectively and both 200mm bending radius)

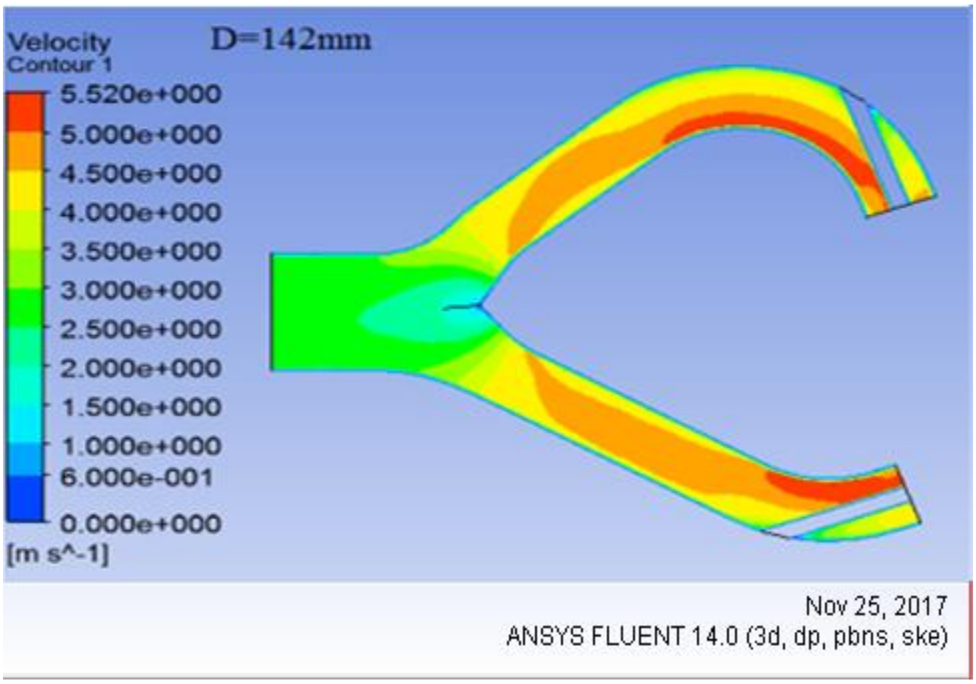

Fig 5.9 Velocity distribution of bifurcation type 4(Lower and upper distributer at splitting angle of 30 and 40 degree, 1 m and 1.2m length respectively and both 300mm bending radius)

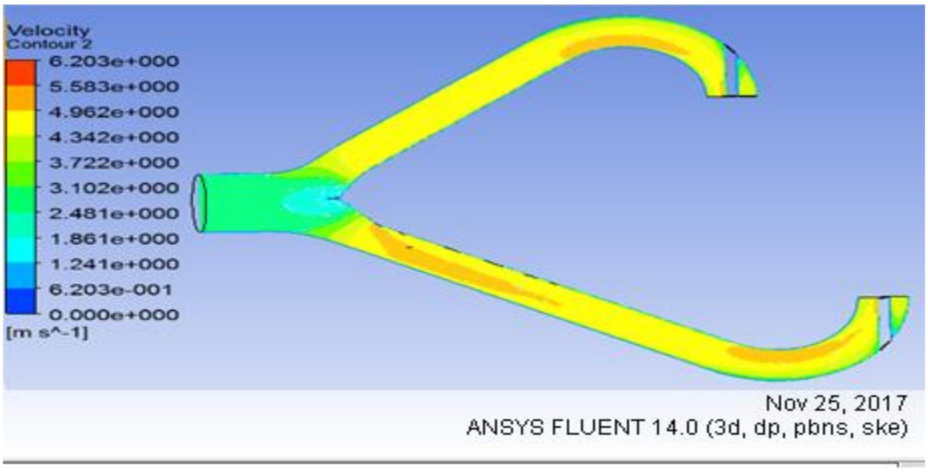

Fig 5.10 Velocity distribution of bifurcation type 5 (Lower and upper distributer at splitting angle of 30 and 40, lower and upper distributer 2 m and 1.7m length respectively and both 300mm bending radius)

Still in velocity contour there is a huge difference between distributer 2, 3, and 4.As you see distributer 2 and 3 the velocity contour is not good because at the curved (bending radius) of the distributer there is very high velocity in red color but when we came to distributer four (4) the distribution is smooth and best especially the lower elbow. Therefore distributer type 4 is best optimized interms of split angle, bending radius and length.

5.1.3 HEAD LOSS CALCULATION BASED ON DIFFERENT DISTRIBUTER DIAMETER

From previous analysis the distributer is optimized interms of bending radius, split angle and length. The next simulation aimed at further optimization based on the diameter optimized and selected diameter. Head loss analysis at different diameter for bifurcation type 4

From appendix F at diameter of 150 mm there is highest head loss. So we can reject it from the comparison. Next since the goal of the thesis focus on optimization, at diameter 160mm and 170mm the head loss is minimum but when we see the outlet velocity which is inlet for the nozzle is very small. A distributer having a diameter of 150mm and 142 mm has highest outlet velocity which enhances the nozzle to produce a high jet power i.e. directly convert into kinetic energy. It is fact that when choosing the distributer diameter, the efficiency of the nozzle has to be observed at different nozzle diameter since there will be high head loss when the efficiency drops a little. This will be verified looking at table 5.11 and Table 5.23. Depending on this fact a distributer having a diameter of 142mm is selected comparing the head loss in distributer and nozzle. The following table summarized for different diameter the head loss has been calculated in the following table.

Table 5.7 The head loss calculation for the 4 different diameters

Bifurcation option	Parts of bifurcation Under consideration	D, (mm)	Split angle	Bending radius, (mm)	Length, (m)	Out let Velocity, (m/s)	Head loss, (m)
4	Inlet	266	Reference Frame			2.52	
	Outlet lower	142	-30	300	1.0	4.697	0.172
	Outlet upper	142	40	300	1.2	4.710	0.226
	Total head loss						0.4
	Inlet	266	Reference Frame			2.52	
	Outlet lower	150	-30	300	1.0	4.12	0.23
	Outlet upper	150	40	300	1.2	4.15	0.23
	Total head loss						0.46
	Inlet	266	Reference Frame			2.52	
	Outlet lower	160	-30	300	1.0	3.62	0.13
	Outlet upper	160	40	300	1.2	3.64	0.17
	Total head loss						0.30
	Inlet	266	Reference Frame			2.52	
	Outlet lower	170	-30	300	1.0	3.25	0.11
	Outlet upper	170	40	300	1.2	3.25	0.13
	Total head loss						0.24

From the Ansys result in appendix G and H the following conclusion are made.

The pressure distribution of a distributer having a diameter of 170mm is smooth comparing to the rest. From the concept of fluid mechanics as the diameter decreases the pressure drop increases but in other word the velocity of the flow getting high i.e. as the flow rate which is multiplication of area and velocity. So decreasing the diameter will let the velocity to be high since flow rate is constant in constant diameter of distributer.

One of the main purpose of distributer is to direct flow to the nozzles. In addition to this the distributer has to be a little bit a converging pipe in need of transition to kinetic energy (convert potential energy to kinetic) and the flow has to be undisturbed to increase the performance of the nozzle. Depending on this fact a distributer having an outlet diameter of 142mm is best suited among the rest since it has a high velocity change at the exit of the distributer as compared to the others. This distribution is clearly seen from the dark red and yellow colors, as they are denoted for higher velocity in *velocity legend bar*. Looking the velocity distribution of a distributer having a diameter 170mm, it has a smooth velocity distribution. But as a function of a distributer this is not the advantage.

As a whole a distributer having a diameter of 142mm is selected even if it has a medium head loss and rough pressure distribution comparing to the others. This is compensated looking the velocity distribution and the higher nozzle efficiency demand.

5.2 NOZZLE AND SPEAR RESULT AND DISCUSSION

The optimization of nozzle and spear shape first requires attention to identifying the most important factors that influence the performance (efficiency) value. To identify this influential parameters the parameter correlation tool in Ansys design explorer are used, so that finally to be able to exclude unimportant parameters in design optimization goal tool and reduce the number of design points(the design points are the nozzle and spear parameters) in design of experiments (DOE).

5.2.1 SAMPLING OF DESIGN POINTS

• The Parameters Correlation method will perform simulations based on a random sampling of the design space (using Latin Hypercube sampling), so as to identify the correlation between all parameters.

• Latin hypercube:-Points are randomly placed, but care is taken to ensure that no two points share input parameters of the same value.

The following tables shows the input parameters used, general setting filled and convergence of design points created in the parameter correlation tab property.

Table 5.8 Sampling of design points to select best nozzle angle from 83 sample

Outline of Schematic B2: Parameters Correlation

	A	B	C
1		Enabled	Quick Help
2	Parameters Correlation		
3	Input Parameters		
4	design parameters (A1)		
5	P15 - bulb_diameter	☑	
6	P16 - blocking_distance	☑	
7	P95 - nozzle_dimater_half	☑	
8	P19 - spear_fillet	☑	
9	P20 - nozzle_curvature	☑	
10	P86 - nozzle_angle	☑	
11	P87 - spear_angle	☑	
12	P93 - extennded_length	☑	

Properties of Outline A2: Correlation

	A	B
1	Property	Value
2	Design Points	
3	Preserve Design Points After DX Run	☑
4	Retain Files for Preserved Design Points	☑
5	Parameters Correlation	
6	Reuse the samples already generated	☑
7	Correlation Type	Spearman
8	Number Of Samples	83
9	Auto Stop Type	Enable Auto Stop
10	Mean Value Accuracy	0.01
11	Standard Deviation Accuracy	0.02
12	Convergence Check Frequency	65
13	Size of Generated Sample Set	82
14	Converged	Yes

Auto Stop Type:-The number of samples required to calculate correlation is determined according to convergences of means and standard deviations of output parameters. At each iteration, convergences of means and standard deviations are checked against accuracy provided. The iteration stops when accuracy is met, or number of samples exceeds the maximum value set by the user, whichever comes first.

The following table shows the input parameters set for the parameter correlation. The checked mark shows the parameter is used for the parameter correlation.

Table 5.9 Set input parameters

Outline of Schematic B2: Parameters Correlation

	A	B	C
1		Enabled	Quick Help
2	Parameters Correlation		
3	Input Parameters		
4	design parameters (A1)		
5	P15 - bulb_diameter	☑	
6	P16 - blocking_distance	☑	
7	P95 - nozzle_dimater_half	☑	
8	P19 - spear_fillet	☑	
9	P20 - nozzle_curvature	☑	
10	P86 - nozzle_angle	☑	
11	P87 - spear_angle	☑	
12	P93 - extennded_length	☑	
13	P94 - rod_diameter_half	☐	
14	P96 - orifice_diameter_half	☐	

The following table shows the bounding limits and properties of checked input parameters

Table 5.10 Properties of checked input parameters

Properties of Outline A5: P15

	A	B
1	Property	Value
2	General	
3	Units	
4	Type	Design Variable
5	Classification	Continuous
6	Values	
7	Initial Value	85
8	Lower Bound	75
9	Upper Bound	100

Properties of Outline A6: P16

	A	B
1	Property	Value
2	General	
3	Units	
4	Type	Design Variable
5	Classification	Continuous
6	Values	
7	Initial Value	45
8	Lower Bound	15
9	Upper Bound	90

Properties of Outline A7: P95

	A	B
1	Property	Value
2	General	
3	Units	
4	Type	Design Variable
5	Classification	Continuous
6	Values	
7	Initial Value	60
8	Lower Bound	60
9	Upper Bound	90

Properties of Outline A8: P19

	A	B
1	Property	Value
2	General	
3	Units	
4	Type	Design Variable
5	Classification	Continuous
6	Values	
7	Initial Value	22.5
8	Lower Bound	15
9	Upper Bound	50

Properties of Outline A9: P20

	A	B
1	Property	Value
2	General	
3	Units	
4	Type	Design Variable
5	Classification	Continuous
6	Values	
7	Initial Value	70
8	Lower Bound	50
9	Upper Bound	85

Properties of Outline A10: P86

	A	B
1	Property	Value
2	General	
3	Units	
4	Type	Design Variable
5	Classification	Continuous
6	Values	
7	Initial Value	45
8	Lower Bound	30
9	Upper Bound	45

Properties of Outline A11: P87

	A	B
1	Property	Value
2	General	
3	Units	
4	Type	Design Variable
5	Classification	Continuous
6	Values	
7	Initial Value	20
8	Lower Bound	20
9	Upper Bound	25

In this setting the analysis is done and the following table shows different sampling design points and the result got from Ansys parameter correlation

Input parameters:- P15 - bulb diameter ; P16 - blocking distance ; P95 - nozzle_dimater_half ; P19 - spear fillet ; P20 - nozzle curvature ; P86 - nozzle angle ; P87 - spear angle.

Output parameters: - P84 - Vout (m s^-1); P98 - inlet static pressure (Pa); P99 - inlet total pressure (Pa); P100 - inlet velocity (m s^-1); P101 - inlet dynamic pressure (Pa); P105 - outlet dynamic pressure (Pa); P107 - outlet total pressure (Pa).

Table 5.11 Sampling points of the parameter correlation and their output parameters results

Name	P15	P16	P95	P19	P20	P86	P87	P84	P98	P99	P100	P101	P105	P107
1	85.4	40.5	80.3	37.0	81.7	40.3	20.2	24.2	468467	478855	4.6	10389	310433	310264
2	99.4	53.2	73.3	47.9	63.9	34.1	24.3	28.3	458065	478855	6.5	20791	414497	414701
3	92.7	69.0	71.6	30.1	68.5	35.7	23.7	28.6	455311	478855	6.9	23545	424744	425261
4	97.8	36.2	75.7	27.2	62.4	44.4	22.8	23.9	465825	478855	5.1	13031	308634	308488
5	75.0	49.5	60.6	28.5	66.4	41.6	23.4	26.6	437233	478855	9.1	41623	374825	374938
6	78.6	28.1	81.9	42.3	83.5	33.2	23.1	23.7	469682	478855	4.3	9173	296969	296799
7	82.7	56.4	73.6	46.7	77.9	44.6	23.2	26.6	460705	478855	6.0	18151	373997	374157

8	99.9	31.4	61.7	44.4	65.1	31.8	22.3	25.4	443754	478855	8.4	35101	339534	339502
9	79.2	38.3	79.0	37.4	55.6	43.4	21.2	23.4	468496	478855	4.6	10359	290639	290449
10	81.6	25.7	64.1	29.0	60.1	42.3	21.6	19.5	461155	478855	6.0	17701	220213	219945
11	77.4	56.9	72.8	17.7	60.6	35.8	21.5	27.7	458450	478855	6.4	20406	396268	396642
12	84.3	60.5	85.8	43.7	50.8	34.9	22.7	28.0	468326	478855	4.6	10530	404893	405451
13	80.1	64.5	89.4	37.9	71.8	36.2	23.1	27.9	470010	478855	4.2	8846	403847	404772
14	83.9	39.4	60.0	25.4	74.0	36.6	23.5	26.1	437046	478855	9.1	41810	361318	361067
15	83.8	15.5	74.1	27.9	84.0	38.7	24.4	14.4	473560	478855	3.3	5295	141017	140584
16	90.0	17.5	84.0	36.3	70.8	42.5	22.9	15.2	475380	478855	2.6	3475	142513	142376
17	84.9	60.1	88.7	32.5	71.1	41.8	24.2	26.9	470280	478855	4.1	8576	382729	383424
18	98.2	51.5	77.3	15.3	69.5	44.0	21.5	26.0	464714	478855	5.3	14141	357437	357347
19	89.0	69.6	66.2	46.5	50.3	37.2	24.7	28.3	446618	478855	8.0	32238	421001	422079
20	94.9	52.3	71.6	41.0	80.1	43.2	22.4	26.4	458767	478855	6.3	20089	370182	370092
21	86.0	58.2	65.5	29.5	79.3	30.9	20.6	28.5	445152	478855	8.2	33704	415829	415953
22	82.9	36.3	86.2	31.0	62.7	39.5	21.4	23.6	471479	478855	3.8	7377	297077	296933
23	91.4	30.5	84.5	45.1	60.8	30.4	20.1	24.2	470421	478855	4.1	8435	309121	308944
24	88.2	41.1	69.0	44.0	75.0	30.7	23.0	27.6	453373	478855	7.1	25483	393360	393511
25	80.9	61.8	70.3	41.1	76.7	40.0	22.6	27.6	455217	478855	6.9	23638	397470	397726
26	86.7	28.3	72.3	31.5	75.5	43.0	24.0	21.5	465997	478855	5.1	12858	260576	260285
27	96.3	22.6	64.4	16.5	72.7	40.8	25.0	19.3	461721	478855	5.9	17134	232029	231638
28	81.1	21.3	77.9	26.1	67.3	40.5	21.8	17.6	472597	478855	3.5	6258	176679	176273
29	75.7	45.6	87.3	48.5	79.8	36.4	23.6	26.6	470046	478855	4.2	8810	367567	367795
30	88.6	44.1	68.1	45.9	77.6	38.7	23.9	26.6	453716	478855	7.1	25140	372475	372523
31	90.6	63.2	67.5	40.3	76.2	38.4	22.2	27.9	450035	478855	7.6	28820	406135	406356
32	87.5	39.3	63.1	33.7	57.7	30.5	20.2	26.8	443497	478855	8.4	35359	373336	373333
33	98.7	62.1	77.3	32.1	55.9	37.3	23.6	28.1	462335	478855	5.8	16520	412215	412573
34	94.2	31.1	75.0	43.1	58.4	44.5	24.2	22.9	466471	478855	5.0	12384	285156	285008
35	96.8	34.5	80.4	17.4	81.6	34.7	21.7	25.2	467612	478855	4.7	11244	334215	334145
36	84.9	38.7	73.1	29.9	74.9	44.0	24.3	24.5	463019	478855	5.6	15837	324397	324161
37	99.3	37.4	63.3	15.4	67.6	42.5	23.2	24.2	450326	478855	7.6	28530	319611	319307
38	92.6	20.8	79.9	43.6	84.9	43.3	20.7	16.3	474055	478855	3.1	4801	153133	152701
39	97.3	52.5	65.6	37.6	58.8	33.1	22.9	28.1	446134	478855	8.1	32721	407273	407291
40	75.3	40.9	71.8	22.2	76.0	41.9	20.3	24.1	462482	478855	5.7	16373	307672	307526
41	78.4	43.0	81.1	32.9	71.3	30.9	23.5	27.4	466080	478855	5.1	12775	387954	388200
42	82.2	32.6	89.3	39.2	55.9	40.2	23.0	23.1	472790	478855	3.5	6066	285298	285204
43	100.0	49.2	61.5	34.5	72.7	30.7	24.7	27.8	436594	478855	9.2	42262	396307	396384
44	79.2	66.4	72.8	17.9	79.9	31.6	24.6	28.9	456396	478855	6.7	22460	432875	433371
45	81.2	66.7	80.5	49.9	60.3	39.6	22.2	27.5	465599	478855	5.2	13256	394697	395460

46	77.0	44.8	85.9	44.4	64.5	44.3	24.7	25.2	470307	478855	4.1	8549	338807	339102
47	83.9	17.5	75.7	30.9	81.3	36.8	24.1	17.0	472252	478855	3.6	6604	175600	175370
48	79.9	18.4	64.5	32.5	82.0	40.0	22.4	16.2	467048	478855	4.9	11808	161467	161162
49	83.6	62.5	68.4	48.4	69.7	39.9	21.3	27.4	452547	478855	7.3	26308	393676	393878
50	83.3	59.2	61.0	43.5	59.6	37.6	24.5	28.1	434134	478855	9.5	44722	409832	409842
51	89.8	68.1	84.5	41.2	65.5	37.0	20.5	27.8	467754	478855	4.7	11101	400992	401222
52	84.4	60.6	82.9	36.6	83.7	38.8	23.3	27.4	467084	478855	4.9	11772	394296	394844
53	97.8	54.7	69.2	16.6	76.9	44.9	24.4	26.8	454806	478855	7.0	24049	381821	381905
54	88.6	33.7	71.4	26.8	78.3	31.3	21.8	26.1	459138	478855	6.3	19718	355202	355173
55	94.6	29.1	76.9	47.6	66.3	37.7	22.0	22.8	467847	478855	4.7	11008	279831	279649
56	85.5	41.8	64.6	45.5	64.0	32.2	22.8	27.4	445539	478855	8.2	33317	389731	389918
57	82.5	65.4	75.8	41.7	66.0	38.2	20.9	27.6	461611	478855	5.9	17244	397779	397990
58	91.3	27.0	89.7	38.1	61.2	36.0	23.4	22.6	473107	478855	3.4	5749	276563	276648
59	87.7	19.4	69.4	48.5	62.5	36.6	20.9	17.7	468616	478855	4.5	10239	179550	179273
60	80.6	21.4	66.9	18.5	54.3	32.8	22.1	20.9	462133	478855	5.8	16723	238432	238123
61	86.8	42.5	74.8	22.7	55.7	40.9	21.8	25.2	463712	478855	5.5	15144	335924	335836
62	95.9	36.1	81.6	33.8	53.6	43.8	24.9	24.0	469190	478855	4.4	9665	314921	314903
63	80.8	68.6	74.0	23.6	82.4	42.4	23.1	27.4	459964	478855	6.1	18891	397679	398531
64	75.8	30.6	79.2	42.7	55.1	36.5	23.9	23.7	468261	478855	4.6	10594	299445	299396
65	88.2	33.0	63.7	46.9	78.7	34.4	22.3	25.4	448373	478855	7.8	30482	340313	340213
66	90.3	63.9	85.3	25.5	53.2	33.4	21.9	28.4	467760	478855	4.7	11095	415464	416114
67	97.2	28.2	82.0	38.6	80.7	30.2	24.0	25.6	468141	478855	4.6	10715	344927	344637
68	85.1	25.0	78.0	32.2	61.4	41.1	25.0	20.4	470418	478855	4.1	8437	238942	238585
69	87.0	22.9	78.6	18.8	80.4	35.3	20.1	19.8	471264	478855	3.9	7592	214030	213819
70	89.0	43.9	79.8	25.9	79.2	34.1	21.1	26.7	465848	478855	5.1	13008	370734	370813
71	86.2	16.6	68.1	40.5	51.5	38.9	21.6	15.4	470510	478855	4.1	8346	142689	142359
72	78.6	26.5	66.4	35.3	72.1	30.4	20.4	23.0	457962	478855	6.5	20894	280696	280518
73	98.2	50.5	83.7	42.4	74.5	34.6	21.4	27.4	467662	478855	4.7	11194	388661	388705
74	80.3	69.5	61.9	24.6	50.2	33.8	20.4	28.6	435405	478855	9.3	43450	420156	420212
75	92.7	22.0	70.2	46.6	51.8	40.5	23.7	19.3	467165	478855	4.8	11691	216777	216743
76	93.4	61.7	87.1	20.6	52.2	35.6	22.6	28.1	468877	478855	4.5	9979	407668	407946
77	92.3	29.5	83.4	39.6	63.4	30.5	20.7	24.2	469988	478855	4.2	8868	308785	308857
78	99.2	31.4	74.6	34.1	83.2	34.9	21.1	24.2	464737	478855	5.3	14119	310834	310817
79	93.8	39.7	86.7	21.6	69.9	35.3	22.4	26.1	470107	478855	4.2	8748	353761	353992
80	82.9	56.9	88.9	25.1	77.9	31.8	24.8	28.5	469425	478855	4.3	9430	418481	419145
81	77.5	23.9	60.2	16.9	62.1	40.8	23.6	19.8	454948	478855	6.9	23908	229485	229074
82	91.6	45.7	78.4	31.5	57.4	32.5	24.2	27.9	463604	478855	5.5	15251	401879	402002

The following fig shows the relationships the input parameters have with output parameters

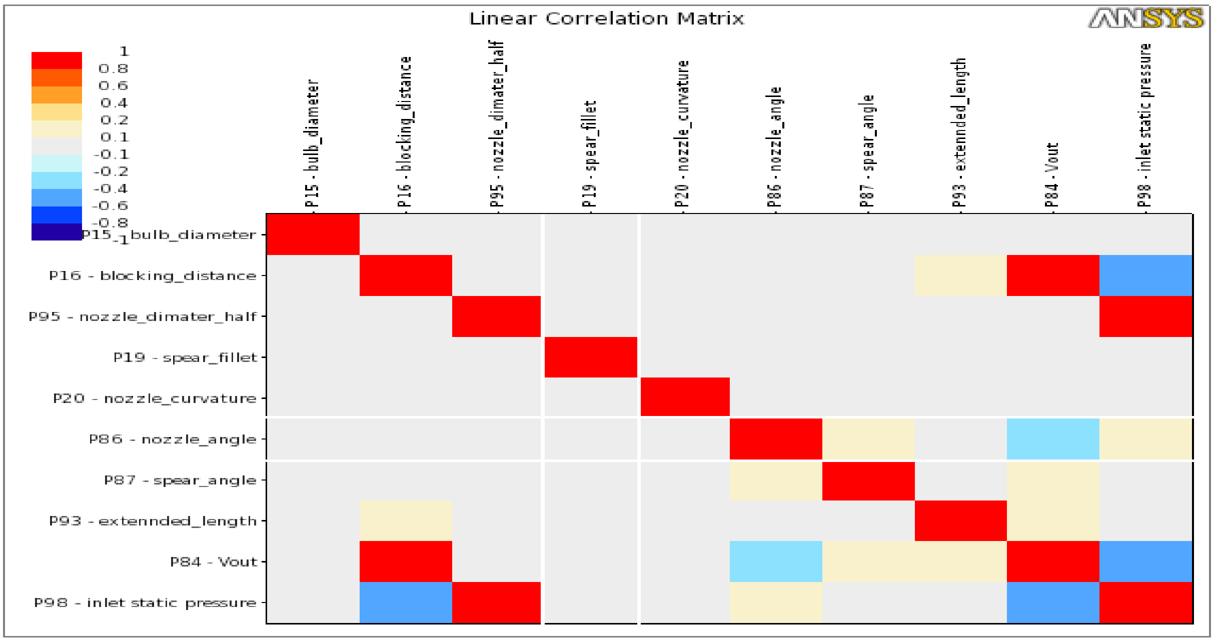

Fig 5.11 Linear correlation between input and output parameters

The closer to the extremes (-1 or 1) the stronger the relationship. The low colors indicate that bulb diameter, spear fillet, and nozzle curvature radius have low impact on the result of V_{out} *and inlet static pressure*. And the blind color and medium intensity colors tells that blocking distance, nozzle diameter, nozzle angle, spear angle and extended length have an impact on the results (V_{out} *and inlet static pressure*) of the analysis.

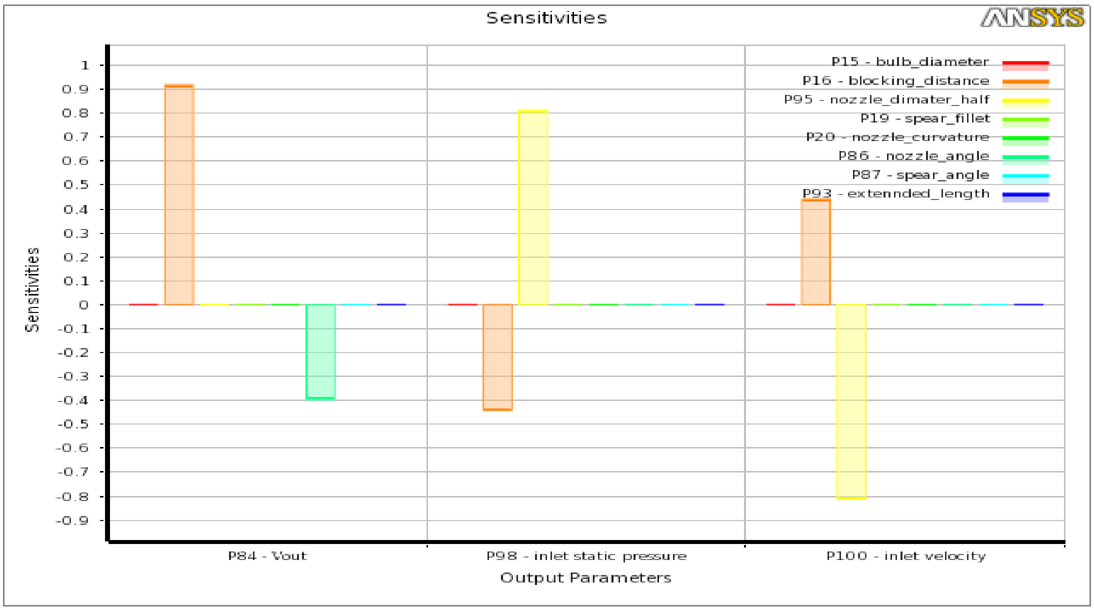

Fig 5.12 Sensitivity bar for defined parameter set

As it can be seen from the sensitivity bar blocking distance have a direct correlation (0.8) and nozzle angle have a reverse correlation (-0.4) to the outlet velocity of the nozzle. On same way nozzle diameter have a direct influence (0.8) and blocking distance a reverse influence (-0.45) on inlet static pressure of the nozzle. For the case of inlet velocity blocking distance have direct impact (0.45) and nozzle diameter a reverse impact (-0.8). Other parameters such as; Bulb diameter, spear fillet, extended length, spear angle and nozzle curvature lies on the horizontal axis (I.e. zero sensitivity or negligible influence on the output parameters). This means that they are unimportant or less influential parameters to the result of the optimization.

After all this analyzing I can conclude that nozzle angle, blocking distance, and nozzle diameter would be the most important parameters in optimizing the design. Optimization of the results using Ansys design explorer direct optimization tool by only altering only the most important parameters predicts well for just screening the first three candidate design points for their highest value of C_D , $C_v, C_c, and\ C_P$.

5.2.2 EFFECT OF NOZZLE ANGLE ON THE OUTPUT RESULTS

While optimizing the $C_v, C_c, and\ C_P$ the nozzle angle is altered in bounds of 30° to 45° to get design of experiments as shown on the following table. The rest of the design parameters are set constant to get only the effect of the nozzle angle.

Table 5.12 DOE only for nozzle angle

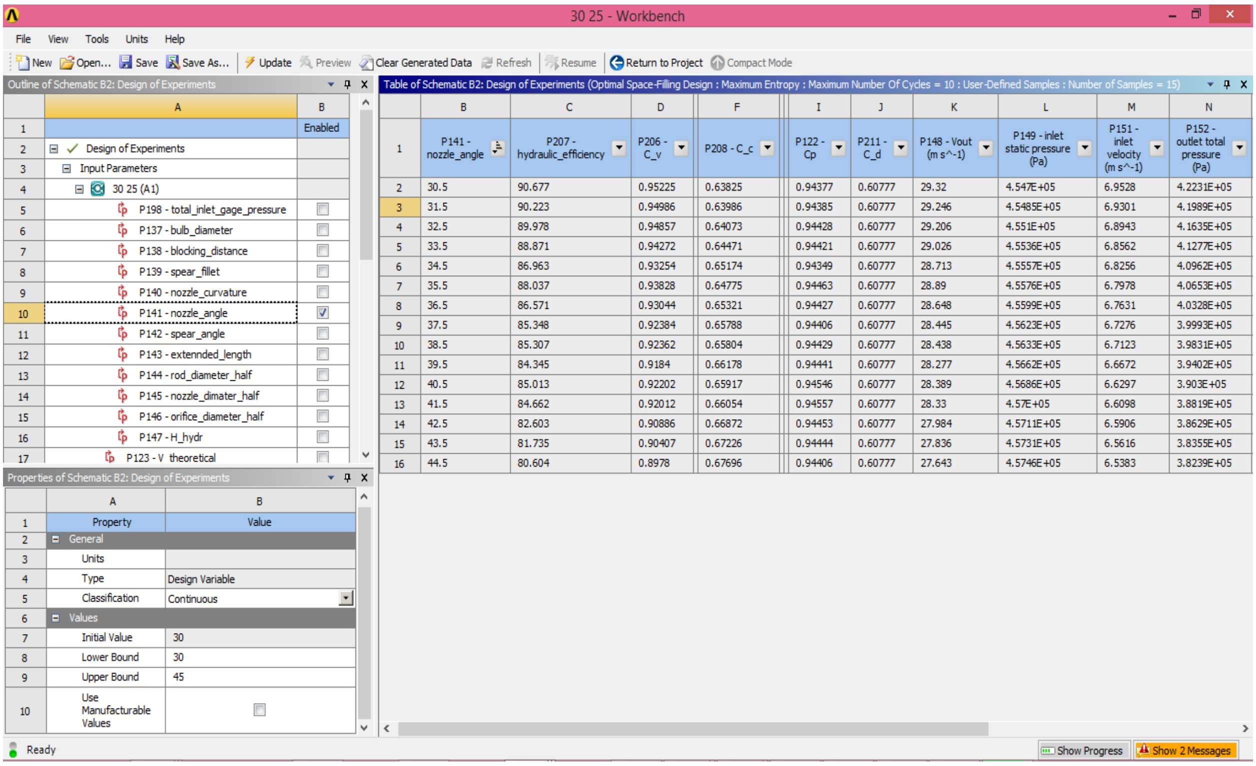

Table of Schematic B2: Design of Experiments (Optimal Space-Filling Design : Maximum Entropy : Maximum Number Of Cycles = 10 : User-Defined Samples : Number of Samples = 15)

	B	C	D	F	I	J	K	L	M	N
1	P141 - nozzle_angle	P207 - hydraulic_efficiency	P206 - C_v	P208 - C_c	P122 - Cp	P211 - C_d	P148 - Vout (m s^-1)	P149 - inlet static pressure (Pa)	P151 - inlet velocity (m s^-1)	P152 - outlet total pressure (Pa)
2	30.5	90.677	0.95225	0.63825	0.94377	0.60777	29.32	4.547E+05	6.9528	4.2231E+05
3	31.5	90.223	0.94986	0.63986	0.94385	0.60777	29.246	4.5485E+05	6.9301	4.1989E+05
4	32.5	89.978	0.94857	0.64073	0.94428	0.60777	29.206	4.551E+05	6.8943	4.1635E+05
5	33.5	88.871	0.94272	0.64471	0.94421	0.60777	29.026	4.5536E+05	6.8562	4.1277E+05
6	34.5	86.963	0.93254	0.65174	0.94349	0.60777	28.713	4.5557E+05	6.8256	4.0962E+05
7	35.5	88.037	0.93828	0.64775	0.94463	0.60777	28.89	4.5576E+05	6.7978	4.0653E+05
8	36.5	86.571	0.93044	0.65321	0.94427	0.60777	28.648	4.5599E+05	6.7631	4.0328E+05
9	37.5	85.348	0.92384	0.65788	0.94406	0.60777	28.445	4.5623E+05	6.7276	3.9993E+05
10	38.5	85.307	0.92362	0.65804	0.94429	0.60777	28.438	4.5633E+05	6.7123	3.9831E+05
11	39.5	84.345	0.9184	0.66178	0.94441	0.60777	28.277	4.5662E+05	6.6672	3.9402E+05
12	40.5	85.013	0.92202	0.65917	0.94546	0.60777	28.389	4.5686E+05	6.6297	3.903E+05
13	41.5	84.662	0.92012	0.66054	0.94557	0.60777	28.33	4.57E+05	6.6098	3.8819E+05
14	42.5	82.603	0.90886	0.66872	0.94453	0.60777	27.984	4.5711E+05	6.5906	3.8629E+05
15	43.5	81.735	0.90407	0.67226	0.94444	0.60777	27.836	4.5731E+05	6.5616	3.8355E+05
16	44.5	80.604	0.8978	0.67696	0.94406	0.60777	27.643	4.5746E+05	6.5383	3.8239E+05

Now when we go to optimization, objective and their importance of levels are set as shown on the following table and the output results of $C_v, C_c, and\ C_P$.

Table 5.13 Optimization of $C_v, C_c, and\ C_P$ by altering only nozzle angle

Table of Schematic B4: Optimization

	A	B	D	E	F	H	I	J
1		P141 - nozzle_angle	P206 - C_v	P203 - A_in	P208 - C_c	P209 - d_jet	P122 - Cp	P211 - C_d
2	Optimization Domain							
3	Lower Bound	30						
4	Upper Bound	45						
5	Optimization Objectives							
6	Objective	No Objective	Maximize	No Objective	Maximize	No Objective	Maximize	No Objective
7	Target Value							
8	Importance		Higher		Lower		Lower	
9	Constraint Handling							
10	Candidate Points							
11	Candidate A	30.008	0.95507	0.015025	0.63637	43.273	0.94383	0.60777
12	Candidate B	31.508	0.94967	0.015025	0.63999	43.519	0.94392	0.60777
13	Candidate C	33.008	0.94372	0.015025	0.64402	43.793	0.94399	0.60777

Optimizing the design by altering nozzle angle only and fixing the other parameters yields a highest value of C_v at 30 degree as shown on the above table.

5.2.3 EFFECT OF NOZZLE DIAMETER ON THE OUTPUT RESULTS

While optimizing the $C_v, C_c, and\ C_P$ the nozzle diameter is altered to get design of experiments as shown on the following table.

The rest of the design parameters are set constant to get only the effect of the nozzle diameter.

Table 5.14 DOE only for nozzle diameter

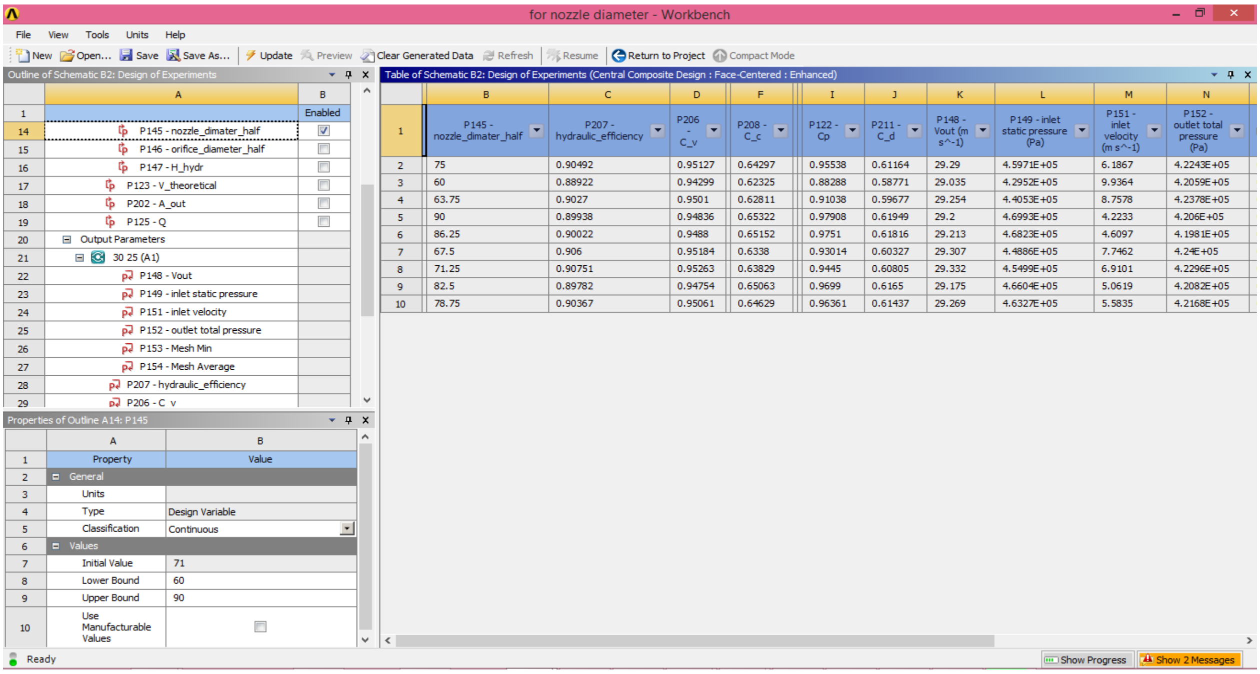

Table of Schematic B2: Design of Experiments (Central Composite Design : Face-Centered : Enhanced)

	B	C	D	F	I	J	K	L	M	N
1	P145 - nozzle_dimater_half	P207 - hydraulic_efficiency	P206 - C_v	P208 - C_c	P122 - Cp	P211 - C_d	P148 - Vout (m s^-1)	P149 - inlet static pressure (Pa)	P151 - inlet velocity (m s^-1)	P152 - outlet total pressure (Pa)
2	75	0.90492	0.95127	0.64297	0.95538	0.61164	29.29	4.5971E+05	6.1867	4.2243E+05
3	60	0.88922	0.94299	0.62325	0.88288	0.58771	29.035	4.2952E+05	9.9364	4.2059E+05
4	63.75	0.9027	0.9501	0.62811	0.91038	0.59677	29.254	4.4053E+05	8.7578	4.2378E+05
5	90	0.89938	0.94836	0.65322	0.97908	0.61949	29.2	4.6993E+05	4.2233	4.206E+05
6	86.25	0.90022	0.9488	0.65152	0.9751	0.61816	29.213	4.6823E+05	4.6097	4.1981E+05
7	67.5	0.906	0.95184	0.6338	0.93014	0.60327	29.307	4.4886E+05	7.7462	4.24E+05
8	71.25	0.90751	0.95263	0.63829	0.9445	0.60805	29.332	4.5499E+05	6.9101	4.2296E+05
9	82.5	0.89782	0.94754	0.65063	0.9699	0.6165	29.175	4.6604E+05	5.0619	4.2082E+05
10	78.75	0.90367	0.95061	0.64629	0.96361	0.61437	29.269	4.6327E+05	5.5835	4.2168E+05

Outline of Schematic B2: Design of Experiments

	A	B
1		Enabled
14	P145 - nozzle_dimater_half	☑
15	P146 - orifice_diameter_half	☐
16	P147 - H_hydr	☐
17	P123 - V_theoretical	☐
18	P202 - A_out	☐
19	P125 - Q	☐
20	Output Parameters	
21	30 25 (A1)	
22	P148 - Vout	
23	P149 - inlet static pressure	
24	P151 - inlet velocity	
25	P152 - outlet total pressure	
26	P153 - Mesh Min	
27	P154 - Mesh Average	
28	P207 - hydraulic_efficiency	
29	P206 - C_v	

Properties of Outline A14: P145

	A	B
1	Property	Value
2	General	
3	Units	
4	Type	Design Variable
5	Classification	Continuous
6	Values	
7	Initial Value	71
8	Lower Bound	60
9	Upper Bound	90
10	Use Manufacturable Values	☐

Now when we go to optimization, objective and their importance of levels are set as shown on the following table and the output results of $C_v, C_c, and\ C_P$.

Table 5.15 Optimization of C_v, C_c, and C_P by altering only nozzle diameter

Table of Schematic B4: Optimization

	A	B	D	F	H	I	J
1		P145 - nozzle_dimater_half	P206 - C_v	P208 - C_c	P209 - d_jet	P122 - Cp	P211 - C_d
2	Optimization Domain						
3	Lower Bound	60					
4	Upper Bound	90					
5	Optimization Objectives						
6	Objective	No Objective	Maximize	Maximize	No Objective	Maximize	Maximize
7	Target Value						
8	Importance		Higher	Lower		Lower	Lower
9	Constraint Handling						
10	Candidate Points						
11	Candidate A	77.655	★★ 0.95096	★ 0.64529	43.88	★★ 0.96145	★★ 0.61365
12	Candidate B	72.105	★★★ 0.95248	− 0.63934	43.475	★ 0.94726	★ 0.60896
13	Candidate C	75.885	★★ 0.95118	★ 0.64378	43.777	★★ 0.95755	★★ 0.61235

Optimizing the design by altering nozzle diameter only and fixing the other parameters yields a highest value of C_v at 72mm half nozzle diameter as shown on the above table.As a whole, reading the tables for objective (higher, default and lower) set for the most important parameters yields best value for the coefficient of velocity, pressure, discharge and contraction in rank of higher value requirement at a nozzle angle of 30^0 and 142mm nozzle diameter by the Ansys optimization tool. Therefore three design points configurations including the current DP ($\alpha=30^0$ -$\beta=20^0$, $\alpha=30^0$ -$\beta=25^0$, $\alpha=35^0$ -$\beta=25^0$) will be analyzed at different nozzle opening by Ansys fluent simulation.

5.2.4.EFFECT OF BLOCKING DISTANCE ON THE OUTPUT RESULTS

Table 5.16 Candidate point's spear and nozzle angle.

Candidate DP'S	Nozzle angle	Spear angle
Candidate $\boldsymbol{A_O}$	35	25
Candidate $\boldsymbol{B_O}$	30	20
Candidate $\boldsymbol{C_O}$	30	25

The following table shows candidateA_O's (current DP) geometrical parametric value interms efficiency at different nozzle opening.

Table 5.17 Dimensional values of current design point

Name	P123 - V_theoretical	P198 - total_inlet_gage_pressure	P20...	P125 - Q	P211 - C_d	P137 - bulb_diameter	P138 - blocking_distance	P139 - spear_fillet	P140 - nozzle_curvature	P141 - nozzle_angle	P142 - spear_angle
Units	m s^-1	Pa		m^3 s^-1							
DP 1	30.68	4.7959E+05	0.0036298	0.07	0.61765	85	20	22.5	120	35	25
DP 11	30.68	4.7959E+05	0.0036298	0.07	0.61765	85	25	22.5	120	35	25
DP 2	30.68	4.7959E+05	0.0036298	0.07	0.61765	85	30	22.5	120	35	25
DP 10	30.68	4.7959E+05	0.0036298	0.07	0.61765	85	34	22.5	120	35	25
Current	30.68	4.7959E+05	0.0036298	0.07	0.61765	85	38	22.5	120	35	25
DP 4	30.68	4.7959E+05	0.0036298	0.07	0.61765	85	50	22.5	120	35	25
DP 12	30.68	4.7959E+05	0.0036298	0.07	0.61765	85	55	22.5	120	35	25
DP 5	30.68	4.7959E+05	0.0036298	0.07	0.61765	85	60	22.5	120	35	25
DP 6	30.68	4.7959E+05	0.0036298	0.07	0.61765	85	66	22.5	120	35	25
DP 7	30.68	4.7959E+05	0.0036298	0.07	0.61765	85	68	22.5	120	35	25
DP 13	30.68	4.7959E+05	0.0036298	0.07	0.61765	85	69	22.5	120	35	25
DP 14	30.68	4.7959E+05	0.0036298	0.07	0.61765	85	70	22.5	120	35	25
DP 15	30.68	4.7959E+05	0.0036298	0.07	0.61765	85	72	22.5	120	35	25
DP 8	30.68	4.7959E+05	0.0036298	0.07	0.61765	85	73	22.5	120	35	25
DP 16	30.68	4.7959E+05	0.0036298	0.07	0.61765	85	75	22.5	120	35	25
DP 17	30.68	4.7959E+05	0.0036298	0.07	0.61765	85	78	22.5	120	35	25
DP 18	30.68	4.7959E+05	0.0036298	0.07	0.61765	85	80	22.5	120	35	25

And its performance determining coefficients are tabulated below

Table 5.18 Output parameter's result of current design point

Name	P207 - hydraulic_efficiency	P206 - C_v	P208 - C_c	P210 - Net_head	P209 - d_jet	P122 - Cp	P148 - Vout	P149 - inlet static pressure	P151 - inlet velocity	P152 - outlet total pressure	P153 - Mesh Min	P154 - Mesh Average
Units						kg kg^-1	m s^-1	Pa	m s^-1	Pa		
DP 1	0.54138	0.73578	0.83945	26.192	57.082	0.97649	22.574	4.736E+05	3.4612	2.3824E+05	0.3095	0.89846
DP 11	0.63186	0.7949	0.77702	30.569	52.837	0.97493	24.387	4.7213E+05	3.8617	2.8871E+05	0.28144	0.895
DP 2	0.70849	0.84172	0.7338	34.277	49.898	0.97432	25.824	4.7103E+05	4.1384	3.2596E+05	0.33138	0.8932
DP 10	0.76698	0.87577	0.70526	37.107	47.958	0.97454	26.869	4.704E+05	4.2873	3.4708E+05	0.35281	0.89102
Current	0.78692	0.88708	0.69627	38.071	47.346	0.97384	27.216	4.699E+05	4.4015	3.6503E+05	0.22655	0.88815
DP 4	0.86184	0.92835	0.66532	41.696	45.242	0.97392	28.482	4.6901E+05	4.5993	3.9543E+05	0.25237	0.88553
DP 12	0.87648	0.93621	0.65974	42.404	44.862	0.97387	28.723	4.6881E+05	4.6428	4.0281E+05	0.35719	0.88712
DP 5	0.86714	0.9312	0.66328	41.952	45.103	0.97316	28.569	4.6863E+05	4.6803	4.0734E+05	0.32646	0.88415
DP 6	0.82048	0.9058	0.68188	39.695	46.368	0.97101	27.79	4.6838E+05	4.7318	4.1854E+05	0.2777	0.88438
DP 7	0.81536	0.90297	0.68402	39.447	46.513	0.97065	27.703	4.6832E+05	4.7459	4.2154E+05	0.36461	0.88739
DP 13	0.80828	0.89904	0.68701	39.105	46.716	0.9703	27.583	4.6828E+05	4.7537	4.2289E+05	0.32289	0.88758
DP 14	0.79273	0.89035	0.69371	38.352	47.172	0.96963	27.316	4.6825E+05	4.7607	4.2382E+05	0.3339	0.88537
DP 15	0.76573	0.87506	0.70584	37.046	47.997	0.96841	26.847	4.6819E+05	4.7717	4.282E+05	0.36477	0.88798
DP 8	0.74466	0.86294	0.71575	36.027	48.671	0.96747	26.475	4.6818E+05	4.7751	4.3059E+05	0.31354	0.88749
DP 16	0.72251	0.85001	0.72664	34.955	49.412	0.96632	26.078	4.6812E+05	4.786	4.3623E+05	0.27701	0.88675
DP 17	0.66479	0.81535	0.75753	32.162	51.512	0.96307	25.015	4.6803E+05	4.8072	4.5068E+05	0.34801	0.8859
DP 18	0.60852	0.78008	0.79178	29.44	53.841	0.95957	23.933	4.68E+05	4.8123	4.6509E+05	0.30848	0.88317

The following table shows candidate B_0's geometrical parametric values at different nozzle opening. The nozzle diameter of this DP candidate is got from the optimization of nozzle performance at nozzle diameter of 72mm. To show this diameter is better than the two (77 and 76) nozzle diameters the results are observed in table.

Table 5.19 Hydraulic efficiency at different nozzle diameter

P174 - blocking_distance	P181 - nozzle_dimater_half	P225 - V_out	P207 - hydraulic_efficiency	P210 - Net_head
		m s^-1		
80	71	30.181	96.77	46.45
80	77	29.508	92.509	44.404
80	80	29.914	95.067	45.632

Table 5.20 Dimensional values of candidate B_o

Name	P123 - V_theoretical	P203 - A_in	P125 - Q	P173 - bulb_diameter	P174 - blocking_distance	P175 - spear_filet	P176 - nozzle_curvature	P177 - nozzle_angle	P178 - spear_angle	P181 - nozzle_dimater_half	P222 - total pressure in
DP 31	30.68	0.015025	0.07	75	5	23	50	30	20	71	4.7959E+05
DP 5	30.68	0.015025	0.07	75	10	23	50	30	20	71	4.7959E+05
DP 4	30.68	0.015025	0.07	75	20	23	50	30	20	71	4.7959E+05
DP 2	30.68	0.015025	0.07	75	30	23	50	30	20	71	4.7959E+05
DP 3	30.68	0.015025	0.07	75	38	23	50	30	20	71	4.7959E+05
DP 7	30.68	0.015025	0.07	75	50	23	50	30	20	71	4.7959E+05
DP 10	30.68	0.015025	0.07	75	55	23	50	30	20	71	4.7959E+05
DP 6	30.68	0.015025	0.07	75	60	23	50	30	20	71	4.7959E+05
DP 14	30.68	0.015025	0.07	75	66	23	50	30	20	71	4.7959E+05
DP 8	30.68	0.015025	0.07	75	68	23	50	30	20	71	4.7959E+05
DP 11	30.68	0.015025	0.07	75	69	23	50	30	20	71	4.7959E+05
DP 12	30.68	0.015025	0.07	75	70	23	50	30	20	71	4.7959E+05
DP 9	30.68	0.015025	0.07	75	73	23	50	30	20	71	4.7959E+05
DP 18	30.68	0.015025	0.07	75	75	23	50	30	20	71	4.7959E+05
DP 19	30.68	0.015025	0.07	75	78	23	50	30	20	71	4.7959E+05
Current	30.68	0.015025	0.07	75	80	23	50	30	20	71	4.7959E+05
DP 24	30.68	0.015025	0.07	80	80	23	50	30	20	71	4.7959E+05
DP 25	30.68	0.015025	0.07	85	80	23	50	30	20	71	4.7959E+05
DP 26	30.68	0.015025	0.07	90	80	23	50	30	20	71	4.7959E+05
DP 27	30.68	0.015025	0.07	70	80	23	50	30	20	71	4.7959E+05
DP 28	30.68	0.015025	0.07	75	80	23	80	30	20	71	4.7959E+05
DP 29	30.68	0.015025	0.07	75	80	23	30	30	20	71	4.7959E+05
DP 30	30.68	0.015025	0.07	75	80	23	120	30	20	71	4.7959E+05
DP 21	30.68	0.015025	0.07	75	85	23	50	30	20	71	4.7959E+05
DP 22	30.68	0.015025	0.07	75	90	23	50	30	20	71	4.7959E+05
DP 23	30.68	0.015025	0.07	75	100	23	50	30	20	71	4.7959E+05

And its performance determining coefficients are tabulated below

Table 5.21 Output parameter's result of candidate B_o

A	S	AL	AM	AN	AO	AP	Y	Z	AA	AB	AC	AE	AF
Name	P214 - C_D	P227 - static pressure in	P228 - total pressue out	P229 - dynamic pressure out	P230 - dynamic pressure in	P231 - C_p	P207 - hydraulic_efficiency	P206 - C_v	P208 - C_c	P210 - Net_head	P209 - d_jet	P226 - V_in	P225 - V_out
Units		Pa	Pa	Pa	Pa							m s^-1	m s^-1
DP 31	0.63537	4.746E+05	92822	93169	4970.2	0.944	18.874	0.43444	1.4625	9.0594	99.451	3.1541	13.329
DP 5	0.63433	4.726E+05	1.3141E+05	1.3214E+05	7001.2	0.93866	24.277	0.49272	1.2874	11.653	87.544	3.7438	15.117
DP 4	0.63243	4.663E+05	2.3313E+05	2.3346E+05	13377	0.94267	49.657	0.70467	0.89748	23.835	61.029	5.1765	21.619
DP 2	0.63079	4.6126E+05	3.2142E+05	3.1932E+05	18442	0.94179	67.409	0.82103	0.76829	32.356	52.244	6.0771	25.189
DP 3	0.62965	4.5871E+05	3.6276E+05	3.6319E+05	20991	0.94198	76.987	0.87742	0.71761	36.954	48.798	6.4844	26.919
DP 7	0.62824	4.5635E+05	4.0537E+05	4.0263E+05	23323	0.94195	85.488	0.9246	0.67947	41.034	46.204	6.8346	28.367
DP 10	0.62775	4.5583E+05	4.1418E+05	4.1126E+05	23851	0.94212	87.668	0.93631	0.67045	42.081	45.591	6.9112	28.726
DP 6	0.62733	4.5511E+05	4.2404E+05	4.2375E+05	24549	0.94205	90.134	0.94939	0.66077	43.264	44.932	7.0117	29.127
DP 14	0.62689	4.5483E+05	4.2623E+05	4.2916E+05	24836	0.94218	91.406	0.95606	0.6557	43.875	44.588	7.0532	29.332
DP 8	0.62677	4.5451E+05	4.3074E+05	4.3504E+05	25140	0.94228	92.674	0.96267	0.65107	44.483	44.273	7.0959	29.535
DP 11	0.62671	4.5464E+05	4.2817E+05	4.3279E+05	25015	0.94223	92.155	0.95997	0.65284	44.234	44.393	7.0788	29.452
DP 12	0.62665	4.5453E+05	4.2985E+05	4.3461E+05	25115	0.94232	92.657	0.96259	0.65101	44.476	44.269	7.0926	29.532
DP 9	0.6265	4.5443E+05	4.327E+05	4.3637E+05	25221	0.94238	93.145	0.96512	0.64914	44.71	44.142	7.1077	29.61
DP 18	0.62641	4.5431E+05	4.3576E+05	4.3808E+05	25336	0.9423	93.455	0.96672	0.64797	44.858	44.062	7.1244	29.659
DP 19	0.62629	4.538E+05	4.4656E+05	4.424E+05	25846	0.94055	92.542	0.96199	0.65103	44.42	44.27	7.1961	29.514
Current	0.62622	4.53E+05	4.6149E+05	4.5569E+05	26584	0.94154	96.77	0.98372	0.63658	46.45	43.288	7.2971	30.181
DP 24	0.62622	4.5374E+05	4.4943E+05	4.4356E+05	25899	0.94146	94.211	0.97062	0.64517	45.221	43.872	7.2048	29.779
DP 25	0.62622	4.5377E+05	4.4898E+05	4.4317E+05	25877	0.94142	94.121	0.97016	0.64548	45.178	43.893	7.2039	29.764
DP 26	0.62622	4.5379E+05	4.4847E+05	4.4262E+05	25857	0.94119	93.922	0.96913	0.64616	45.082	43.939	7.2104	29.733
DP 27	0.62622	4.5377E+05	4.489E+05	4.4314E+05	25864	0.94159	94.213	0.97064	0.64516	45.222	43.871	7.197	29.779
DP 28	0.62622	4.5368E+05	4.485E+05	4.4387E+05	25960	0.94059	92.991	0.96432	0.64939	44.636	44.158	7.2112	29.585
DP 29	0.62622	4.5364E+05	4.4955E+05	4.4521E+05	26000	0.94154	94.647	0.97287	0.64368	45.431	43.77	7.2167	29.848
DP 30	0.62622	4.5374E+05	4.4866E+05	4.4356E+05	25903	0.9414	94.066	0.96987	0.64567	45.151	43.906	7.2029	29.756
DP 21	0.62609	4.5344E+05	4.5199E+05	4.4763E+05	26191	0.94044	93.633	0.96764	0.64703	44.944	43.998	7.2451	29.687
DP 22	0.62602	4.5334E+05	4.5547E+05	4.5281E+05	26276	0.94136	95.435	0.97691	0.64082	45.809	43.576	7.2579	29.972
DP 23	0.62606	4.5348E+05	4.598E+05	4.6183E+05	26127	0.94243	96.677	0.98325	0.63673	46.405	43.297	7.2379	30.166

The following table shows candidateC_o's geometrical parametric values interms efficiency at different nozzle opening.

Table 5.22 dimensional values of candidate $\boldsymbol{C_o}$

Name	P123 - V_theoretical	P198 - total_inlet_gage_pressure	P125 - Q	P211 - C_d	P137 - b...	P219 - blockin...	P139 - sp...	P140 - no...	P141 - nozzle_angle	P142 - spear_angle
Units	m s^-1	Pa	m^3 s^-1							
DP 6	30.68	4.7959E+05	0.07	0.60885	90	10	25	80	30	25
DP 1	30.68	4.7959E+05	0.07	0.60885	90	20	25	80	30	25
DP 2	30.68	4.7959E+05	0.07	0.60885	90	30	25	80	30	25
DP 4	30.68	4.7959E+05	0.07	0.60885	90	38	25	80	30	25
DP 5	30.68	4.7959E+05	0.07	0.60885	90	50	25	80	30	25
Current	30.68	4.7959E+05	0.07	0.60885	90	55	25	80	30	25
DP 7	30.68	4.7959E+05	0.07	0.60885	90	60	25	80	30	25
DP 8	30.68	4.7959E+05	0.07	0.60885	90	70	25	80	30	25
DP 10	30.68	4.7959E+05	0.07	0.60885	90	73	25	80	30	25
DP 11	30.68	4.7959E+05	0.07	0.60885	90	80	25	80	30	25
DP 13	30.68	4.7959E+05	0.07	0.60885	85	80	25	80	30	25
DP 14	30.68	4.7959E+05	0.07	0.60885	80	80	25	80	30	25
DP 17	30.68	4.7959E+05	0.07	0.60885	90	85	25	80	30	25
DP 18	30.68	4.7959E+05	0.07	0.60885	90	90	25	80	30	25
DP 19	30.68	4.7959E+05	0.07	0.60885	90	100	25	80	30	25

And its performance determining coefficients are tabulated below

Table 5.23 Output parameter's result of candidate C_o

Name	P207 - hydraulic_efficiency	P206 - C_v	P208 - C_c	P210 - Net_head	P209 - d_jet	P221 - C_p	P148 - Vout	P149 - inlet static pressure	P151 - inlet velocity	P152 - outlet total pressure
Units						kg kg^-1	m s^-1	Pa	m s^-1	Pa
DP 6	0.28322	0.53218	1.1441	13.702	77.796	0.96748	16.327	4.7525E+05	2.9444	1.2103E+05
DP 1	0.62709	0.79189	0.76885	30.339	52.282	0.95156	24.295	4.6529E+05	5.3472	2.8189E+05
DP 2	0.79372	0.89091	0.6834	38.4	46.471	0.94862	27.333	4.604E+05	6.1955	3.6198E+05
DP 4	0.84936	0.92161	0.66064	41.092	44.923	0.94686	28.275	4.5835E+05	6.518	3.959E+05
DP 5	0.90346	0.95051	0.64055	43.71	43.558	0.94693	29.162	4.5703E+05	6.7177	4.1882E+05
Current	0.92429	0.9614	0.63329	44.717	43.064	0.94739	29.496	4.5668E+05	6.7654	4.2543E+05
DP 7	0.90658	0.95214	0.63945	43.86	43.483	0.94509	29.212	4.5615E+05	6.8455	4.3104E+05
DP 8	0.857	0.92574	0.65769	41.462	44.723	0.94027	28.402	4.5547E+05	6.9414	4.4619E+05
DP 10	0.78667	0.88694	0.68646	38.059	46.679	0.93482	27.211	4.554E+05	6.9469	4.5796E+05
DP 11	0.78092	0.88369	0.68898	37.781	46.851	0.93405	27.112	4.5528E+05	6.9624	4.5892E+05
DP 13	0.77828	0.8822	0.69015	37.653	46.93	0.93374	27.066	4.5529E+05	6.9671	4.5937E+05
DP 14	0.77395	0.87974	0.69208	37.444	47.061	0.93335	26.991	4.5531E+05	6.968	4.592E+05
DP 17	0.77525	0.88049	0.69149	37.507	47.022	0.93353	27.013	4.5523E+05	6.9644	4.5943E+05
DP 18	0.77093	0.87802	0.69343	37.297	47.153	0.93322	26.938	4.5522E+05	6.9611	4.6046E+05
DP 19	0.76398	0.87406	0.69658	36.962	47.367	0.93305	26.816	4.552E+05	6.9386	4.6086E+05

Organizing and ordering the values of the coefficients in table summarized as follows. These values are calculated using the formula in chapter three after the actual velocity and pressure founded in Ansys simulation.

Table 5.24 Values of coefficient of velocity, contraction, and pressure for the three candidate points @ different blocking distance.

Closing distance		C_v	C_c	C_d	C_p
20	A	0.73	0.84	0.62	0.97
	B	0.7	0.89	0.63	0.94
	C	0.79	0.77	0.6	0.95
30	A	0.84	0.73	0.62	0.97
	B	0.82	0.77	0.63	0.94
	C	0.89	0.68	0.6	0.95
38	A	0.88	0.69	0.62	0.97
	B	0.877	0.71	0.62	0.94
	C	0.92	0.66	0.6	0.94
50	A	0.92	0.66	0.62	0.97
	B	0.95	0.64	0.61	0.94
	C	0.95	0.64	0.6	0.94
55	A	0.936	0.66	0.62	0.97
	B	0.93	0.67	0.62	0.94
	C	0.96	0.63	0.6	0.95
60	A	0.93	0.66	0.62	0.97
	B	0.949	0.66	0.62	0.94
	C	0.95	0.64	0.6	0.94
70	A	0.89	0.69	0.62	0.97
	B	0.962	0.65	0.62	0.94
	C	0.92	0.65	0.6	0.94
80	A	0.78	0.79	0.62	0.97
	B	0.983	0.63	0.62	0.94
	C	0.88	0.69	0.6	0.93

The comparison of the candidate DPs is based on coefficient of velocity, discharge, contraction, and pressure. The green, yellow, and red colors indicates the highest, medium and lowest value respectively. The higher these values the best will be the overall performance of the nozzle. But it so hard to get all of them higher, that is why optimization needed. Comparing the results candidate DP B_0 has an optimized result having higher importance for C_v at closing distance of 80mm. But it's C_c, C_d, and C_p values are low, medium and medium respectively. The pressure and velocity distribution are listed on appendix I and J from the result the flowing conclusion are made.

The pressure contour of the three DP (design point) candidates shows that the pressure is higher at the inlet of the nozzle and getting lower and lower as the cross -section is converging.

The velocity distribution is smoothly increasing as the flow gets out of the nozzle in contrary to the pressure distribution. Looking the velocity contours, the velocity contour of $\alpha=35^0$ -$\beta=25^0$ has a little bit rough especially at the inlet of the nozzle, which is unwanted.

The following charts shows the relation of nozzle efficiency, static pressure, and net head at different nozzle openings for different spear and nozzle configuration.

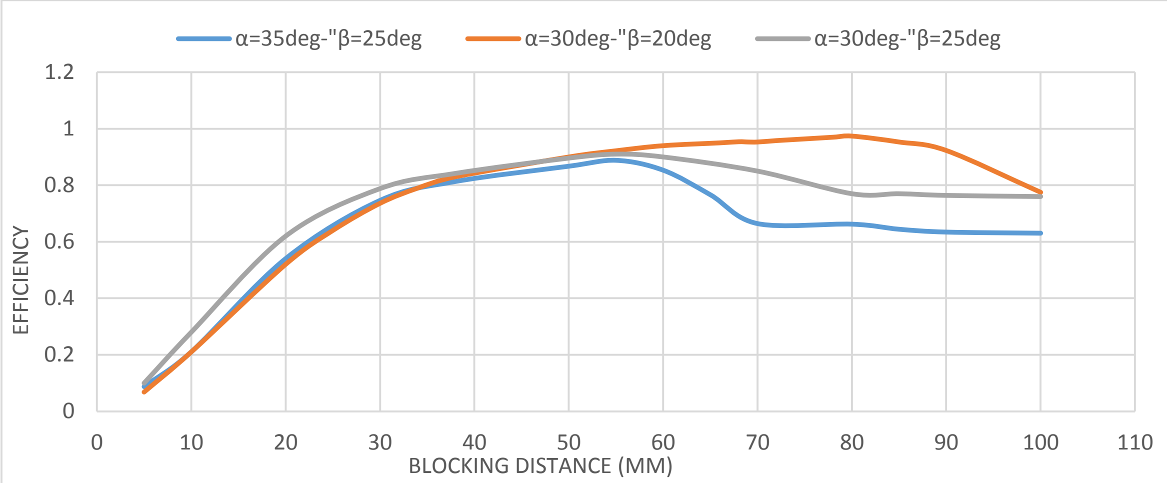

Fig 5.13 Efficiency vs. blocking distance for A, B, C design point candidates

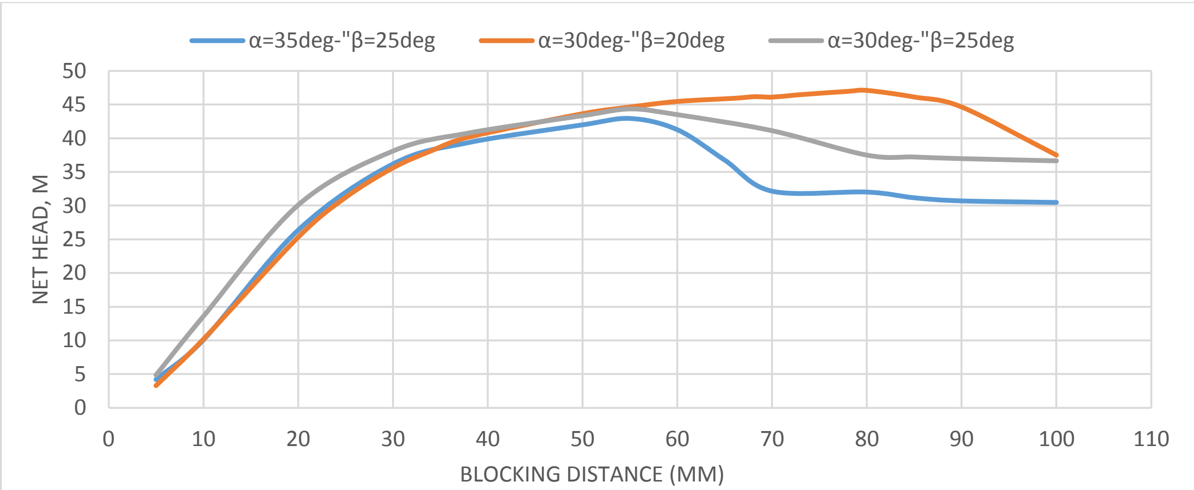

Fig 5.14 Net head vs. blocking distance for A, B, C design point candidates

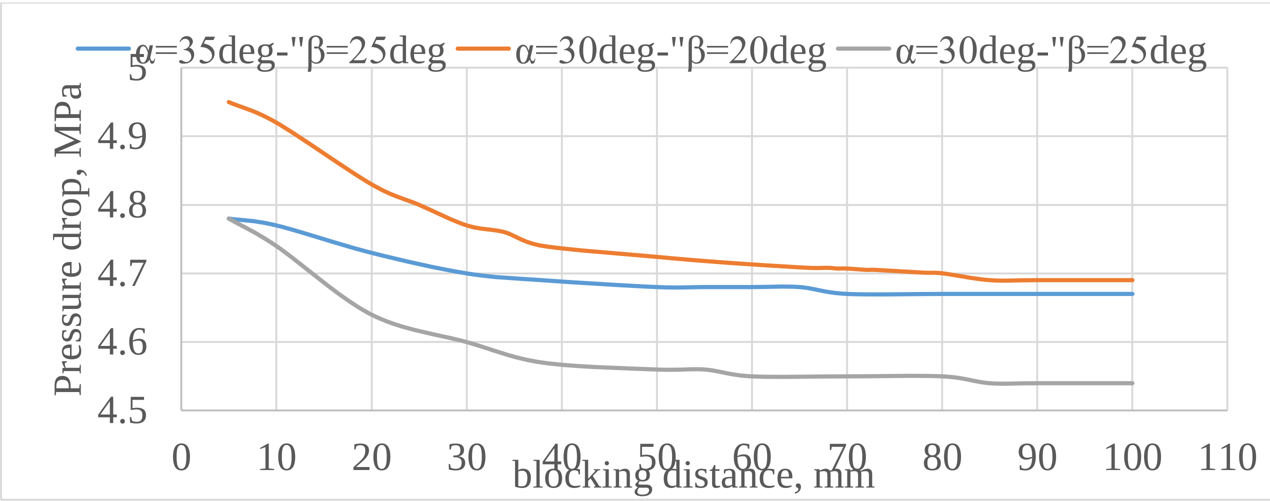

Fig 5.15 Pressure drop vs. blocking distance for A_o, B_o, C_o design point candidates

Analyzing the efficiency versus nozzle opening graph the red color ($\beta = 30°, \alpha = 20°$) has a higher efficiency than the other colored curves but looking inlet static pressure curve versus blocking distance it has the most higher value than the other curves in whole of its nozzle opening range. Interms of pressure drop the light dark color ($\beta = 35°, \alpha = 25°$) curve has an advantage over the other curves, but in contrary it has the second lowest value interms of efficiency in most of nozzle opening range. The blue colored curve ($\beta = 35°, \alpha = 20°$) is the second chosen interms of the pressure drop versus blocking distance in most of its entire nozzle opening range. Interms of efficiency and pressure drop optimization the orange colored curve is the best optimized one.

5.3 COMPARISON BETWEEN THE BASE LINE DESIGN AT AN ANGLE OF (25, 35) DEGREES AND OPTIMIZED DESIGN AT ANGLE OF (20, 30) DEGREES

The comparison clearly shows that how the efficiency and performance of the nozzle at different flow rate are improved. At different season the flow rate is not the same, due to this reason the simulations has performed at different flow rate ranging from 0.009 to 0.1 as the given or reference flow rate is 0.07 m^3/s for each nozzle.

Table 5.25 Input parameter for reference design of spear and nozzle angle (25, 35) degree respectively.

P123 - V_theoretical	P198 - total_inlet_gage_pressure	P125 - Q	P137 - bulb_diameter	P138 - blocking_distance	P139 - spear_fillet	P140 - nozzle_curvature	P141 - nozzle_angle	P142 - spear_...	P212 - hydra_diameter
30.68	4.6992E+05	0.009	85	38	22.5	120	35	25	0.138
30.68	4.7022E+05	0.02	85	38	22.5	120	35	25	0.138
30.68	4.7139E+05	0.04	85	38	22.5	120	35	25	0.138
30.68	4.7332E+05	0.06	85	38	22.5	120	35	25	0.138
30.68	4.7458E+05	0.07	85	38	22.5	120	35	25	0.138
30.68	4.7604E+05	0.08	85	38	22.5	120	35	25	0.138
30.68	4.7952E+05	0.1	85	38	22.5	120	35	25	0.138

Table 5.26 Output parameter for reference design of spear and nozzle angle (25, 35) degrees respectively

P207 - hydraulic_efficiency	P206 - C_v	P208 - C_c	P210 - Net_head	P209 - d_jet	P122 - Cp	P148 - Vout	P149 - inlet static pressure	P151 - inlet velocity	P152 - outlet total pressure	P211 - C_d
0.77103	0.87808	0.70341	37.303	47.832	0.97384	26.94	4.6043E+05	4.3569	3.5767E+05	0.61765
0.77154	0.87837	0.70317	37.327	47.816	0.97384	26.949	4.6073E+05	4.3584	3.579E+05	0.61765
0.77345	0.87946	0.70231	37.419	47.757	0.97384	26.982	4.6187E+05	4.3637	3.5879E+05	0.61765
0.77663	0.88127	0.70087	37.573	47.659	0.97384	27.037	4.6377E+05	4.3727	3.6026E+05	0.61765
0.7787	0.88244	0.69993	37.673	47.596	0.97384	27.073	4.65E+05	4.3785	3.6122E+05	0.61765
0.78109	0.88379	0.69886	37.789	47.523	0.97384	27.115	4.6642E+05	4.3852	3.6233E+05	0.61765
0.78681	0.88703	0.69632	38.066	47.349	0.97384	27.214	4.6984E+05	4.4012	3.6498E+05	0.61765

Table 5.27 Input parameter for optimized design by CFD of spear and nozzle at an angle of (20, 30) degrees respectively

P125 - Q	P173 - bulb_diameter	P174 - blocking_distance	P175 - spear_fillet	P176 - nozzle_curvature	P177 - nozzle_angle	P178 - spear_angle	P181 - nozzle_dimater_half	P222 - total pressure in	P212 - hydra_dimeter	P123 - V_theoretical
0.009	75	80	23	50	30	20	71	4.6992E+05	0.11	30.68
0.01	75	80	23	50	30	20	71	4.6993E+05	0.11	30.68
0.02	75	80	23	50	30	20	71	4.7022E+05	0.11	30.68
0.04	75	80	23	50	30	20	71	4.7139E+05	0.11	30.68
0.06	75	80	23	50	30	20	71	4.7332E+05	0.11	30.68
0.07	75	80	23	50	30	20	71	4.7458E+05	0.11	30.68
0.08	75	80	23	50	30	20	71	4.7604E+05	0.11	30.68
0.1	75	80	23	50	30	20	71	4.7952E+05	0.11	30.68

Table 5.28 output parameter for optimized design by CFD of spear and nozzle at an angle of (20, 30) degrees respectively

P207 - hydraulic_efficiency	P206 - C_v	P208 - C_c	P210 - Net_head	P209 - d_jet	P226 - V_in	P225 - V_out	P227 - static pressure in	P228 - total pressue out	P231 - C_p
94.914	0.97424	0.64278	45.559	43.709	7.2268	29.89	4.4384E+05	4.5264E+05	0.94154
94.92	0.97427	0.64276	45.562	43.707	7.227	29.891	4.4386E+05	4.5267E+05	0.94154
94.976	0.97456	0.64257	45.588	43.695	7.2291	29.899	4.4413E+05	4.5293E+05	0.94154
95.15	0.97545	0.64198	45.672	43.655	7.2357	29.927	4.4525E+05	4.5376E+05	0.94154
95.487	0.97717	0.64085	45.834	43.578	7.2485	29.98	4.4709E+05	4.5537E+05	0.94154
95.812	0.97883	0.63976	45.99	43.504	7.2609	30.031	4.4826E+05	4.5692E+05	0.94154
96.024	0.97992	0.63905	46.091	43.456	7.2689	30.064	4.4966E+05	4.5793E+05	0.94154
96.719	0.98346	0.63675	46.425	43.299	7.2952	30.173	4.5296E+05	4.6124E+05	0.94154

Comparison table and graph of modified design and base line.

This portion is simulated due to seasonal variation of flow rate even if the given flow rate is $0.07 m^3/s$ it is not constant throughout the year at summer and winter there is a flow rate variation. The following table shows the last optimized nozzle at different flow rate and the first designed nozzle without optimization in different flow rate. Since all of the above simulation is done by assuming the flow rate is the same for all condition.so now the optimized nozzle performs a good efficiency at different season as shown in the table.

Table 5.29 Comparison table for different flow rate condition at (20, 30) and (25, 35) degrees

Q	**20-30 degree(Modified Design by CFD)**	**25-35 degree (Reference Design)**
flow rate(m3/s)	Efficiency (%)	Efficiency (%)
0.009	85.91400084	70.10323628
0.01	86.92027569	75.10626439
0.02	94.97600909	77.15400639
0.04	95.14984421	77.34493298
0.06	95.48675408	77.66314931
0.07	95.81154814	77.86998244
0.08	96.02367801	78.10865386
0.1	96.7194482	78.68143915

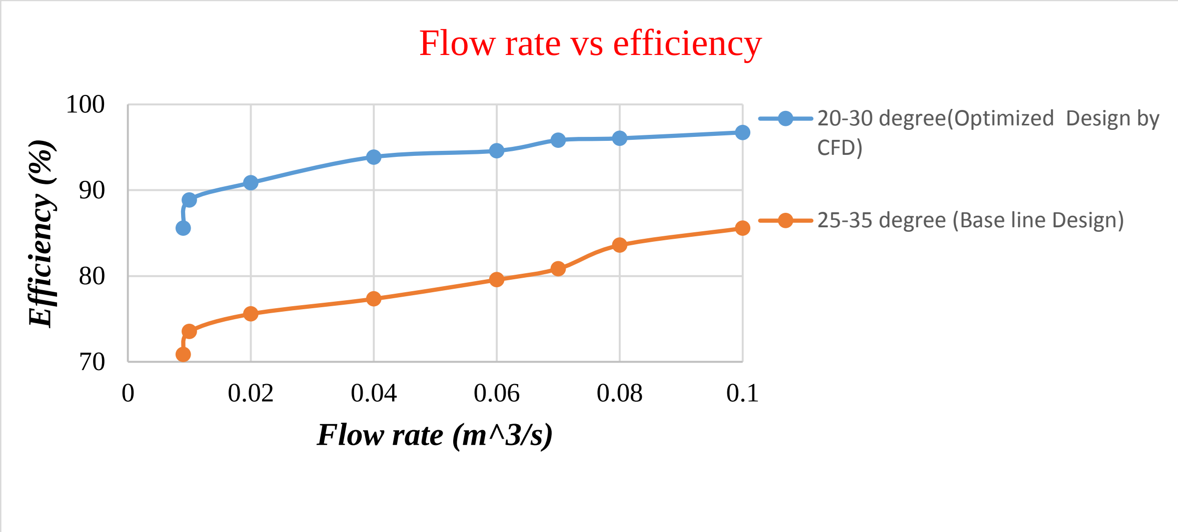

Fig 5.31 Efficiency vs flow rate for the reference design and modified(improved) design

5.4 STRESS ANALYSIS AND STRUCTURAL SIMMULATION

5.4.1 STRESS ANALYSIS OF NOZZLE

$$t_n = P_i \times \frac{dn}{2(S_d \times 0.7 - 0.6 \times P_i)}$$

Where t_n = minimum wall thickness of the nozzle,

P_i = internal pressre of Nozzle, S_d = strength of material.

The material selected is 13Cr 4Ni stainless steel (martensitic, its yield strength is

$S_y = 154$MPA)

Then we have the design strength $S_d = 0.66 * S_y = 0.66 * 154 = 101.6MPA$

The total head is the summation of gross and surge head:

$H_t = H_g + H_s = 50 + 118.8 = 168.8m$

The maximum pressure at which the nozzle subjected is therefore:

$Pi = H_t * \rho g = 168.8 * 998.2 \times 9.806 = 1.6MPA$

$$t_n = P_i \times \frac{dn}{2(S_d \times 0.7 - 0.6 \times P_i)} = 1.6 * \frac{0.17}{2(101.6 * 0.7 - 0.6 * 1.6)} = 2mm$$

$to\ be\ more\ safe\ take\ 3mm$

5.4.2 STRUCTURAL ANALYSIS OF NOZZLE USING ANSYS SOFTWARE

Structural analysis of nozzle using Ansys software for its stress, deformation, and safety factor is that to prove that the analytical design safe i.e. the selected material and its safety factor are good or not in handling the flow. The following table shows the engineering data of material of nozzle [40]

Table 5.30 Engineering data for nozzle material

Outline of Schematic A2: Engineering Data

Properties of Outline Row 3: 13Cr 4Ni stainless steel

	A	B	C
1	Property	Value	Unit
2	Density	7850	kg m^-3
3	Isotropic Secant Coefficient of Thermal Expansion		
6	Isotropic Elasticity		
7	Derive from	Young's Modulus and Po...	
8	Young's Modulus	2E+11	Pa
9	Poisson's Ratio	0.3	
10	Bulk Modulus	1.6667E+11	Pa
11	Shear Modulus	7.6923E+10	Pa
12	Alternating Stress Mean Stress	Tabular	
16	Strain-Life Parameters		
24	Tensile Yield Strength	154	MPa
25	Compressive Yield Strength	154	MPa
26	~~Tensile Ultimate Strength~~	4.6E+08	Pa
27	~~Compressive Ultimate Strength~~	0	Pa

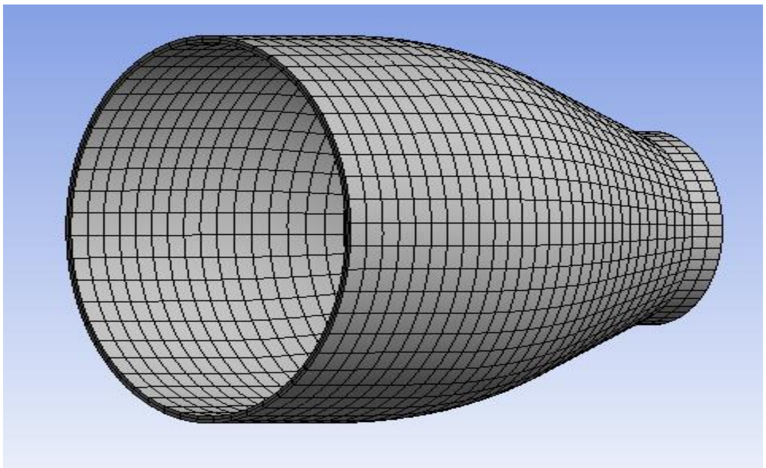

Fig 5.17 Mesh style used in discretization of nozzle

Table 5.31 Result verification of mesh refinement

P13 - Pressure Magnitude	P17 - Mesh Min Size	P18 - Mesh Proximity Min Size	P12 - Mesh Max Face Size	P11 - Mesh Max Size	P16 - Equivalent Stress Maximum	P14 - Total Deformation Maximum	P15 - Safety Factor Minimum	P9 - Mesh Min	P10 - Mesh Average
MPa	mm	mm	mm	mm	MPa	mm			
1.6	0.1	0.1	15	15	42.227	0.017662	3.647	0.37213	0.78223
1.6	7	6	10	12	42.988	0.017786	3.5824	0.44852	0.73561
1.6	13	10	20	20	42.322	0.017671	3.6388	0.53102	0.89202
1.6	5	4.5	5	5	42.396	0.017678	3.6324	0.89242	0.99195

Looking at table 5.31, as the mesh refined the stress, deformation and factor of safety are not changing that much.

The factor of safety is therefore 3.6 we can say that the nozzle is safe against internal pressure that will develop during the operation.

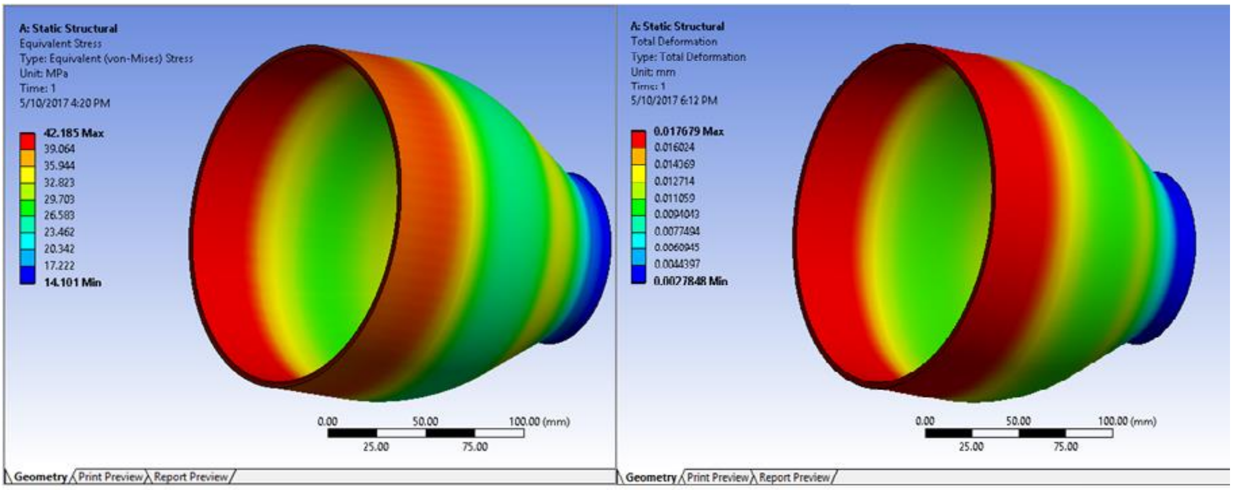

Fig 5.18 Equivalent von miss stress and deformation contour of nozzle

The stress and deformation distribution is higher at the inlet periphery of the nozzle and they are decreasing to the exit periphery of the nozzle.

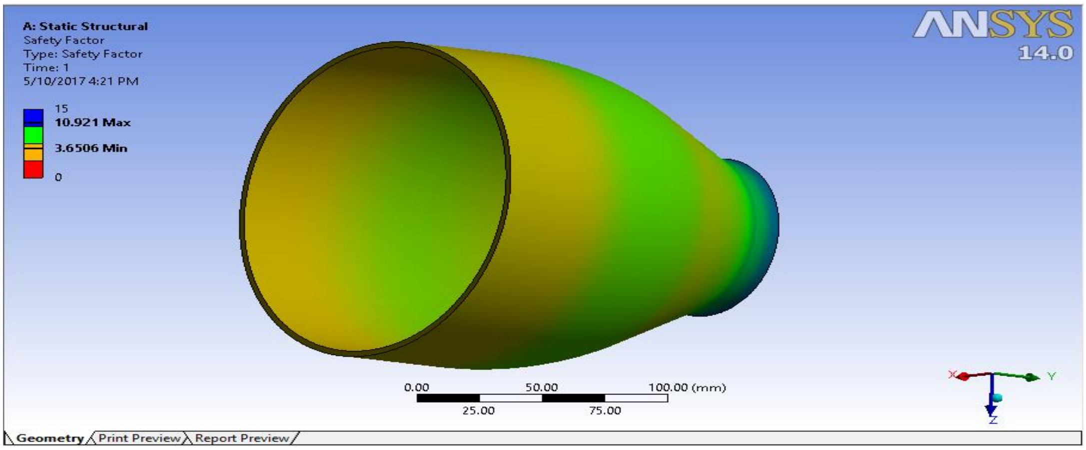

Fig 5.19 Safety factor distribution of nozzle

The safety factor distribution along the axis of the nozzle is increasing from 3.6 to 15 where the minimum safety around the inlet periphery of the nozzle and maximum at the exit periphery.

5.4.3 STRESS ANALYSIS OF SPEAR ROD

The needle will be constantly under tension because the rod diameter is smaller than the diameter of the nozzle outlet diameter.

$d_b > d_1$ where d_b = is nozzle out let diameter and d_1 = rod diameter

The maximum stress developed on the needle is calculated by:

$$S_s = \rho \times \frac{H_t({d_b}^2 - {d_1}^2)}{{d_1}^2} - - - - - - - - - - - - - - - 4.10$$

$$S_s = 998.2 \times 168.8 \times 9.81 \times \frac{\pi}{4}\left(\frac{0.068^2 - 0.032^2}{0.032^2}\right) = 4.56 \text{ Mpa}$$

The stress must be less than 66% of the yield stress of the material that I have used. Stainless steel is recommended because the needle is submerged all the time. Then AISI 1006 (Martensitic hot rolled Steel $Sy170MPA$), were used which yield stress is much higher, but is selected its corrosion resistance properties

Table 5.32 Property of hot rolled and cold rolled material [46]

1 UNS No.	2 SAE and/or AISI No.	3 Processing	4 Tensile Strength, MPa (kpsi)	5 Yield Strength, MPa (kpsi)
G10060	1006	HR	300 (43)	170 (24)
		CD	330 (48)	280 (41)
G10100	1010	HR	320 (47)	180 (26)
		CD	370 (53)	300 (44)
G10150	1015	HR	340 (50)	190 (27.5)
		CD	390 (56)	320 (47)
G10180	1018	HR	400 (58)	220 (32)
		CD	440 (64)	370 (54)

The maximum force applied to the needle shaft when regulating the needle at the turbine inlet will be:

$$F_a = \pi \times \frac{{d_1}^2 \times S_s}{4} = \pi * 0.032^2 * \frac{4.56}{4} = 3.67 \text{ K N}$$

Safety factor check of the needle shaft for Axial stress that resist for crushing

$$The\ design\ yeild\ strength\ of\ the\ rod, S = 0.66Sy = 0.66 * 170 = 112.2\ MPA$$

The yield strength of the material is higher than the maximum effort that will develop.

Therefore the needle valve is safe!

BUCKLING CHECK:-Checking for buckling the spear rod: critical slenderness ratio is calculated by:

$$\left(\frac{l}{k}\right)_1 = \sqrt{\frac{2\pi^2 CE}{Sy}} \qquad 4.11$$

$\text{Where C} = \text{end codition(for fixed} - \text{fixed end condition it is 1.2)}$

since the spear is fixed by stator guide on the nozzle side and fixed by the other side by bearings.

$\text{E} = \text{modulus of elasticity(207GPA)}, \quad \text{Sy} = \text{yield strength(170MPA), and}$

$$\text{k} = \text{radius of gyration} = \frac{\text{spear rod diameter}}{2} = \frac{32}{2} = 16\text{mm},$$

$\text{L}_r = \text{length of rod}$

$$\left(\frac{\text{L}_r}{\text{k}}\right) \le \left(\frac{\text{L}_r}{\text{k}}\right)_1 = \sqrt{\frac{2\pi^2\text{CE}}{\text{Sy}}} = \sqrt{\frac{2\pi^2 * 1.2 * 207000}{170}} = 169.8,$$

The maximum length of the rod keeping the rod diameter 32mm will be:

$$\left(\frac{\text{L}_r}{\text{k}}\right) \le 169.8, \quad \text{l}_{\text{max}} = 169.8\text{k} = 169.8 \times 16\text{mm} = 2.7\text{m}$$

5.4.4 STRUCTURAL ANALYSIS OF SPEAR USING ANSYS

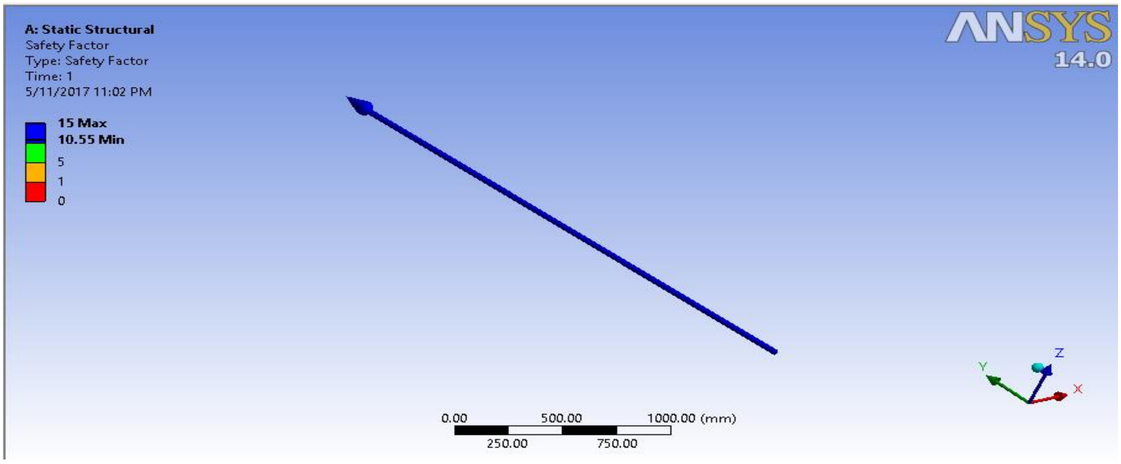

Fig 5.20 Safety factor distribution along the rod length for static(crushing) at critical length

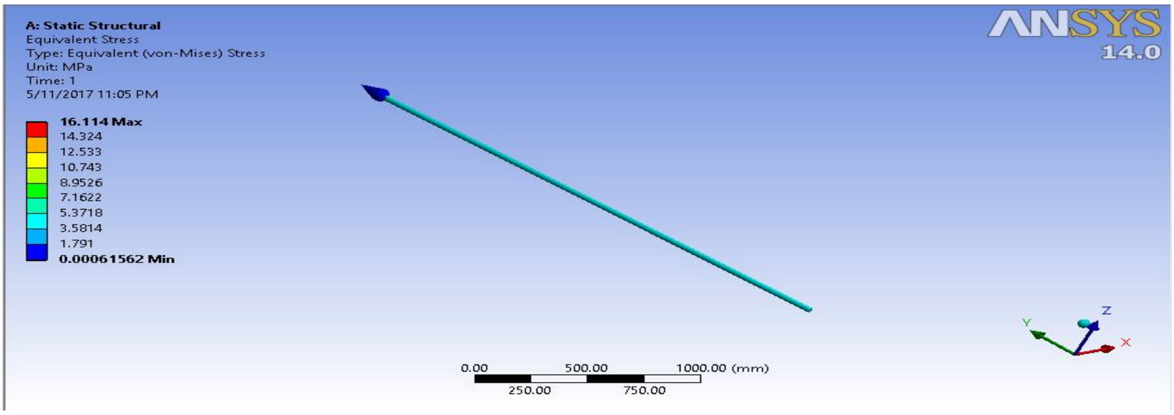

Fig 5.21 Stress distribution along rod length

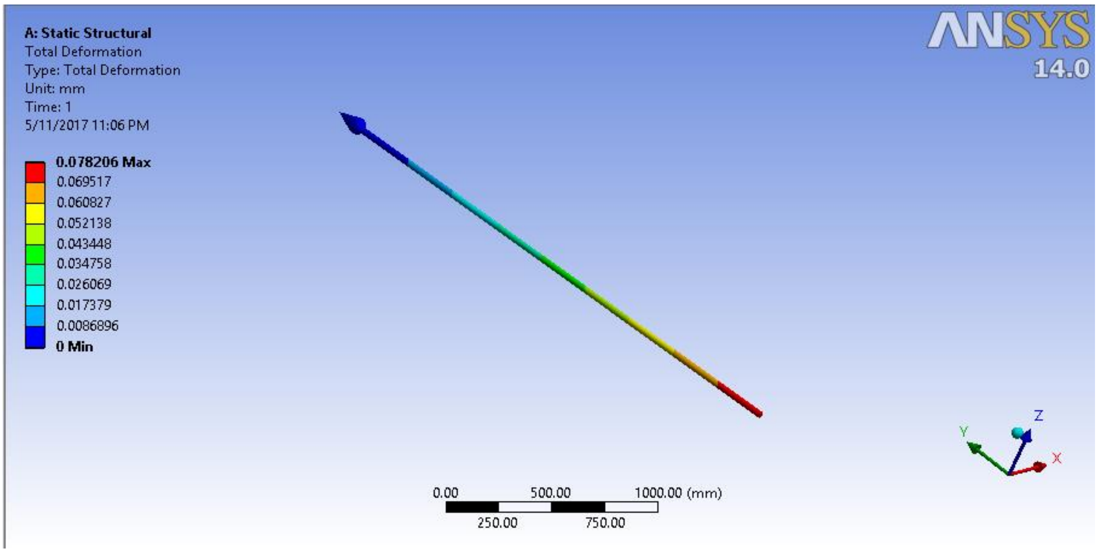

Fig 5.22 Total deformation along the rod axis

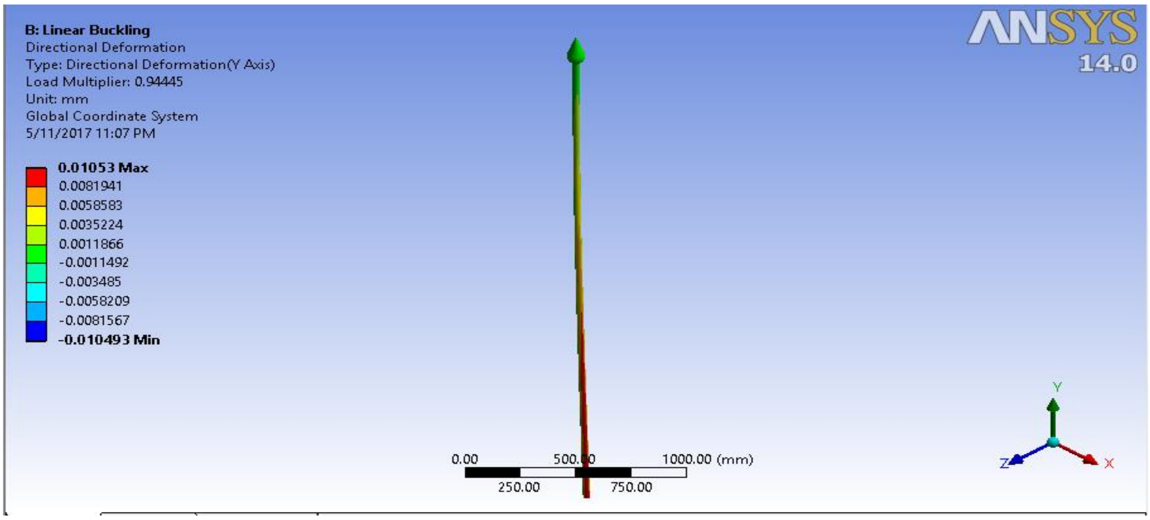

Fig 5.23 Buckling deformation along rod axis at load multiplier of 0.944

As proved by the ansys simmulation shown in the above picture the safety factor is 0.9445 at a length of 2.7m and therfore the length of the spear to be manufactured should be less than 2.7m.becuase when I design analiticaly I used slender ness ratio which is the critical length is $less\ than\ or\ equal\ to$ 2.7m.the safty factor at that critical point is 1. If we use less than 2.7m we are safe.

From the structural analysis the designed spear is safe because the minimum safety factor in the simmulation is 10.55,because the stress developed on the spear and the selected material of the spear are related by safety factor.

5.4.5 DEFLECTOR DESIGN

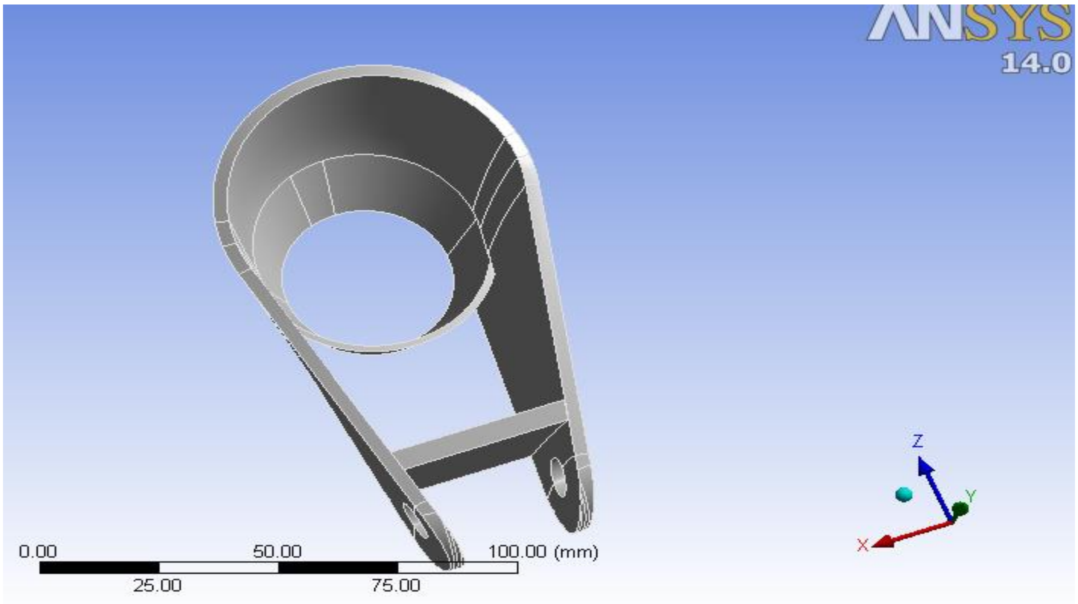

Fig 5.24 3D model of deflector

Deflectors have the function of diverting the water flow or part of it between the nozzle and the runner in such a way that it does not hit the buckets. These may be used for an emergency stop or to regulate the turbine.

If the power has to be reduced quickly, the governor moves the jet deflector into the jet, thus diverting part of the water from the buckets and reducing the power transferred to the runner. The governor then adjusts the discharge by slowly moving the needle. Meanwhile the deflector is gradually withdrawn.

Instead of a costly regulating mechanism with needle and spear it is often easier and cheaper to regulate the turbine with a jet deflector. If the necessary quantity of water is always available, this method has also other advantages. In combination with a slow closing, hand operated penstock valve the allowable pressure of the penstock pipe would not be much higher than the static head because no water hammer effects occur[1,3]

5.4.6 THE HYDRO-DYNAMIC FORCE IN EACH DEFLECTOR

The following figure shows that R_d is the total length of the deflactor that is the torque acting on the deflactor and r_d is the radius at which the pivot is applied and F_d is hydrodynamic force on the deflactor [2].

$$F_d = \frac{\rho * Q_n * V_j}{2} = \frac{998.2 * 0.07 * 30.95}{2} = 1.06KN$$

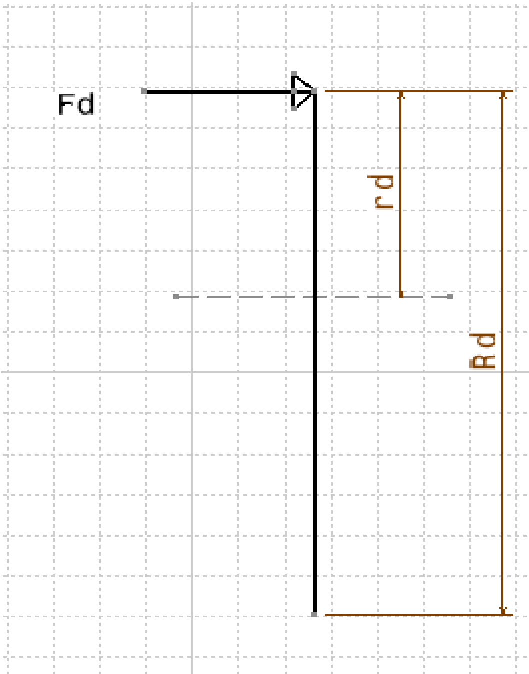

Fig 5.25 Hydrodynamic force acting on the deflactor

The required force in each deflector is given as:

$$F_{dr} = F_d \times r_d \times s.f/(R_d - r_d)$$

Take safety factor 1.5,

$$\text{Therefore } F_{dr} = 1.5 * 1.06 \times r_d/(R_d - r_d)$$
$$= 1.59 \times r_d/(R_d - r_d)$$

The bending moment acting on the deflector arm given as:

$$T_d = \left(1.59 \times \frac{r_d}{R_d - r_d}\right) \times (R_d - r_d) = 1590 r_d (N.m)$$

The moment required acting on the deflector arm given as:

$$T_{dr} = T_d * F_c$$

Where F_C *is* friction factor acted upon by bearings (≅1.2)

$T_{dr} = T_d * F_c = 1590 r_d * 1.2 = 1908 r_d (N.m)$ Where

r_D is moment arm in m

5.4.7 DESIGN THE DEFLECTOR FOR THE BENDING STRESS DUE TO THE WATER JET FORCE CREATED ON THE DEFLECTOR

$\sigma_B = \frac{T_{dr} * r_d}{I_{xx}}$, Where I_{xx} second moment of inertia of the cross section of the deflector

The second moment of inertia for hollow tube with circular cross-section would be:

$$I_{xx} = \frac{\pi {r_o}^4}{4} - \frac{\pi {r_i}^4}{4}$$

Where r_o *is outside circle radius, and* r_i *is inner circle radius*

$$r_o = r_i + t$$

Where t is the thickness of the deflector

$$I_{xx} = \frac{\pi (r_i + t)^4}{4} - \frac{\pi {r_i}^4}{4} = \frac{\pi}{4}((r_i + t)^4 - {r_i}^4)$$

When designing the cross-section of the deflector must be large enough to deflect the whole water jet. This means the inner radius must be greater than the water jet radius.

Material Fe E220 is used recommended as per IS: 1871(Part I) -1987. The data table is put on appendix C at table 5.38.

Factor of safety incorporated: $\mathrm{n} = \dfrac{0.66\mathrm{S_y}}{\sigma_\mathrm{B}}$ Substituting each parameters

$$\mathrm{n} = \frac{0.66\mathrm{S_y}}{\left(\dfrac{\mathrm{T_{dr}} * \mathrm{r_d}}{\frac{\pi}{4}((r_i + t)^4 - {r_i}^4)}\right)} = \frac{0.66 * 220 * 10^6}{\left(\dfrac{1908\mathrm{r_d} \times \mathrm{r_d}}{\frac{\pi}{4}((r_i + t)^4 - {r_i}^4)}\right)} = \frac{46185.36((r_i + t)^4 - {r_i}^4)}{{\mathrm{r_d}}^2}$$

Rearranging the terms for moment arm:

$$r_d(m) = \sqrt{\frac{46185.36((r_i + t)^4 - {r_i}^4)}{n}}$$

As the moment arm varies the torque needed to deflect the water jet also varies so the optimum moment arm has to be set regarding the available space and the material cost needed due to the change in moment arm. The following table shows the relation of the moment arm, $\mathrm{r_d}$, safety factor, internal diameter and thickness of the deflector, and torque required to deflect the water.

Table 5.33 The torque requirement versus moment arm interms of safety factor and thickness

n	$r_i = \frac{d_{jet}}{2}$(mm)	t(mm)	$r_d(mm)$	$T_{dr} = 1.908\mathrm{r_d}(\mathrm{N.m})$
1	27.2	2	91	174
2	27.2	3	81	154
2.6	27.2	3	70	133
2.5	27.2	4	86	164
2.5	27.2	5	99	189

$For\ t = 3mm, r_i = 27.2mm, r_d = 70mm,$

$n\ and\ T_{dr}\ becomes\ 2.6\ \ and\ 133\ N.m\ respectively$

5.4.8. ANALYSIS OF DEFLECTOR USING ANSYS SOFTWARE

The design is safe as shown in the simulated figure the minimum safety factor is 2.67.

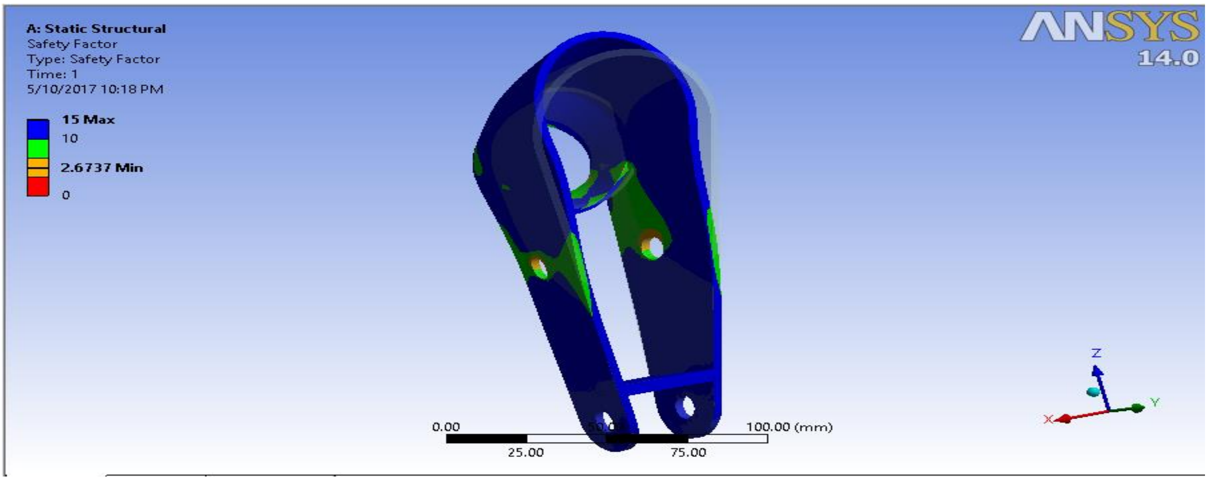

Fig 5.26 Deflector safety factor using Ansys

5.4.9 DEFORMATION OF DEFLECTOR AND STRESS ANALYSIS

From the relation of safety factor and stress $n = \frac{0.66S_y}{\sigma_B}$ the maximum stress that the selected material with stand loads up to 72MPa at safety factor of 2 and simulation (numerical analysis) and analytical solution is very much nearest each other so it is best and safe design.

The following two figures shows the deformation and stress respectively.

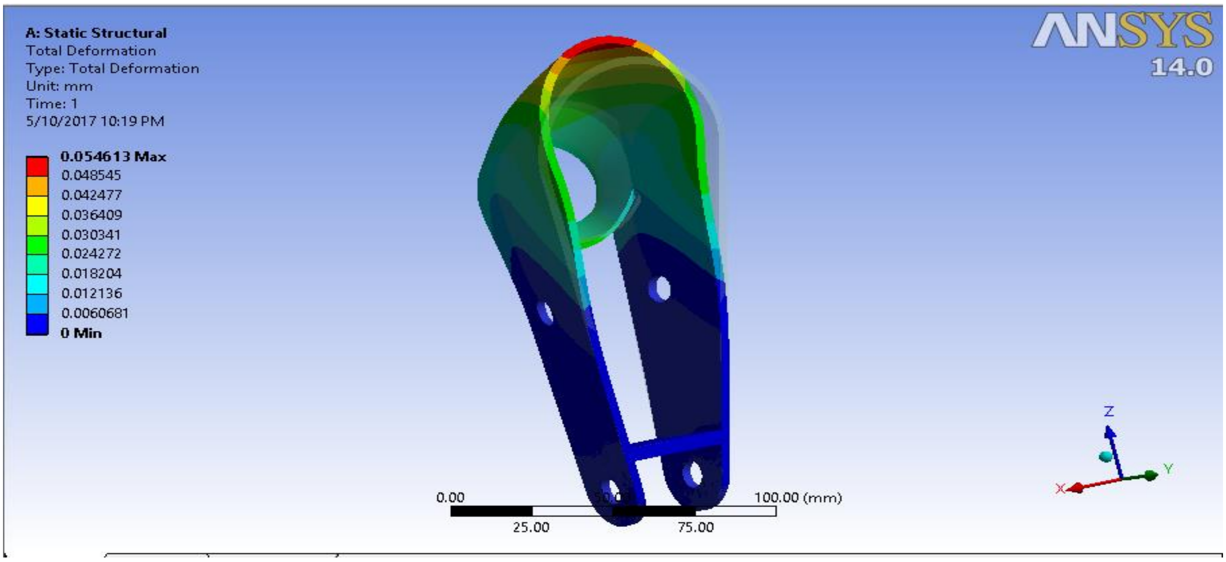

Fig 5.27 Total deformation of deflector

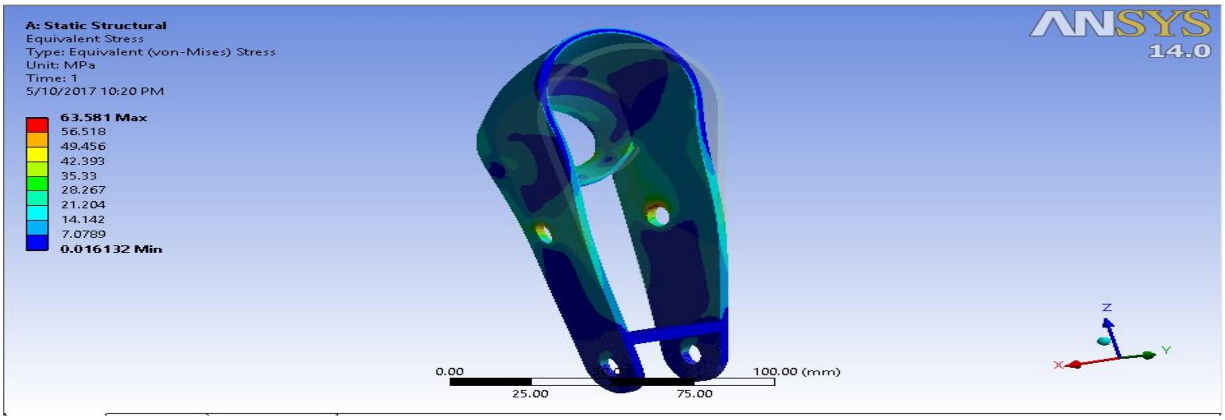

Fig 5.28 Equivalent (von mises) stress of deflector.

5.4.10. DESIGN OF CIRCULAR FLANGED PIPE JOINT

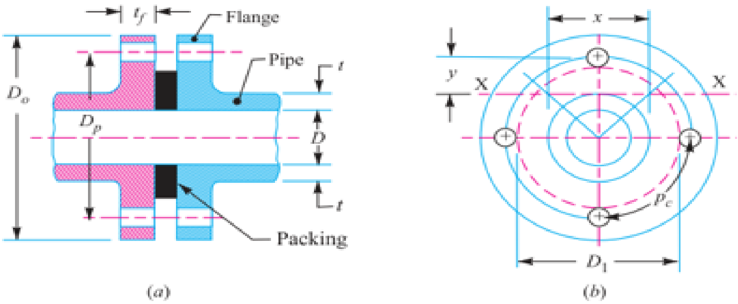

Fig 5.29 Circular flanged pipe joint [46]

Consider a circular flanged pipe joint as shown in Figure 5.30. In designing such joints, it is assumed that the fluid pressure acts in between the flanges and tends to separate them with a pressure existing at the point of leaking. The bolts are required to take up tensile stress in order to keep the flanges together.

The effective diameter on which the fluid pressure acts, just at the point of leaking, is the diameter of a circle touching the bolt holes. Let this diameter be D_1. If d_1 is the diameter of bolt hole and D_p is the pitch circle diameter, then $D_1 = D_P - d_1$

Therefore force trying to separate the two flanges, will be $F = \frac{\pi}{4}(D_1)^2 * P$

Let $n =$ Number of bolts,

$d_c =$ core diameter of the bolts, and σ_t Permissible stress for the material of the bolts.

Therefore resistance to tearing of bolts, $\frac{\pi}{4}(d_c)^2 * \sigma_t * n$

The thickness of the flange is obtained by considering a segment of the flange as in fig.

The bending moment is taken about the section X-X, which is tangential to the outside of the pipe. Let the width of the segment is x and the distance of this section from the center of the bolt is y.Therefore bending moment on each bolt due to the force F, $\frac{F}{n} * y$ And resisting moment on the flange, $\sigma_b * Z$ Where σ_b = bending or tensile stress for the flange material, and

$$Z = \text{section modulus of the cross} - \text{section of the flange} = \frac{1}{6} * x * (t_f)^2$$

The pipes may be strengthened by providing greater thickness near the flanges (equal to $\frac{(t+tf)}{2}$. The flange may be strengthened by providing ribs equal to thickness of (t +tf)/2

The flange material is cast iron:$t = \frac{P*D}{2*\sigma_t} + C$, the value of 'C' according to Weisback, are given in the following table.

Table 5.34 Weisback constant [46].

Material	Cast iron	Mild steel	Zinc and Copper	Lead
Constant (C) in mm	9	3	4	5

Allowable tensile stress will be:

$\sigma_t = 14\text{MPa}$ and from the table, $C = 9$ mm, for cast iron

and D internal diameter of the nozzle 142mm

Other dimensions of a flanged joint for a cast iron pipe may be fixed as follows:

Nozzle thickness, $t = 3mm$

Nominal diameter of bolts, $d = 0.75t + 10mm \geq 16mm$ to make the joint leak proof

$d = 0.75 * 3 + 10mm = 13mm$ (*not accepted*) As recommended by design considerations the bolt nominal diameter s never be less than 16mm so in my case 13mm. therefore the nominal diameter for my design of flange joint is 16mm

Number of bolts, $n = 0.0275D + 1.6 = 0.0275 * 142 + 1.6 = 5.5$ say 6 bolts

Thickness of flange, $t_f = 1.5t + 3mm = 1.5 * 3 + 3mm = 7.5mm$

Width of flange, $B = 2.3d = 2.3 * 16 = 36.8mm$ say 37mm

Outside diameter of flange, $D_o = D + 2t + 2B = 142 + 2 * 3 + 2 * 37 = 185mm$

Pitch circle diameter of bolts,

$D_P = D + 2t + 2d + 12mm = 142 + 2 * 3 + 2 * 16 + 12 = 192mm$

The circumferential pitch of the bolts is given by: $P_c = \frac{\pi}{n} D_P = \frac{\pi}{7} * 192 = 86\text{mm}$

In order to make the joint leak-proof, the value of P_c should be between $20\sqrt{d_1}$ and $30\sqrt{d_1}$.

Let us take $d1 = d + 3 = 13 + 3 = 16\text{mm}$ Since the circumferential pitch as obtained above (i.e. 86) is within $20\sqrt{d_1} = 80$ to $30\sqrt{d_1} = 120$, therefore the design is satisfactory.

5.5 THE PRESSURE AND VELOCITY CONTOUR OF THE INTEGRATED NOZZLE-DISTRIBUTER ANSYS SIMULATION RESULT

The pressure is very high at the inlet of the distributer while the velocity is very low at the inlet. The reverse is true at the exit of the nozzle the pressure is almost negligible while the velocity is very high i.e. the potential energy at the nozzle exit is converted to kinetic energy. The following simulation result clearly shows this fact.

Table 5.35 The result of integrated nozzle-distributer

Name	P7 - Mesh Min	P8 - Mesh Average	P5 - Mesh Elements	P6 - Mesh Nodes	P9 - total pressure in	P11 - V_jet_lower	P12 - V_jet_upper	P14 - total pressure lower	P15 - total pressure upper
Units					Pa	m s^-1	m s^-1	Pa	Pa
Current	0.18202	0.89734	5.027E+05	1.5089E+05	4.7692E+05	29.553	29.025	4.7518E+05	4.7578E+05

5.5.1 The Pressure Contour of the Integrated Nozzle-Distributer Design.

As it can be seen from the following figure the pressure is very high throughout the cross section (4.77 x 10^5 pa) and at the exit the pressure energy converted to kinetic energy.so at the exit pressure is almost zero.

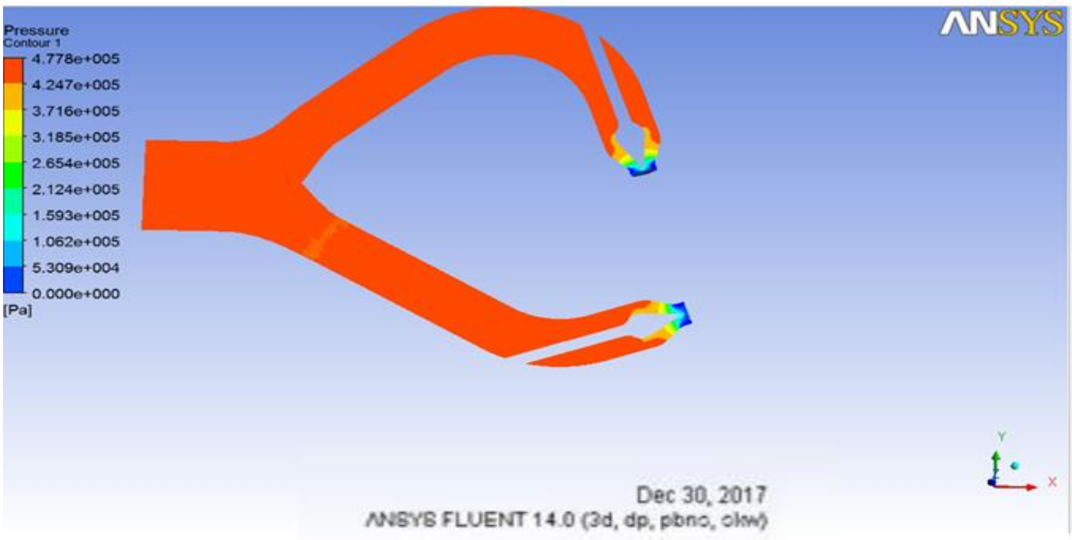

Fig 5.30 The pressure contour of the integrated nozzle –distributer geometry

5.5.2 The velocity contour of the integrated nozzle-distributer

The velocity is very low except at the nozzle exit which is around 30m/s as it is listed on the velocity legend bar.at the split angle the velocity is below 3m/s i.e between 0m/s to 3m/s.

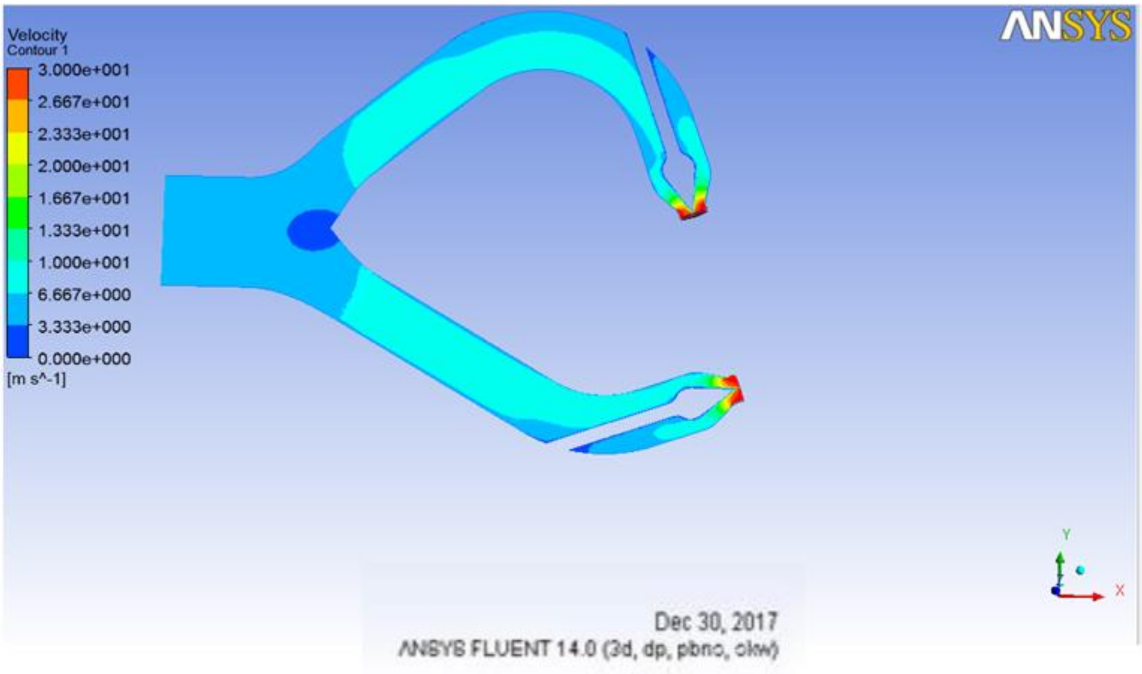

Fig 5.31 The velocity contour of the integrated nozzle –distributer .

CHAPTER SIX

CONCLUSION AND RECOMMENDATION

6.1 CONCLUSION.

The objective of the study was to optimize efficiency of nozzle and distributer by varying their corresponding parameters. Accordingly design analysis and simulations were made for each of the following nozzle parameters: - nozzle angle, spear angle, spear fillet radius, blocking distance, nozzle diameter, bulb radius, nozzle curvature, and spear radius. The numerical values obtained from the resulting analysis shows the insignificance of those parameters but, blocking distance, nozzle angle and nozzle diameter. So due to their significance, blocking distance, nozzle angle, and nozzle diameter were the main concerns of this study in optimizing nozzle efficiency. And then further investigation was made on blocking distance, nozzle diameter, nozzle angle, and spear angle to be analyzed for best flow pattern and less head loss.

To optimize the distributers; split angle, bending radius, length of the distributer and their diameters were essential parameters to select minimum head loss and maximum efficiency. The bending radius from 200mm to 300mm , the diameter from 142mm to 170mm and the splitting angle from 0 degree to 70 degree variation was used to meet the turbine blade properly which is by using 400mm pitch circle diameter of the runner. When the length of the distributer increase the head loss increase due to this, the effect of length has been considered in minimizing the head loss.

The results obtained from the study shows that increasing the pipe diameter of distributer results in the reduction of head loss. However, since the optimal diameter is 142 mm due to its high total gauge pressure, further increment in pipe diameter causes the fall in the total gauge pressure at the inlet of nozzle because the exit of the distributer is the inlet for the nozzle. Total gauge pressure inlet was used due to hydraulic energy at the inlet of the distributer and nozzle due to effect of head and flow rate. Moreover, an increase in diameter of the distributer for specified flow rate has decreased total gauge pressure at the nozzle inlet which in turn leads to high head loss and decreased nozzle efficiency. Yet, continual increment in pipe diameter causes the rise in cost of pipe too. The distributer at 300mm bending radius, 70 degree splitting angle, 1m and 1.2 m length of lower and upper distributer respectively, and 142mm distributer diameter is selected as optimal design and simulation results of the investigation.

For the design and simulation of nozzle, a jet diameter of 54.4mm, flow rate of 0.14m^3/s and the total head of 50m was taken. The nozzle angle of (30-45) in degree and the spear angle of (20-25) in degree was fed to Ansys and then it generates 82 samples. So, the effect of each angle in the range was analyzed on the performance and efficiency of the nozzle and spear alignment in the parameter correlation subpart of Ansys software. The value obtained from Ansys parameter correlation depicts that nozzle angle of 30 degree and spear angle of 20 degree is where maximum efficiency and performance is obtained.

Then further simulation was done by using three candidates of nozzle and spear -angle i.e. (25, 35), (20, 30) and (25, 30) in degree are used with variation of blocking distance from (0-93) mm and nozzle diameter 142 mm to 160mm and finally nozzle and spear angle (20, 30) at a blocking distance of 80 mm with 142 mm nozzle diameter achieved nozzle efficiency of 96.8%.

The critical and notable factor form the simulation of the nozzle was as it can be seen from the study was the nozzle angle and nozzle efficiency. i.e. As the nozzle angle increases the nozzle efficiency decreases due to back flow at the exit of the nozzle when the con angle is very high.

Since flow rate varies seasonally, its range from 0.1 to 0.009 m^3/s were analyzed. And then the optimized nozzle performs well at various values of flow rate compared to the baseline design. After both nozzle and distributer were optimized separately, they were integrated and simulated to compare their corresponding results. The result obtained shows the additive values of head loss obtained from nozzle and distributer equals to the head loss in their integration. Lastly structural simulation of each components are analyzed and as the result shown all the mechanical components were enough to handle the fluid flow through each component with enough safety factor. After the whole simulation was conducted, the best optimized design and simulation geometry of the distributer and the nozzle components were prepared for manufacturing and each of the components were drawn in detail.

6.2. RECOMMENDATION

6.2.1 Recommendation

For further investigation and fulfilling this micro hydro pelton turbine project in generating electric power for off grid area the following recommendations are very important for future work.

- As the design, fluid flow simulation, structural simulation, and the manufacturing drawing are completed here the next recommendation will be manufacturing of each components, as the details of the manufacturing drawing specification and design parameters.
- During load variation there is damage on the mechanical components so there must be automatic controlling unit to control the load variation i.e. servomotor.
- Lastly it is recommended to prepare mini manual to operate properly the micro hydro pelton turbine.

REFERENCE

[1] Aung Kyaw Minn, Htay Win and Nyein Aye San international journal of scientific Design of 225kW Pelton Turbine Mandalay technological University Vol.03, Issue.24 September-2014, Pages: 4836-4842

[2] Bilal Abdullah Nasir international journal of (ijeet) Design of high efficiency pelton turbine for micro hydro power Plant Volume 4, Issue 1, January- February (2013), pp. 171-183

[3] Abhishek Sharma, Vishnu Prashad and Anil Kumar Numerical Simulation of Pelton Turbine Nozzle for Different Shapes of Spear Maulana Azad National Institute of Technology, Bhopal (India).(Received: November 09, 2010; Accepted: December 11, 2010)

[4] Michele Manno Hydraulic Turbines and Hydroelectric Power Plants Department of Industrial Engineering University of Rome «Tor Vergata» 22/05/2013

[6] Vishal Gupta, Dr. Vishnu Prasad and Dr. Ruchi Khare Effect of Jet Shape on Flow and Torque Characteristics of Pelton Turbine Runner. *Vol. 4, Issue 1(Version 1), January 2014.*

[7] Mario Peron, Etienne Parkinson, Lothar Geppert and Thomas Staubli importance of jet quality on pelton efficiency and cavitation 2008 – milano 3rd-6th September International Conference on Hydraulic Efficiency Measurements

[8] Mesa associates, Oak ridge national laboratory for the U.S. department of energy Best Practice Catalog *Pelton Turbine on* 07/24/2012

[9] Aravinda/l kottasamy design and fabrication of laboratory scale micro-hydro pelton turbine Mechanical Engineering University Malaysia Pahang NOVEMBER 2010

[10] Deepak Bisen1, Prof. Sunil Shukla and Dr. P.K.Sharma Optimization and Simulation of Hydro-Turbine Nozzle in Based on Ansys Analysis International Journal of Advance Engineering and Research Development *Volume 1, Issue 10, October-2014*

[11] M. M. Alnakhlani, Mukhtar, D. A. Himawanto, A. Alkurtehi1 & D. Danardono Effect of the Bucket and Nozzle Dimension on the Performance of a Pelton Water Turbine Mechanical Engineering Department, Sebelas Maret University, Surakarta, Indonesia November 18, 2014

[12] J. Veselý and M. Varner A Case Study of upgrading of 62.5MW Pelton Turbine mechanical Engineering a.s., Czech Republic

[13]Water for agriculture and energy in Africa ministerial conference on water for agriculture and energy in Africa: the challenges of climate change: Sirte, Libyan Arab Jamahiriya, and 15-17 December 2008

[14] Micro Hydro Power Resource Assessment Handbook Prepared for Asian and Pacific Centre for Transfer of Technology of the United Nations – Economic and Social; Commission for Asia and the Pacific (ESCAP); By Dilip Singh; September 2009

[15] Dr. M.N. Shesha Prakash, Professor, J.N.N. College of Engineering, Shimoga Hydraulics and Hydraulic Machines

[16] Takashi Kubota and hitomi kawekami Observation of jet interference in 6-Nozzle pelton turbine modernization of large Kaplan runner (updating of U.S wells hydroelectric project)

[17] Cavado Portugal English electric and Bersimis Canada (English electric) impulse turbine pelton wheel

[18] Bilal Abdullah Nasir Design of Micro - Hydro - Electric Power Station International Journal of Engineering and Advanced Technology (IJEAT) ISSN: 2249 – 8958, Volume-2, Issue-5, June 2013

[19] Zh. Zhang Pelton Turbines Swiss Federal Institute of Technology in Zurich Switzerland January 2016

[20] Prof. Q.H. Nagpurwala hydraulic turbine ppt

[21] Reiner Mack, Bartlomiej Gola, Martin Smertnig, Bernhard Wittwer and Peter Meusburger Modernization of vertical Pelton turbines with the Help of CFD and model on 12/04/2016 [22] Mohammed Taih Gatte and Rasim Azeez Kadhim Hydro Power project

[22] M. Sahu, Kishanjit Kumar Khatua, Kanhu Charan Patra, and T. Naik developed laminar flow in pipe using computational Fluid dynamics Rourkela India February 2009

[23] E Hernández Design and construction of an impulse turbine Florida, Colombia November 2013

[24] Phoevos-Charalampos K. Koukouvinis development of a meshfree particle method for the simulation of steady and unsteady free surface flows: application and validation of the method on impulse hydraulic turbines**.** National Technical University of Athens School of Mechanical Engineering July 2012

[25] Muh. Anis Mustaghfirin, Akio Miyara, Azridjal Aziz and Fumiaki Sugino; Uniformity of Two-phase Flow Distribution in Curved Round Distributor Department of Mechanical Engineering, Saga University ***vol.33 (2012)***

[26] Amod Panthee, Hari Prasad Neopane and Bhola Thapa CFD Analysis of Pelton Runner International Journal of Scientific and Research Publications, Volume 4, Issue 8, August 2014

[27] Professor Arne Kjølle HYDROPOWER IN NORWAY Norwegian University of Science and Technology December 2001

[28] Dilip Singh Micro Hydro Power Resource Assessment Handbook Asian and Pacific Centre for Transfer of Technology Of the United Nations – Economic and Social Commission for Asia and the Pacific **September 2009**

[29] M V Subbarao Professor Mechanical Engineering Department CFD Analysis of Free Jets & Flows In Air Nozzles & Jets for Pelton Wheels ppt 2009

[30] Faiz Ahmed Meeran, Muhammad Arslan, Ali Raza Mansha and Aamir Sajjad Design and Optimization of Pelton Wheel Turbine for Tube-well international journal of multidisciplinary sciences and engineering, vol. 6, no. 9, September 2015

[32]http/www.codecogs.compagescatgen.phpcategory-engineering fluid mechanics pipes head loss.

[33] Trainers Textbook Small Hydro Power (SHP) Module Ministry of New and Renewable Energy Government of India

[34] Prof. J.-L. KUENY Objectives for Small Hydro technology Institute national polytechnique de Grenoble ecole nationale supérieure d'hydraulique et de mécanique de grenoble

[35] Professor Maarten J. Kamper design and implementation of a low cost grid connected 10kw hydro power system March 2010

[36] A. Carvalho Quintela *Guideline for Design of small hydropower plants* July 1999.

[37] andreas von flotow micro hydro penstock design oregon state university me 406: independent projects june 2, 2012

[38] Fluent User Services Center www.fluentusers.com

[39]Markus Eisenring harnessing water power on small scale series of micro hydro pelton turbine hand book manual volume 9

[40] Tilahun Nigussie micro hydro pelton turbine design and manufacturing PHD Research at Addis Ababa institute of Technology 2016

[41] Aldo Cateni, Livio Magri and Gianalberto Grego Optimization of hydro power plants performance Importance of rehabilitation and maintenance Economics of Efficiency Testing and Monitoring 7th International Conference on Hydraulic Efficiency Measurements, September 3rd-6th 2008, Milan, Italy

[42] Matthew Gass, and Hetch Hetchy Modification of Nozzles for the Improvement of Efficiency of Pelton Type Turbines Moccasin Ca USA 2002

[43] Fluid Mechanics and Thermodynamics of Turbomachinery Sixth Edition 2010 S.L. Dixon, and C.A. Hall.

[44] Akhilesh Arvind Nimje and Gopal Dhanjode Pico-Hydro-Plant for Small Scale Power Generation in Remote Villages Issue 1 Ver. III (Jan. 2015), PP 59-67

[45] Bryan Patrick Ho-Yan Design of a Low Head Pico Hydro Turbine for Rural Electrification in Cameroon university of Guelph, Ontario, Canada April, 2012

[46]R.S. KHURMI and J.K. GUPTA text book of machine design fourteenth edition 2005

APPENDICES

APPENDIX A: MANUFACTURING DRAWINGS OF THE COMPONENTS

I. Nozzle

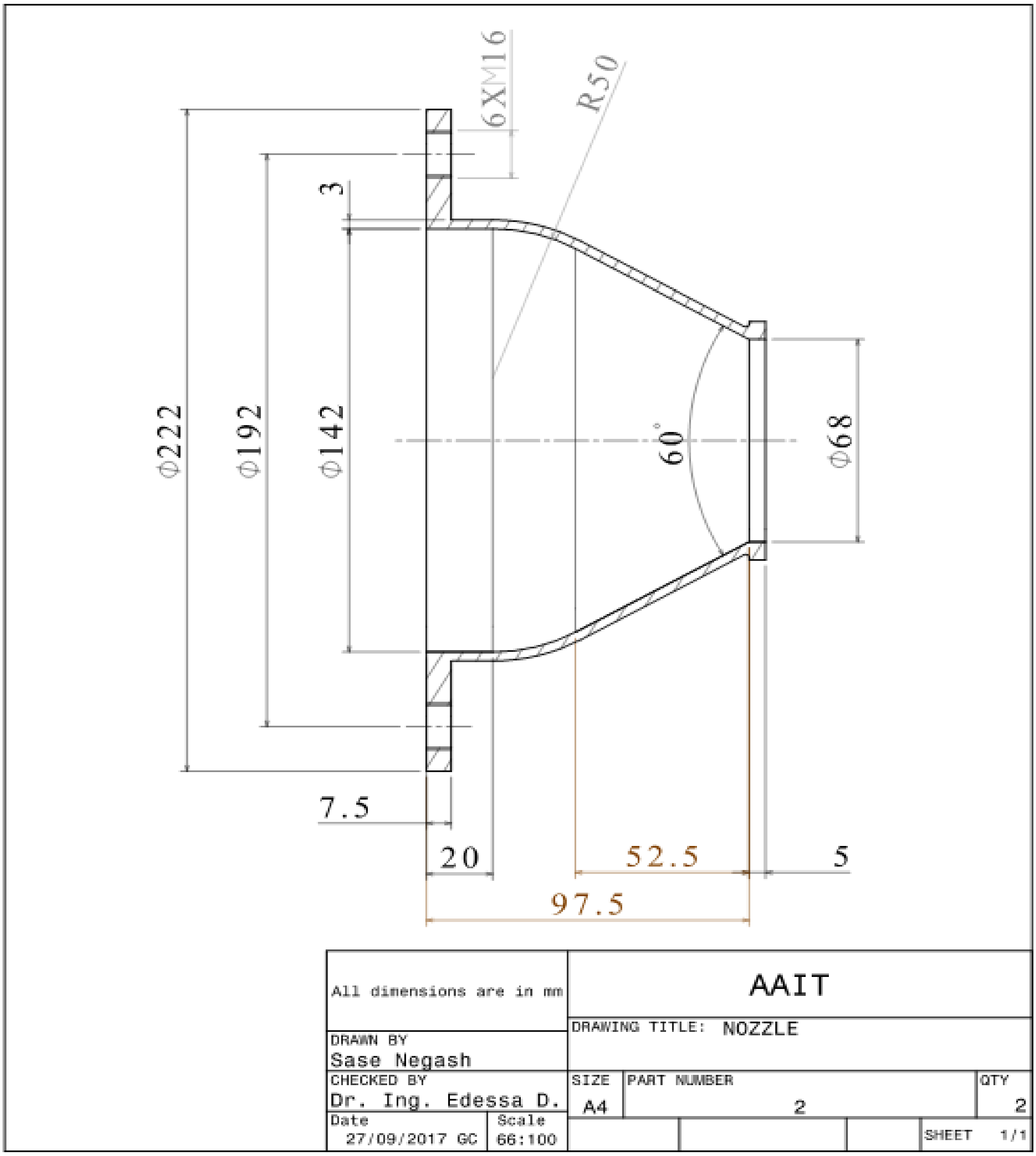

II. Spear

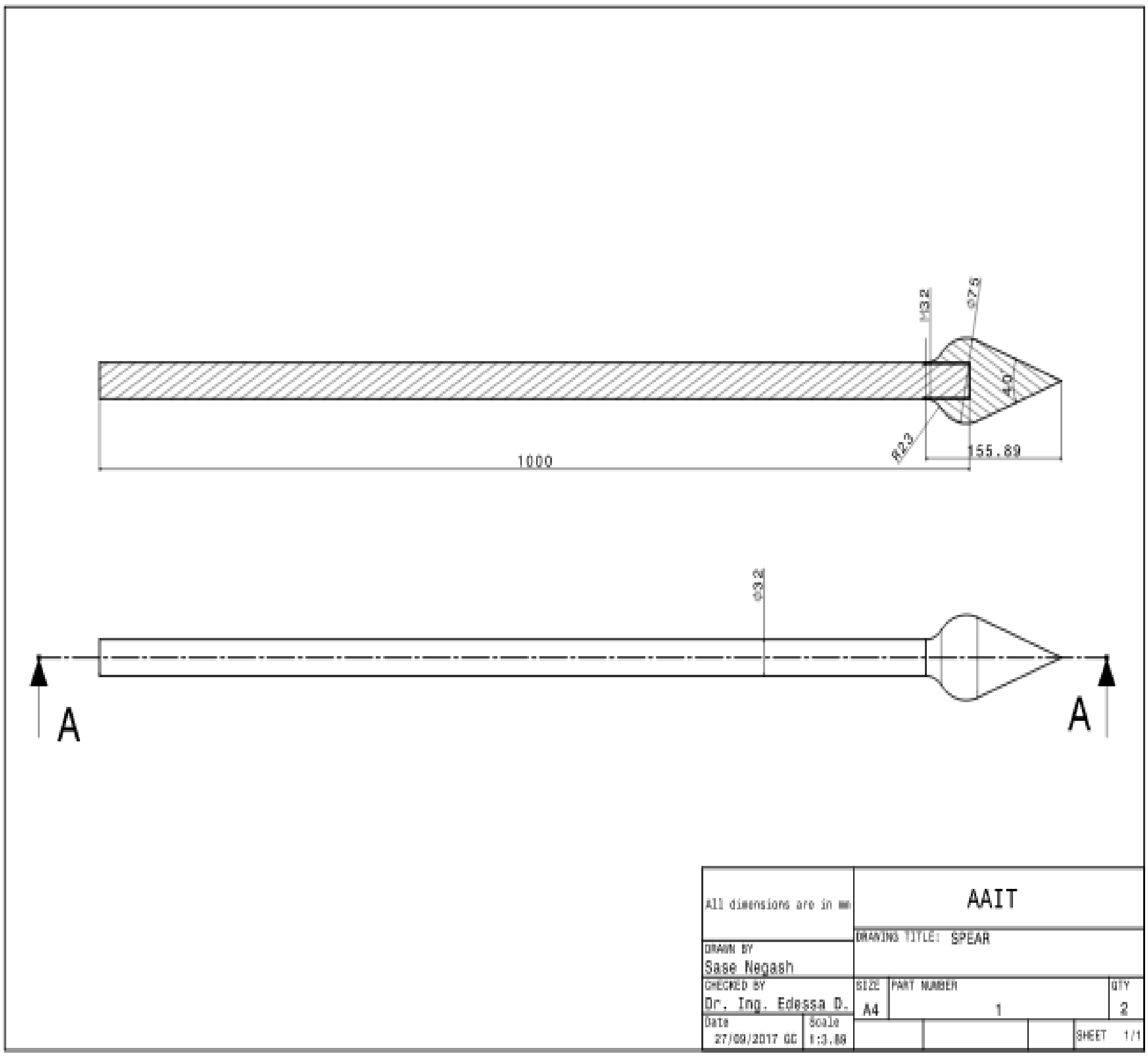
H32
Ø75
40
R23
155.89
1000
Ø32
A
A
All dimensions are in mm
AAIT
DRAWING TITLE: SPEAR
DRAWN BY
Sase Negash
CHECKED BY
Dr. Ing. Edessa D.
SIZE
A4
PART NUMBER
1
QTY
2
Date
27/09/2017 GC
Scale
1:3.88
SHEET 1/1

III. Stator guide

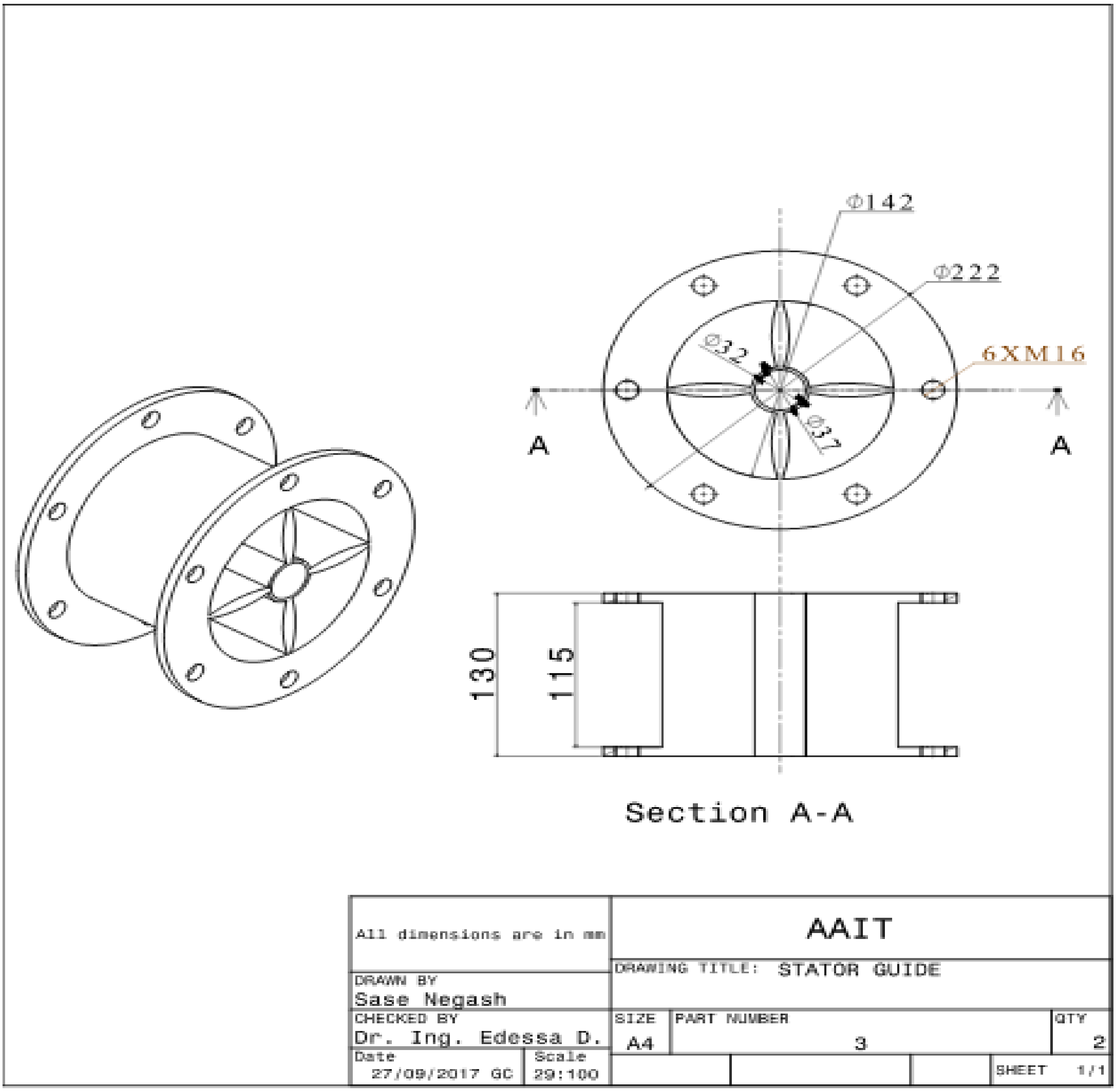

IV. Bifurcation

i. upper bifurcation

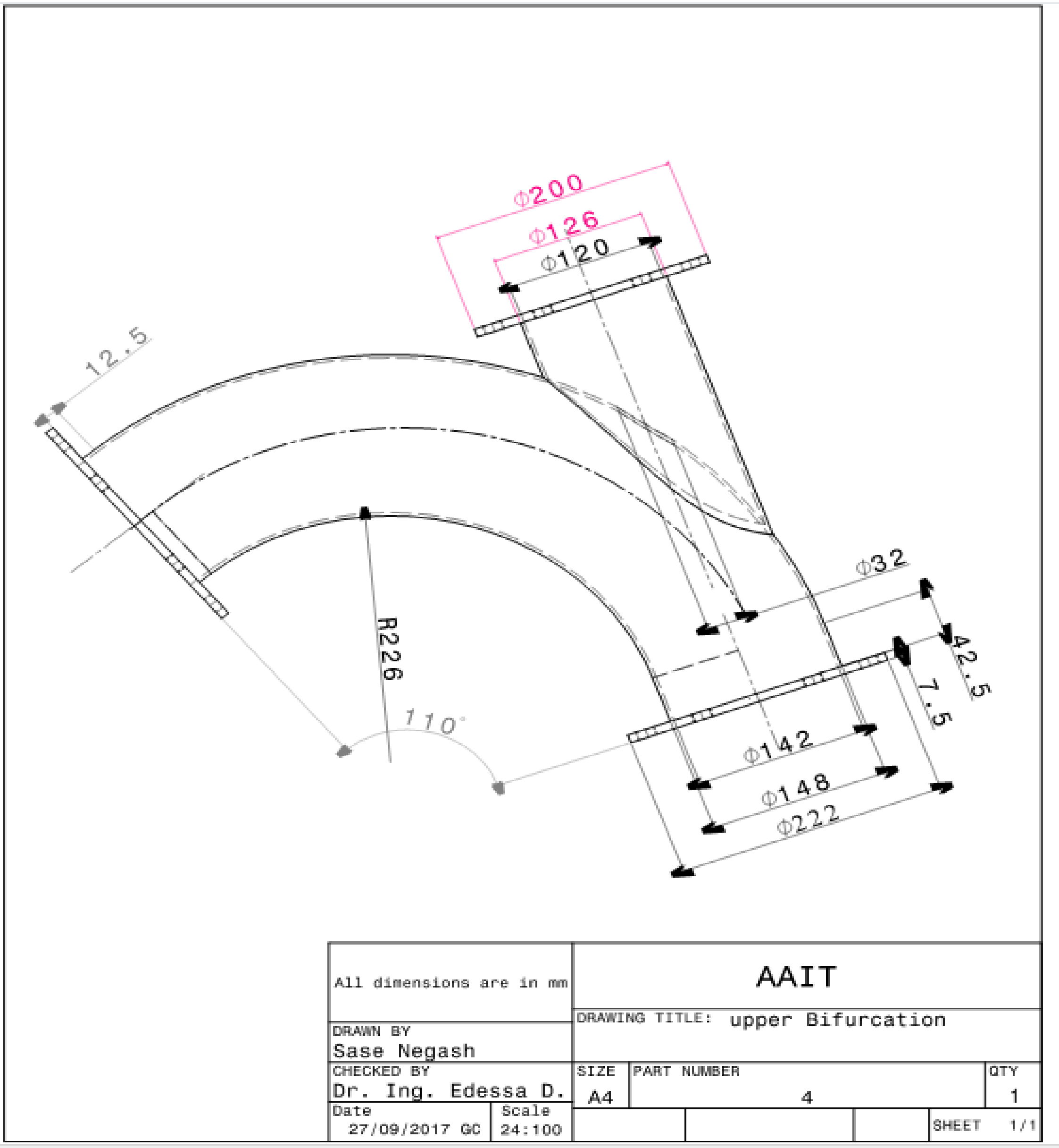

ii. Lower bifurcation

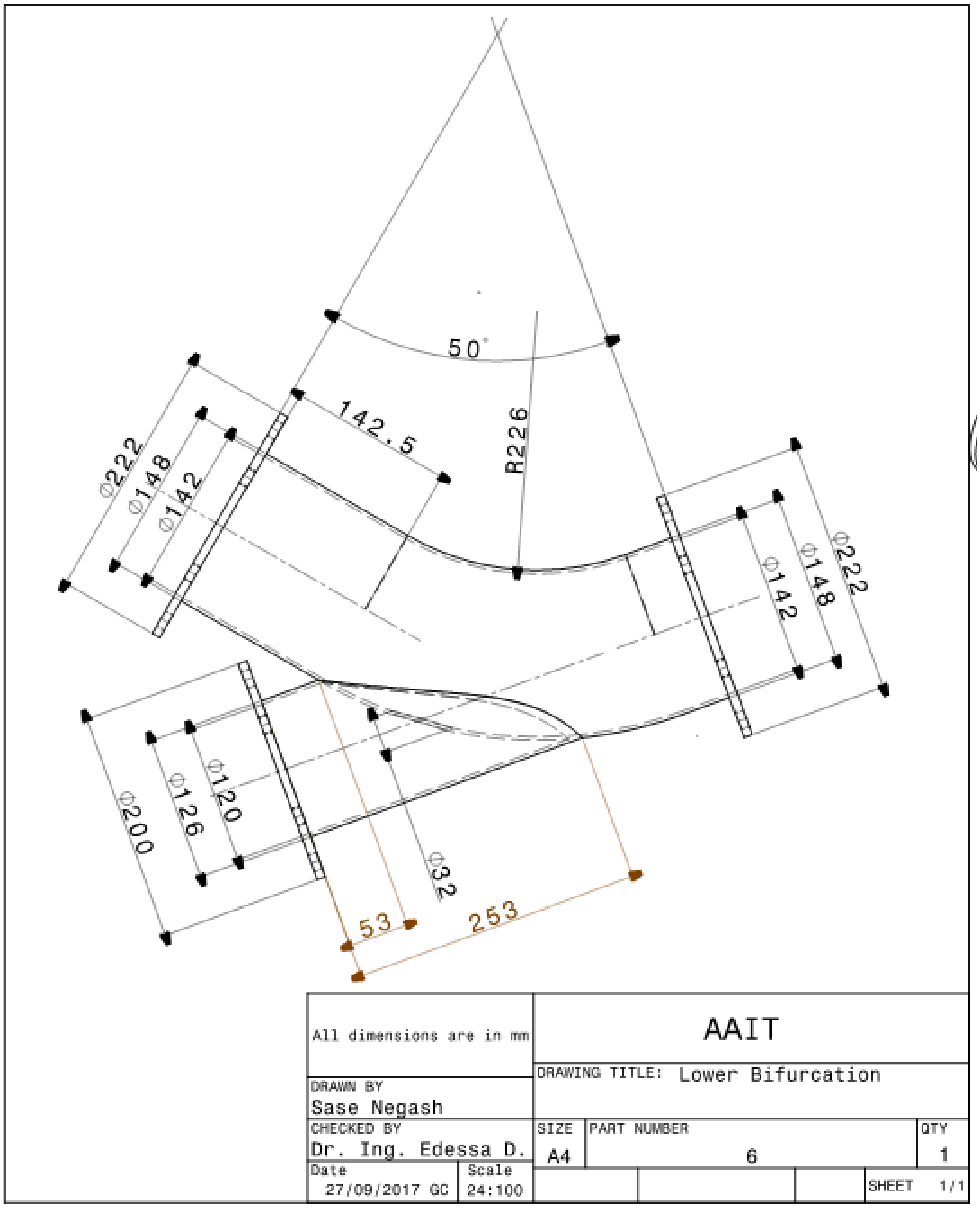

V. Straight Bifurcation

i. upper Straight Bifurcation

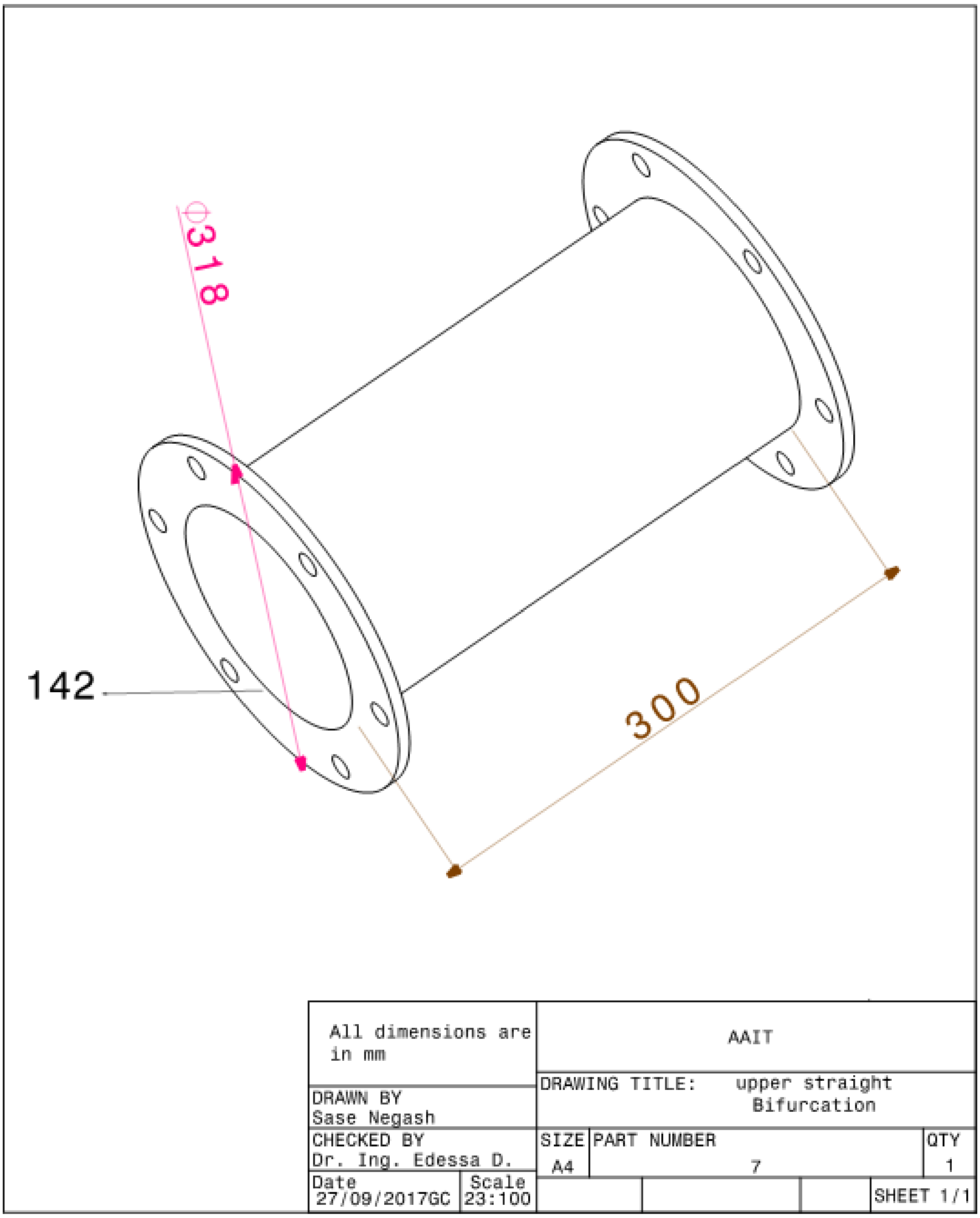

ii. Lower straight Bifurcation

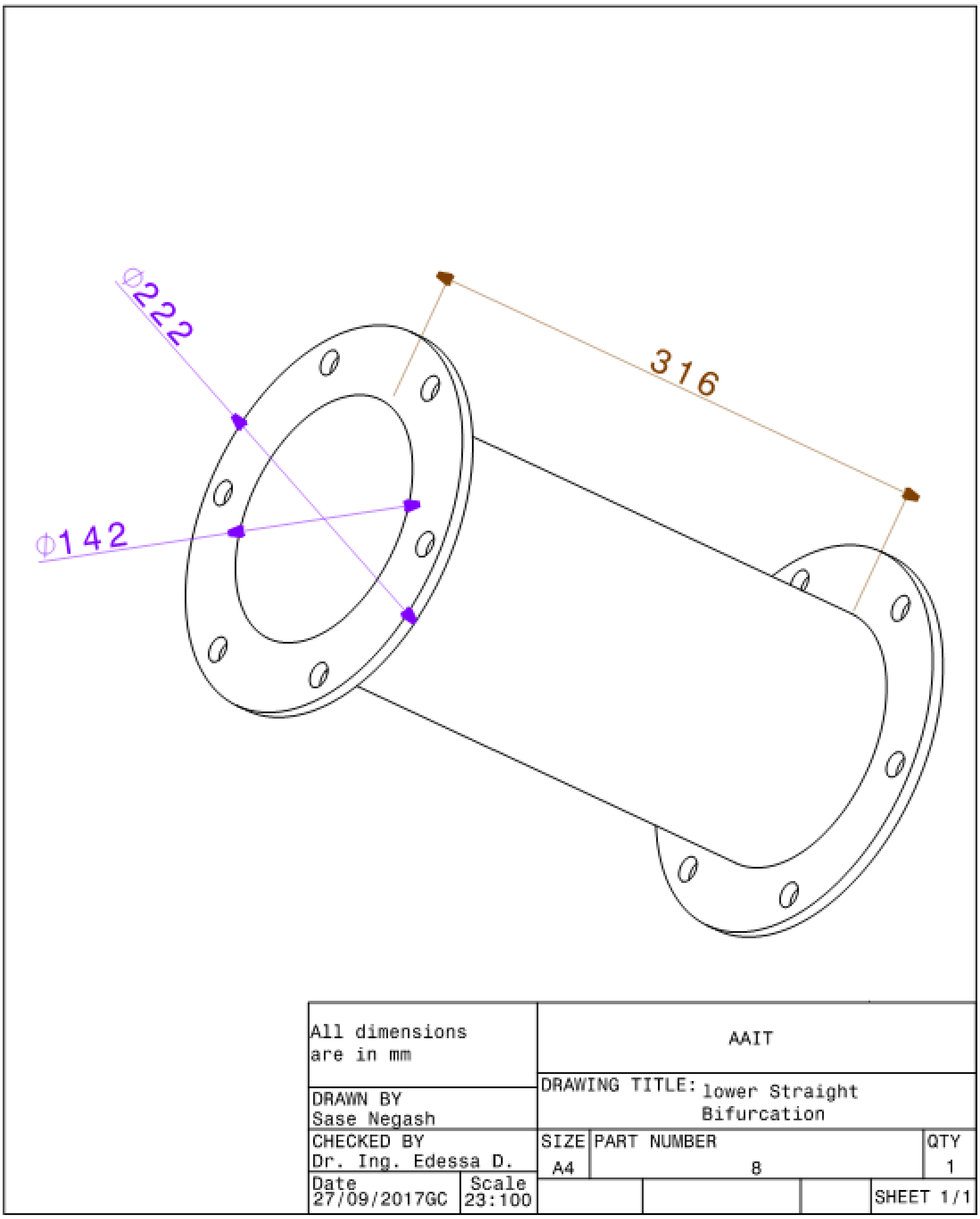

VI. Nozzle packing box

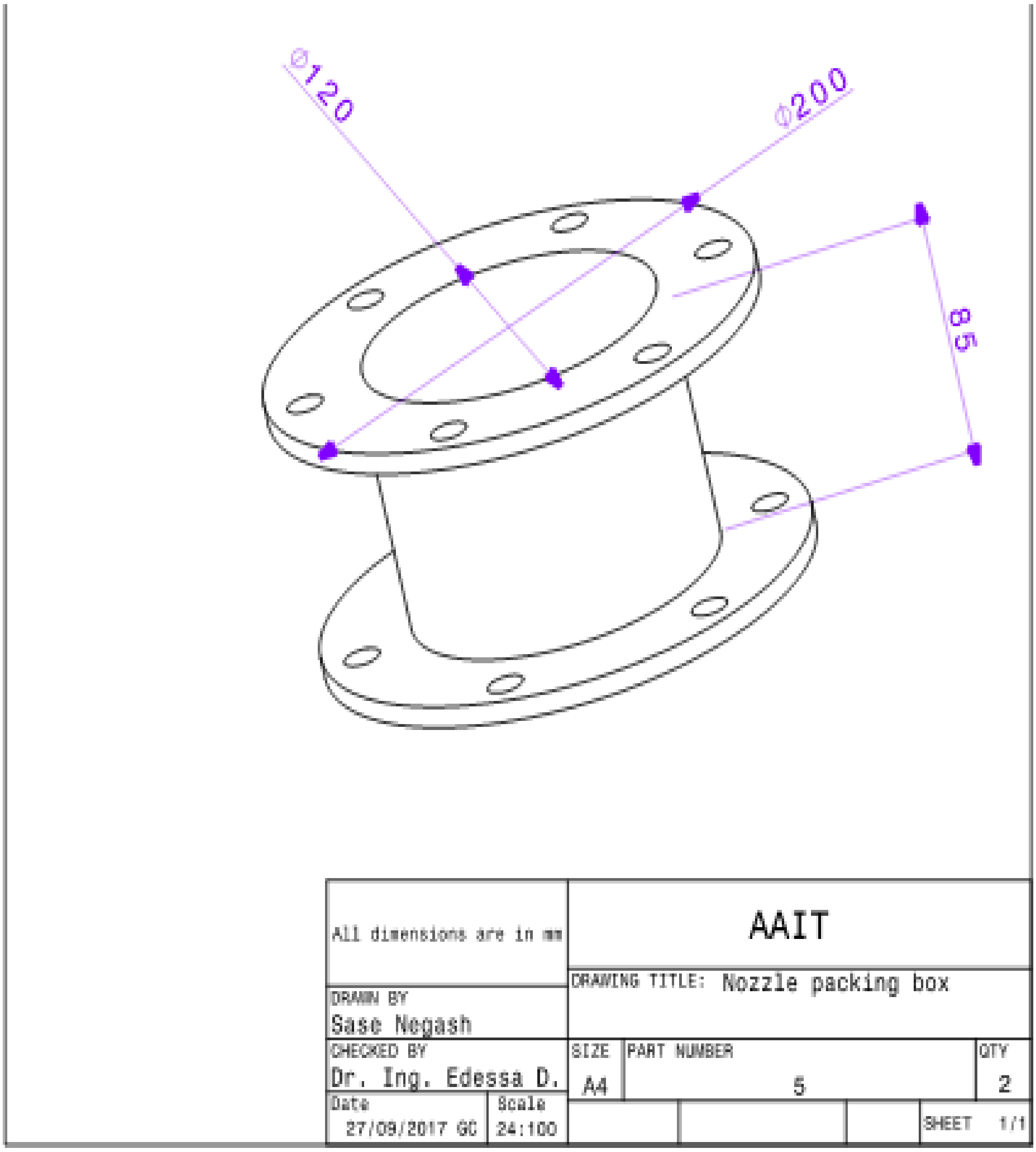

VII. Three junction distributer

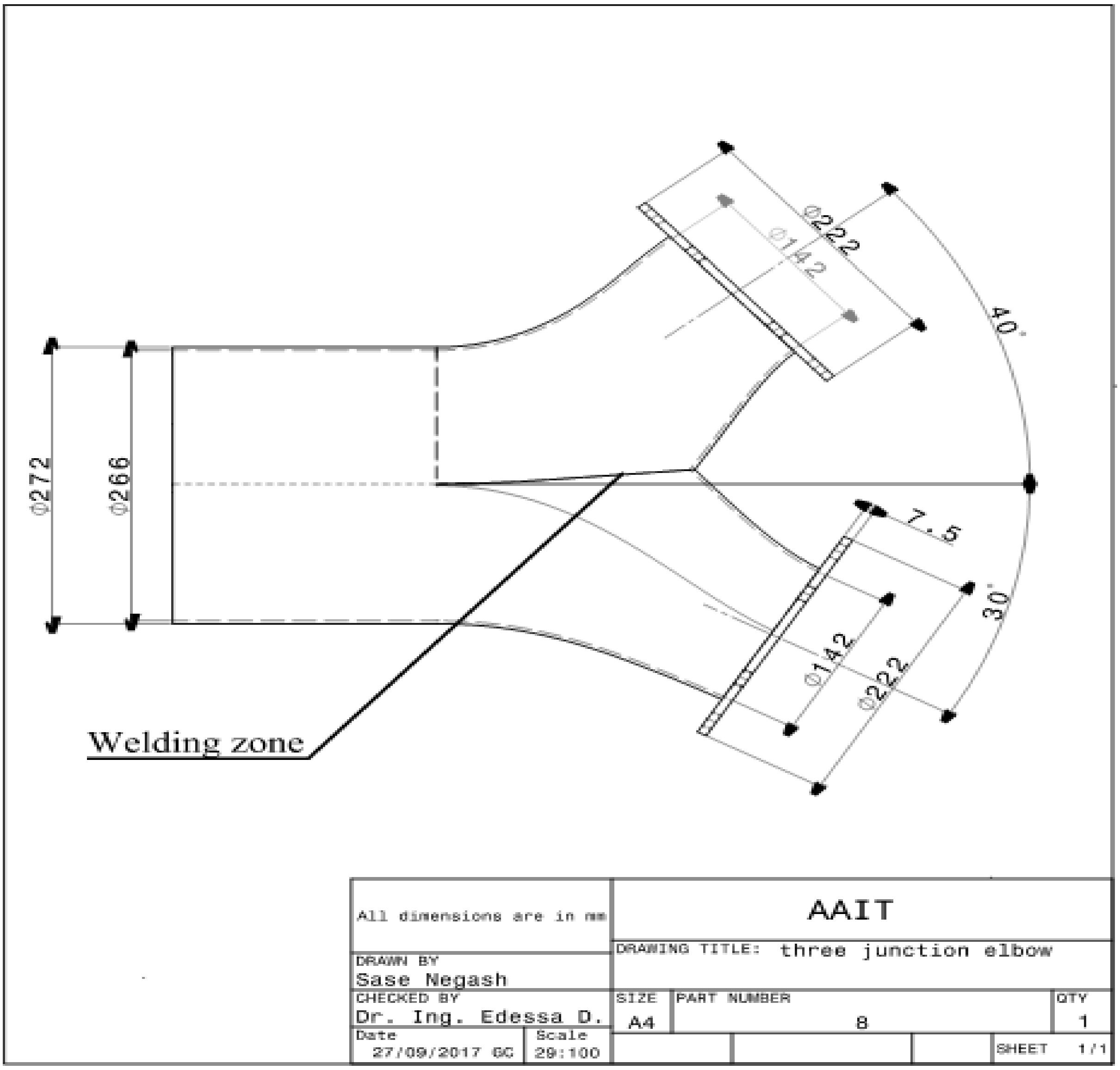

VIII. Deflector

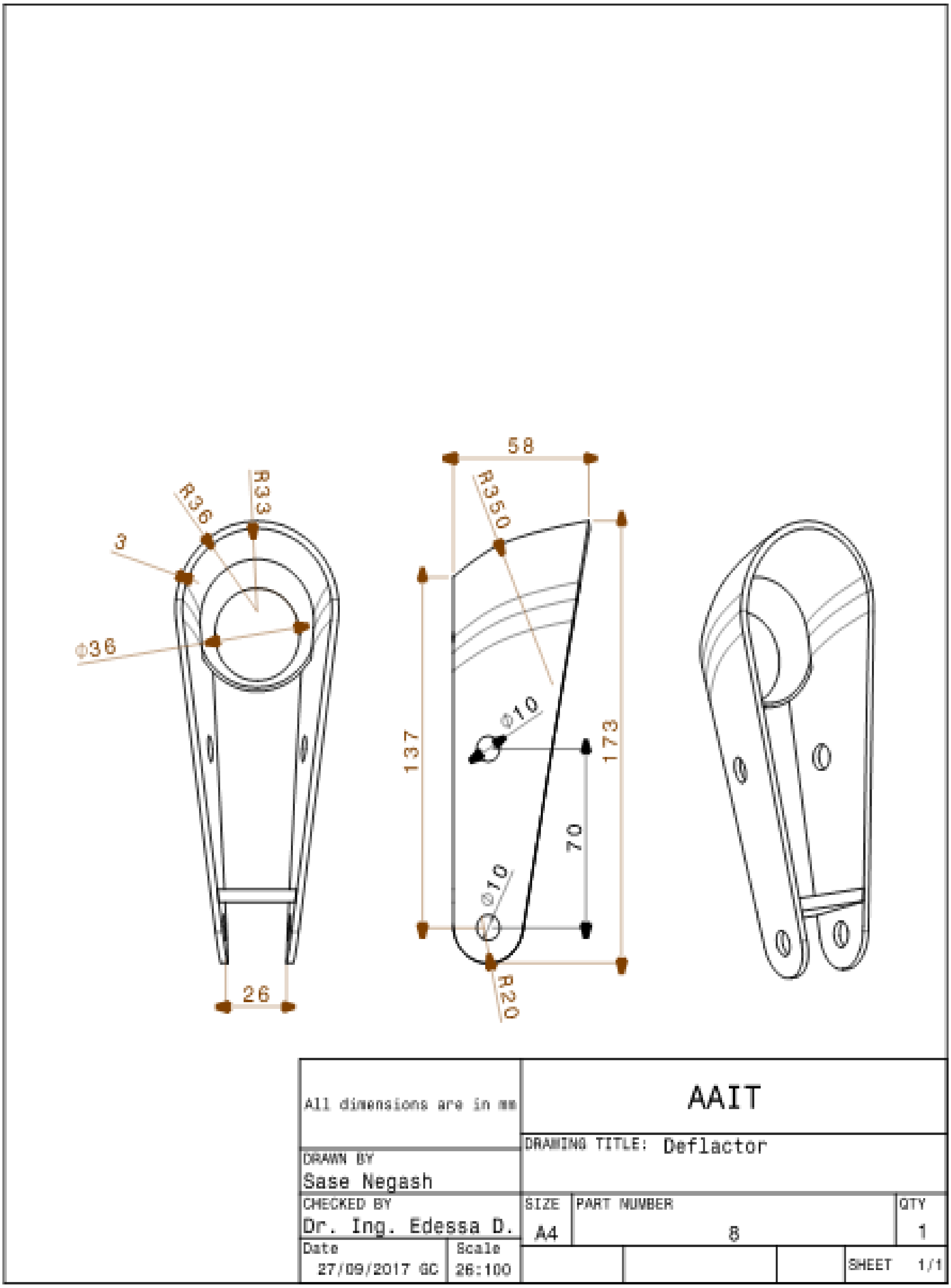

IX. Assembly drawing.

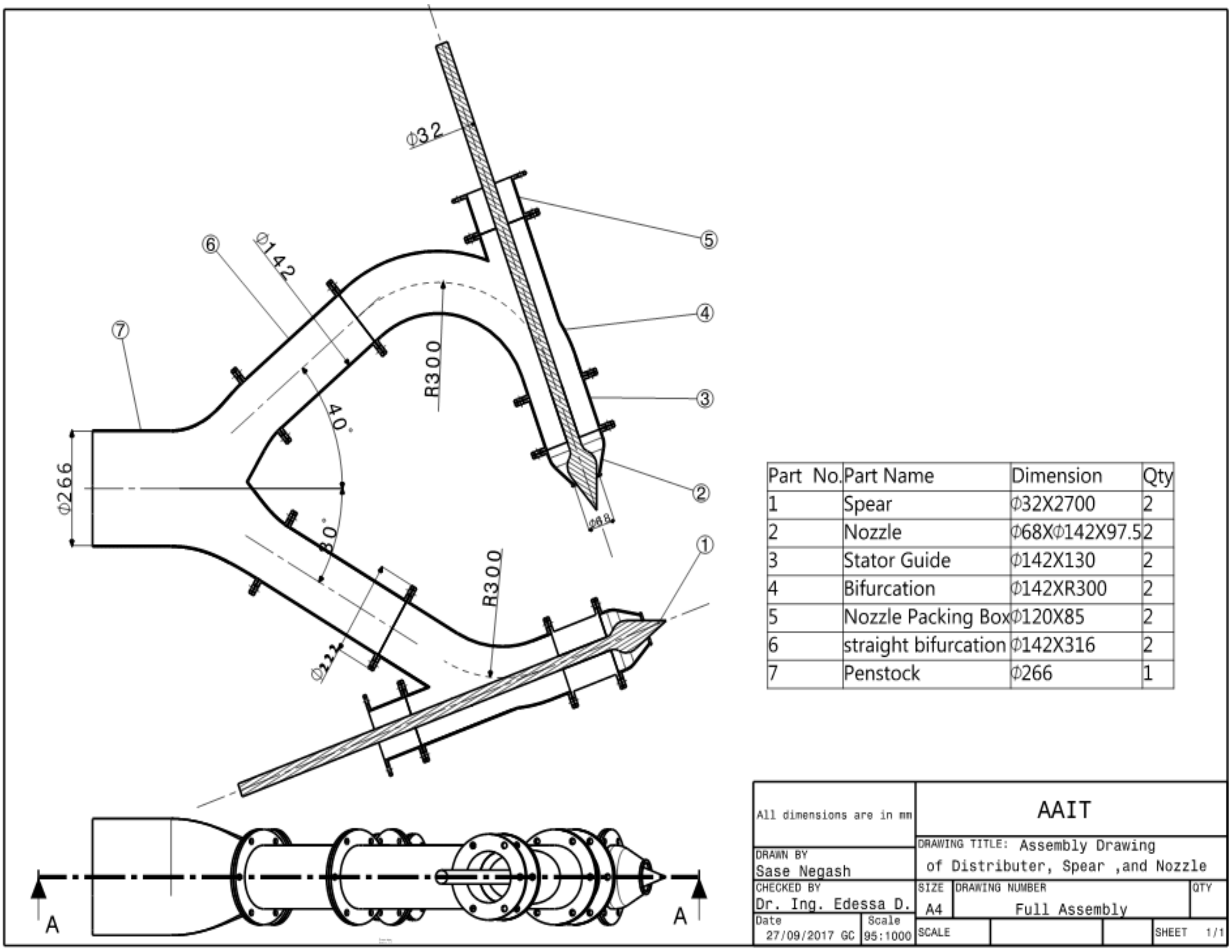

Part No.	Part Name	Dimension	Qty
1	Spear	Φ32X2700	2
2	Nozzle	Φ68XΦ142X97.5	2
3	Stator Guide	Φ142X130	2
4	Bifurcation	Φ142XR300	2
5	Nozzle Packing Box	Φ120X85	2
6	straight bifurcation	Φ142X316	2
7	Penstock	Φ266	1

APPENDIX B: MOODY CHART

Friction factor as a function of $\boldsymbol{R_e}$ and $\boldsymbol{\epsilon/D}$ for round pipes- the Moody chart

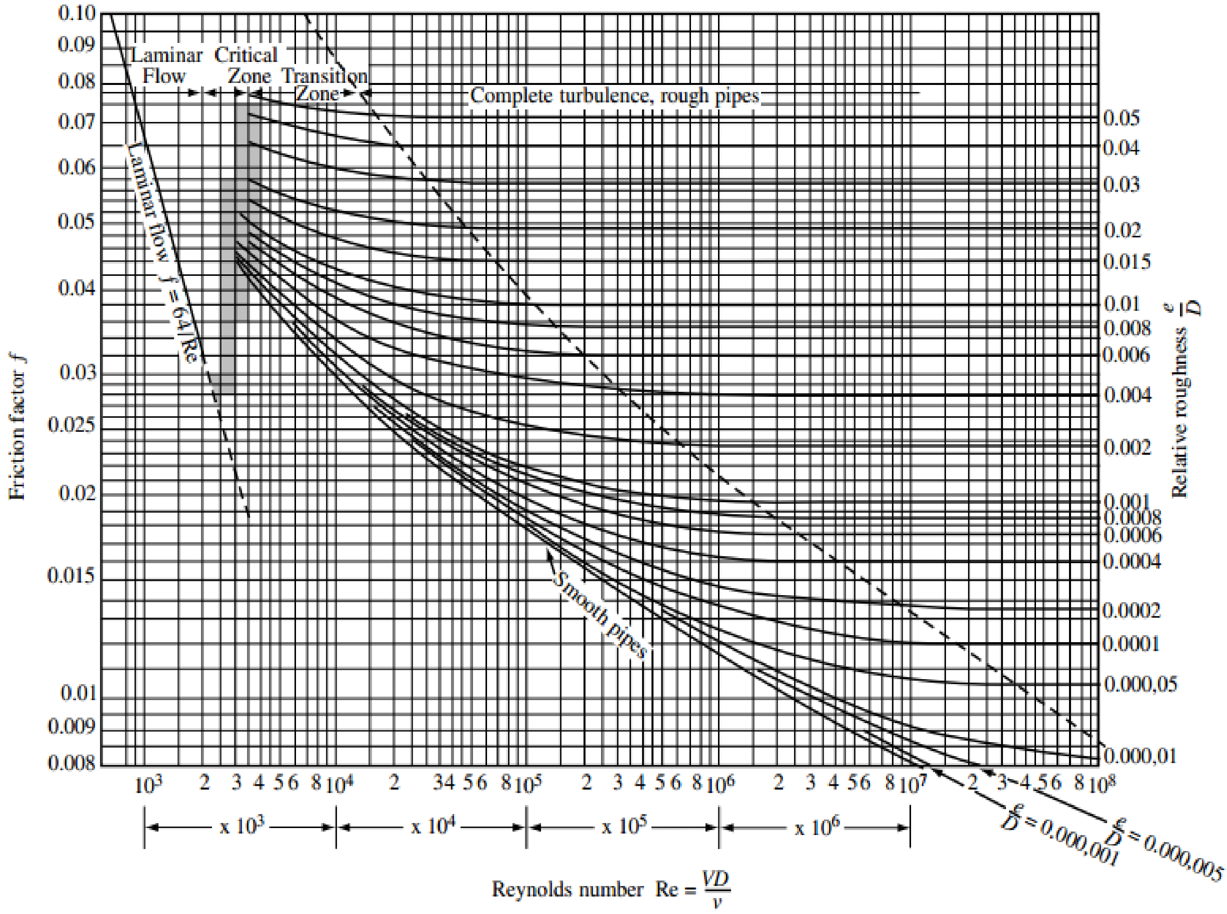

APPENDIX C- DATA TABLES FOR DIFFERENT DESIGN

Table 3.1 Comparison of penstock material [35]

Charactersticks of commom pipe material	Steel	Unplasticized Poly Vinyl cholride Upvc	High-density Polyethlene (HDPE)
Cost	Expensive	Cheapest	Cheap
Friction	It has moderat resistance	Low resistance to flow	Low resistance to flow
Sunlight	Susceptible to sunlight	Deteriorates when subjected to sunlight	Suscpectible to sunlight
Corrosion	Does corrode	Good resistance to corrosion	Good resistance to corrosion
Weight	Heavy	Light	Light
Max. pressure	189.9barr	25 bar	25 barr
Max diameter	600mm	500mm	1000mm
Joining	Moderat pipes are either welded or bolted together	Easy, features a spigot and socket joint;	Difficult, different pipes need to be welded together
Fragile	Very resistance to damage	Very fragile specially at low tempratures	Less fragile than Upvc
Expansition and contraction	Little	About ten times more than steel	About ten times more than steel

Table 3.2 Nominal steel pipe size as per ASTM from

U.S./METRIC

NOMINAL PIPE SIZE	OD	SCHEDULE DESIGNATIONS			WALL THICKNESS		WEIGHT		ID	
INCH MM	INCH MM	ASME			INCH	MM	LBS/ FOOT	KG/ METER	INCH	MM
9 225	9.625 244.5	STD	40	40S	0.342	8.69	33.94	50.54	8.941	227.12
		XS	80	80S	0.500	12.70	48.77	72.60	8.625	219.10
		XX			0.875	22.23	81.85	121.85	7.875	200.04
10 250	10.750 273.0			5S	0.134	3.40	15.21	22.61	10.482	266.20
				10S	0.165	4.19	18.67	27.78	10.420	264.62
					0.188	4.78	21.23	31.62	10.374	263.44
		20			0.250	6.35	28.06	41.76	10.250	260.30
		30			0.307	7.80	34.27	51.01	10.136	257.40
		STD	40	40S	0.365	9.27	40.52	60.29	10.020	254.46
		XS	60	80S	0.500	12.70	54.79	81.53	9.750	247.60
		80			0.594	15.09	64.49	95.98	9.562	242.82
		100			0.719	18.26	77.10	114.71	9.312	236.48
		120			0.844	21.44	89.38	133.01	9.062	230.12
		140	XX		1.000	25.40	104.23	155.10	8.750	222.20
		160			1.125	28.58	115.75	172.27	8.500	215.84
11 275	11.750 298.5	STD	40	40S	0.375	9.53	45.60	67.91	11.000	279.44
		XS	80	80S	0.500	12.70	60.13	89.51	10.750	273.10
		XX			0.875	22.23	101.72	151.46	10.000	254.04

Table 3.3 Roughness value for different material type [35]

Pipe material	Roughness, ε(mm)
Cast iron	0.26
Commercial steel and wrought iron	0.045
Concrete	0.3-3.0
Drawn tubing	0.0015
Galvanized iron	0.15
Plastic, (and glass)	0.0(smooth)
Riveted steel	0.9-9.0

Table 3.4 Flow Regime Vs Reynolds No [38]

Reynolds no	Flow regime	Y+(first cell height)
$Re \leq 2000$	Laminar	$Y+= Pipe\ radius/38$
$2000 < Re < 15000$	Turbulent, enhanced wall treatment	$Y+ < 5$
$Re \geq 15000$	Turbulant, standard wall function	$Y+ > 30$

Table 5.38 Indian standard designation of steel according to IS: 1570(part I) 1978(reaffirmed 1993)

IS : 1570 (Part I)-1978 (Reaffirmed 1993).

Indian standard designation	Tensile strength (Minimum) N/mm²	Yield stress (Minimum) N/mm²	Minimum percentage elongation	Uses as per IS : 1871 (Part I)—1987 (Reaffirmed 1993)
Fe 290	290	170	27	It is used for plain drawn or enamelled parts, tubes for oil well casing, steam, water and air passage, cycle, motor cycle and automobile tubes, rivet bars and wire.
Fe E 220	290	220	27	
Fe 310	310	180	26	These steels are used for locomotive carriages and car structures, screw stock and other general engineering purposes.
Fe E 230	310	230	26	
Fe 330	330	200	26	
Fe E 250	330	250	26	

APPENDIX D- Ansys simulation result table for distributer type 4 at different diameter

At D=142mm

P224 - mass flow out	P223 - total pressure in	P154 - Q	P132 - dynamic pressure lower	P131 - dynamic pressure upper	P125 - V_in	P126 - V_lower	P127 - V_upper	P128 - static pressure in	P129 - static pressure lower	P130 - static pressure upper	P155 - Q_lower	P156 - Q_upper
kg s^-1	Pa	m^3 s^-1	Pa	Pa	m s^-1	m s^-1	m s^-1	Pa	Pa	Pa	m^3 s^-1	m^3 s^-1
69.874	4.7692E+05	0.14	10952	10957	2.5193	4.6973	4.7104	4.7375E+05	4.6423E+05	4.6363E+05	-0.07	-0.07

At D=150mm

P247 - mass outflow	P246 - total pres... in	P248 - d_hyd	P249 - static pressure in	P250 - static pressure lower	P251 - static pressure upper	P253 - total pressure upper	P252 - total pressure lower	P254 - V_in	P255 - V_lower	P256 - V_upper
kg s^-1	Pa	m	Pa	Pa	Pa	Pa	Pa	m s^-1	m s^-1	m s^-1
69.874	4.7692E+05	0.118	4.7375E+05	4.6663E+05	4.6607E+05	4.7484E+05	4.7542E+05	2.5206	4.1246	4.1539

At D=160mm

P232 - outflow mass	P231 - total pressure in	P235 - static pressure lower	P234 - static pressure in	P236 - static pressure upper	P239 - V upper	P238 - V lower	P237 - V in	P242 - dynamic pressure in	P241 - dynamic pressure lower	P240 - dynamic pressure upper
kg s^-1	Pa	Pa	Pa	Pa	m s^-1	m s^-1	m s^-1	Pa	Pa	Pa
69.874	4.7692E+05	4.6904E+05	4.7374E+05	4.6859E+05	3.6422	3.6276	2.5209	3178	6734.3	6713.1

At D=170mm

P293 - total pressure in	P294 - mass outflow	P295 - d_hyd	P296 - static pressure in	P297 - static pressure lower	P298 - static pressure upper	P299 - V_upper	P300 - V_lower	P301 - V_in
Pa	kg s^-1	m	Pa	Pa	Pa	m s^-1	m s^-1	m s^-1
4.7692E+05	69.874	0.138	4.7374E+05	4.7074E+05	4.7034E+05	3.2485	3.2489	2.524

Appendix E- Pressure contour of the distributer for the different diameter

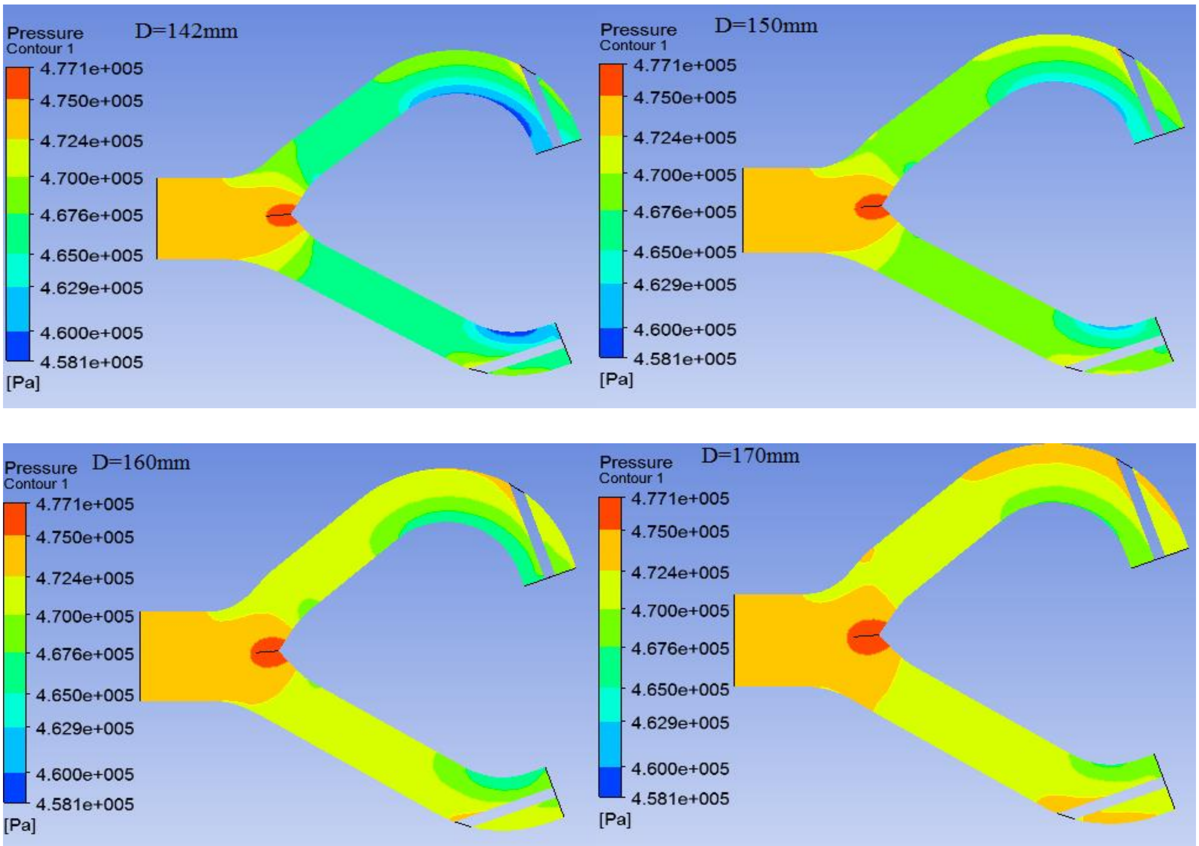

Appendix F-Velocity contour of distributer for different diameter.

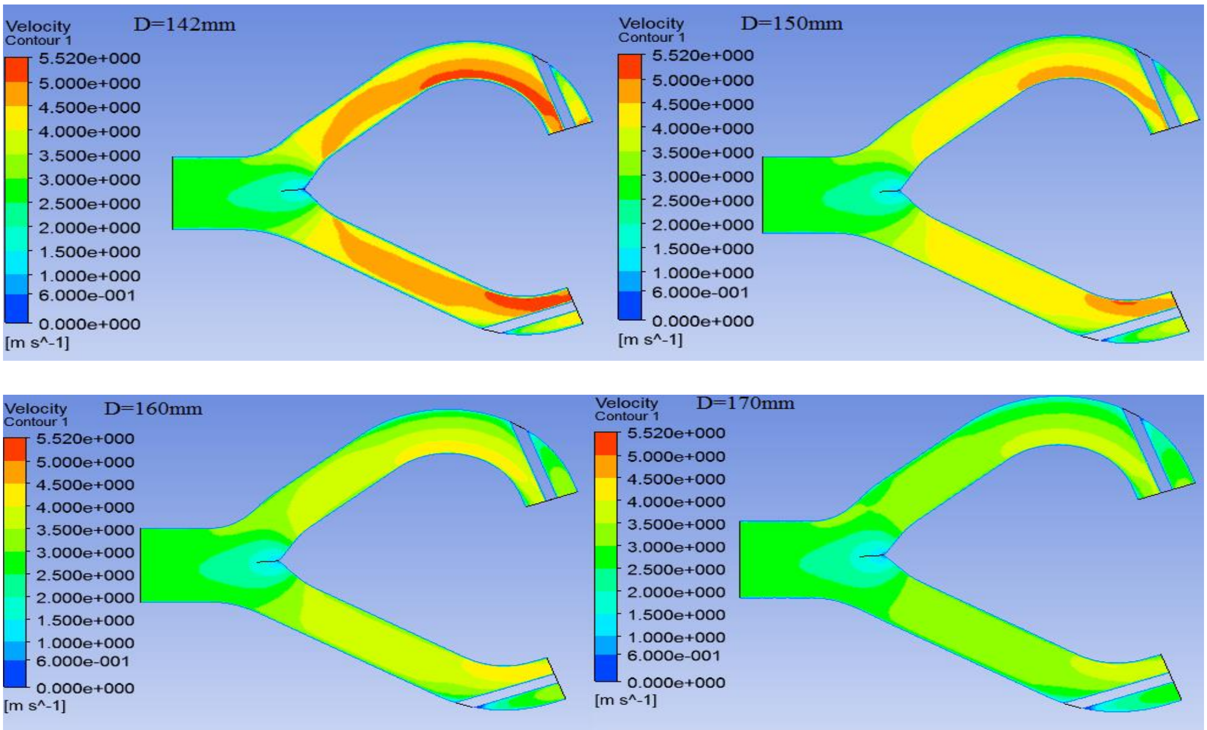

Appendix G Pressure Contour Of Nozzle At Different Nozzle and spear Angles

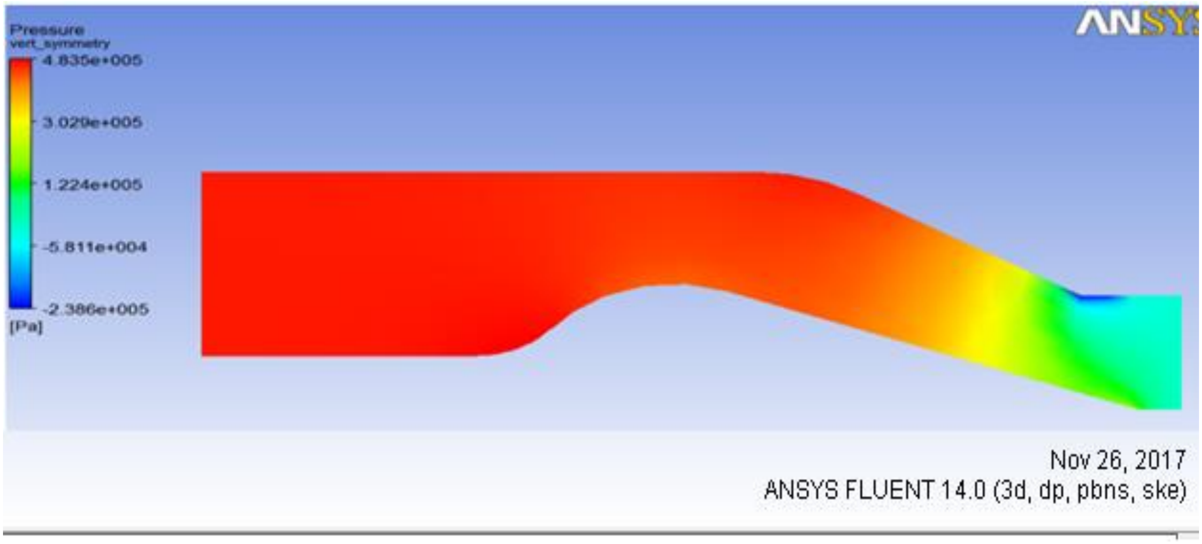

pressure contour of $\alpha=30^0$ -$\beta=20^0$

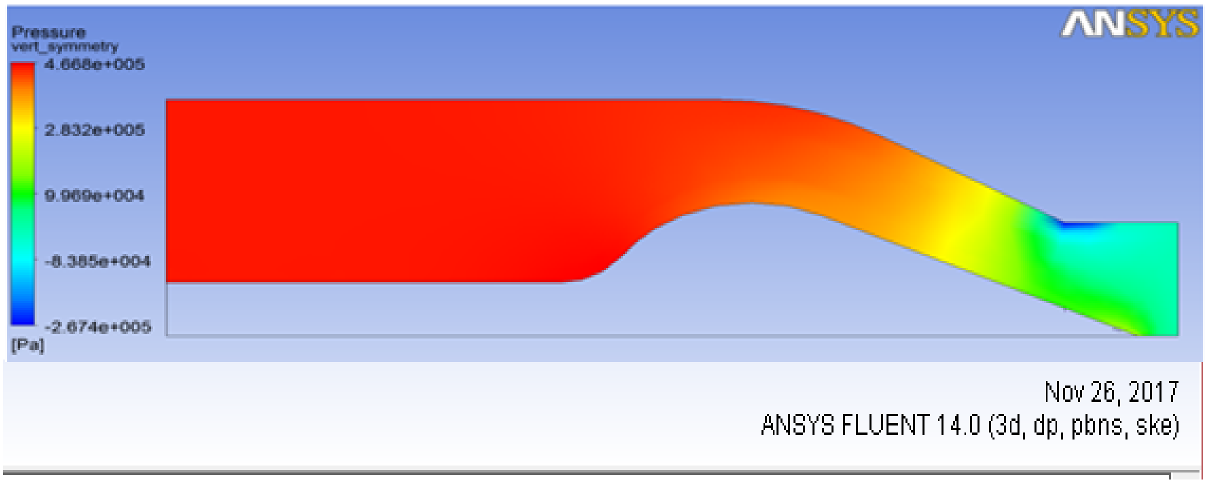

Pressure contour of $\alpha=30^0$ -$\beta=25^0$

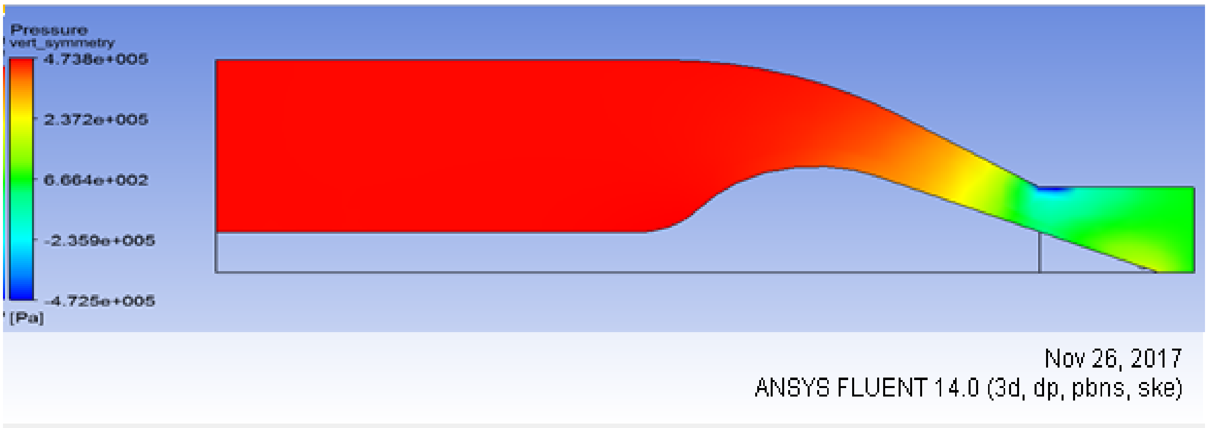

Pressure contour of $\alpha=35^0$ -$\beta=25^0$

APPENDIX H- Velocity Contour Of Nozzle For Different Nozzle And Spear Angles

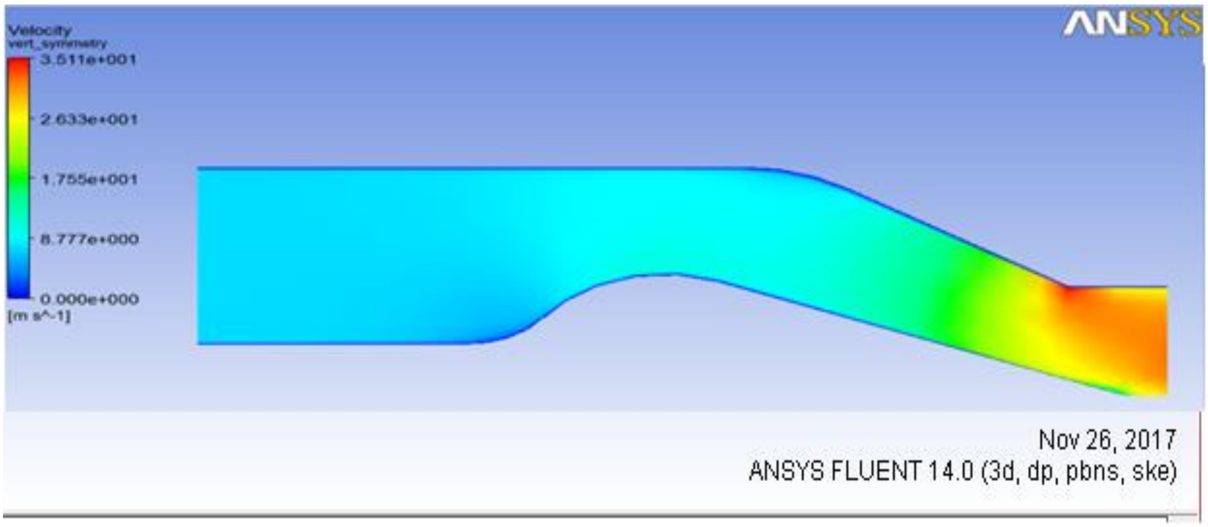

Velocity contour of $\alpha=30^0$ -$\beta=20^0$ at closing distance of 80mm

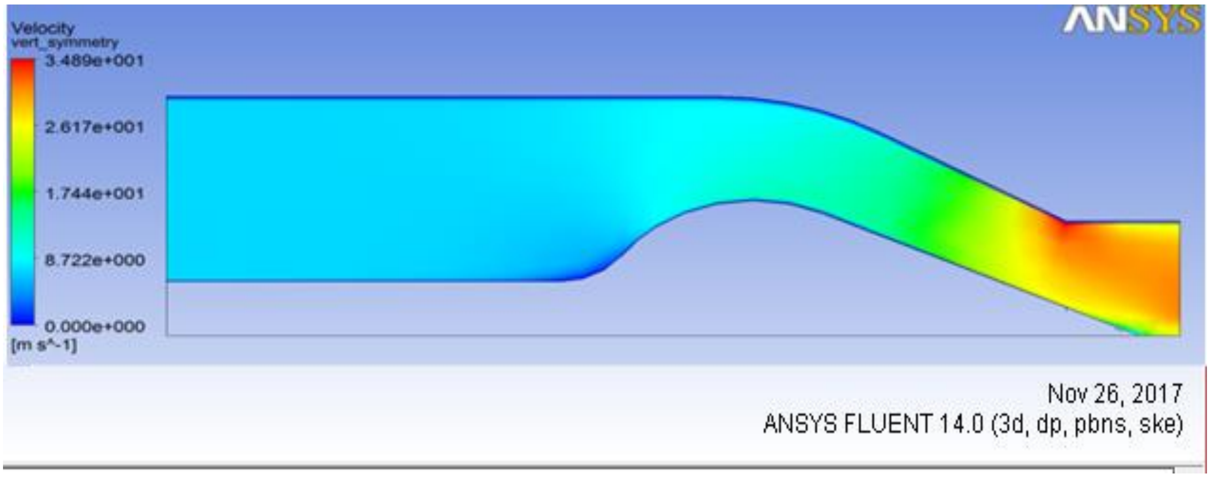

Velocity contour of $\alpha=30^0$ -$\beta=25^0$

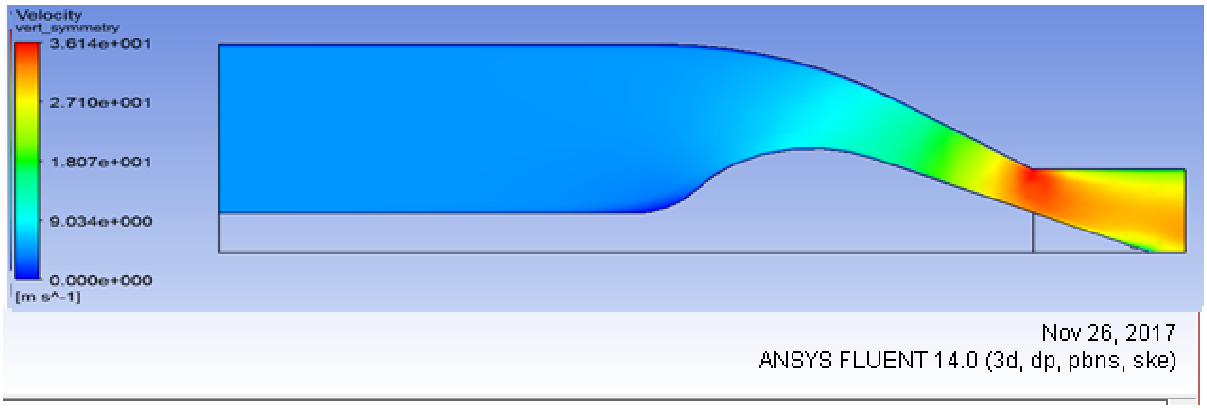

Velocity contour of $\alpha=35^0$ –$\beta=25^0$

ADDIS ABABA UNIVERSITY

SCHOOL OF GRADUATE STUDIES

INSTITUTE OF TECHNOLOGY

DEPARTMENT OF MECHANICAL ENGINEERING

DECLARATION

I, the undersigned, declare that this is to certify that the thesis prepared by **Sase Negash**, entitled: "***Design and Simulation of the Distributer and Nozzle of a Micro Hydro Pelton Turbine***" is my original work and has not been presented for any degree in any university and all the sources of materials used for the thesis have been duly Acknowledged.

SASE NEGASH	______________	______________
Name	Signature	Date

Addis Ababa Institute of Technology, Addis Ababa University, Addis Ababa

Date of Submission_____march 2018 G.C